5-2007

Modeling the Quorum Sensing Signaling Regulatory Network in *Vibrio fischeri*

Ling Yan
University of Tennessee, Knoxville

To the Graduate Council:

I am submitting herewith a dissertation written by Ling Yan entitled "Modeling the Quorum Sensing Signaling Regulatory Network in *Vibrio fischeri*." I have examined the final electronic copy of this dissertation for form and content and recommend that it be accepted in partial fulfillment of the requirements for the degree of Doctor of Philosophy, with a major in Civil Engineering.

Chris D. Cox, Major Professor

We have read this dissertation and recommend its acceptance:

Michael L. Simpson, Bruce Robinson, Alice C. Layton

Accepted for the Council:

Carolyn R. Hodges

Vice Provost and Dean of the Graduate School

(Original signatures are on file with official student records.)

To the Graduate Council:

I am submitting herewith a dissertation written by Ling Yan entitled "Modeling the Quorum Sensing Signaling Regulatory Network in *Vibrio fischeri*." I have examined the final paper copy of this dissertation for form and content and recommend that it be accepted in partial fulfillment of the requirements for the degree of Doctor of Philosophy, with a major in Civil Engineering.

Chris D. Cox, Major Professor

We have read this dissertation
and recommend its acceptance:

Accepted for the Council:

Vice Provost and Dean of the Graduate School

Modeling the Quorum Sensing Signaling Regulatory Network in *Vibrio fischeri*

A Dissertation

Presented for the

Doctor of Philosophy Degree

The University of Tennessee, Knoxville

Ling Yan

May 2007

Acknowledgments

I would like to express my special appreciation to Dr. Chris D. Cox for the significant suggestions on the modeling and the supervising overall the project. I also want to thank Dr. Michael L. Simpson for the encouragements and supports; Dr. Alice C. Layton for providing helps in the molecular microbiological experiments; and Dr. Bruce Robinson for the suggestions on the dissertation writing. Others who provided assistant or comments for this research include Dr. Gray Sayler, Dr. Paul Frymier, Dr. David Nivens, Dr. Hong Guo, Dr. Michael S. Allen, John Wilgus, Dr. Steve Ripp, Dr. James T. Fleming, Dr. John Sanseverino, Dr. Shawn A. Hawkins, Dr. Randall W. Gentry, Stephanie Osbourne, Christopher S. Chewning, Scott Moser, Sharon Hall, Boris Horris as well as other CEB personnels. Last, but not least, I am indebted to my family whose understanding and support made this work possible.

Abstract

Quorum sensing is a mechanism by which bacteria can sense the levels of signaling molecules and respond by controlling the expression of target genes. The marine bacterium, *Vibrio fischeri*, has been extensively studied as a model for the quorum sensing mechanism in Gram-negative bacteria. In order to systematically investigate the quorum sensing regulatory network in *V. fischeri*, a conceptual model was first established based on the existing knowledge. Next, molecular microbiology and bioinformatics techniques were employed to both qualitatively and quantitatively characterize the system. These techniques included the quantification of the 3-oxo-C6-HSL concentrations in the cell culture supernatant using a bioluminescent bioreporter strain of *E. coli*, the measurements of the messenger RNA levels of quorum sensing genes (*luxI, luxR, ainS* and *litR*) using the reverse transcription-polymerase chain reaction (RT-PCR), as well as the sequence analysis of the promoter regions of quorum sensing related genes. A mathematical model composed of ordinary differential equations was created to characterize the regulatory process. The simulated annealing method was used to minimize the weighted discrepancy between the modeling output and the experimental data. The simulations from the calibrated model agree well with the experimental data with correlations ranging from 0.85 to 0.99. This study, mathematically modeled the comprehensive quorum sensing regulatory system, which encompasses 3-oxo-C6-HSL, *lux* operon (*luxR* and lux*ICDABEG*), C8-HSL, *ainS, ainR*, *luxO*, and *litR*, and can benefit the understanding of dozens of similar quorum sensing regulatory systems.

TABLE OF CONTENTS

CHAPTER 1. INTRODUCTION 1

1.1 Background knowledge 1
1.1.1 Quorum sensing 1
1.1.2 Vibrio fischeri 2

1.2 The motivations to study the quorum sensing system in *Vibrio fischeri* 3

1.3 Research objectives 5

1.4 Research overview 5

CHAPTER 2. THE QUORUM SENSING REGULATORY SYSTEM IN *VIBRIO FISCHERI* (LITERATURE REVIEW) 7

2.1 AI-1 signaling molecules and intracellular signaling regulation 7
2.1.1 *lux* Operon and 3-oxo-C6-HSL signaling regulation 7
2.1.2 *ain* genes and C8-HSL signaling regulation 13
2.1.3 LuxO regulation 14

2.2 AI-2 and intercellular regulation 18

CHAPTER 3. BIOINFORMATICS ANALYSIS OF THE QUORUM SENSING REGULATORY NETWORK IN *VIBRIO FISCHERI* 24

3.1 Introduction 24
3.1.1 Motivation to use bioinformatics tools 24
3.1.2 The genomic properties of *Vibrio fischeri* ES114 24
3.1.3 The important components involved in the dynamic quorum sensing regulatory process 25

3.2 Important sequences in the quorum sensing regulatory network 27
3.2.1 The regulatory region between the LuxI and LuxR coding sequences 27
3.2.2 The litR promoter region and the possible LitR binding site 34
3.2.3 *ain* Genes 38
3.2.4 Sigma-54 dependent sRNAs 40

CHAPTER 4. DIRECT QUANTIFICATION OF *N*-(3-OXO-HEXANOYL)-*L*-HOMOSERINE LACTONE IN CULTURE SUPERNATANT USING A WHOLE-CELL BIOREPORTER 48

4.1 Introduction 48

4.2 Materials and methods 50
4.2.1 Bioreporter strain and its cultivation 50
4.2.2 Bioreporter detection of HSLs 51
4.2.3 Data reading and processing 51

4.3 Results and discussion 51

CHAPTER 5. MODELING AND SIMULATION OF QUORUM SENSING REGULATION IN *VIBRIO FISHCERI* 59

5.1 Introduction 59

5.2 The quorum sensing regulatory network in *Vibrio fischeri* 60
5.2.1 Important components of the network 60
5.2.2 The components in the *lux* operon- 3-oxo-C6-HSL system 60
5.2.3 The components in the *ain* genes- C8-HSL system 61
5.2.4 The cell-density dependent dynamic regulatory process 62

5.3 Experimental methods and data analysis 63

5.4 Model formulation and calibration 70
5.4.1 Conceptual model 70
5.4.2 Mathematical model 70

5.5 Discussion 78

5.6 Supporting information 85

CHAPTER 6. CONCLUSION 87

Appendix A. The Sigma factors analysis 106

Appendix B. The procedures for sequencing the putative sRNA DNA sequence... 107

Appendix C. The important proteins in the QS regulatory network 109

Appendix D. The Fortran 77 codes 112

VITA 120

Chapter 1. INTRODUCTION

1.1 Background knowledge

1.1.1 Quorum sensing

Quorum sensing is a mechanism by which bacteria can sense and respond to their own cell density via signaling molecules (Fuqua et al., 1994). During this process, signaling molecules (autoinducers) are synthesized by synthase proteins, and then either diffuse or are transported into the surrounding environment (Kaplan and Greenberg, 1985). The autoinducer concentration increases with cell population, and the receptor proteins of the bacteria can detect the status and take actions by controlling the expression of target genes through either activating or repressing their transcription levels (Parsek and Greenberg, 2000).

Quorum sensing mechanisms have been studied in many systems, such as bioluminescence production, plant and animal pathogenesis, and biofilm formation (Kievit and Iglewski, 2000; Pesci and Iglewski, 1997; Visick and Ruby, 2006). The marine bacterium, *Vibrio fischeri*, is a typical example of a bioluminescent bacterium. Among a group of low-density *V. fischeri,* almost no bioluminescence can be detected; however, with the accumulation of the cell population, they luminescent strongly (Fuqua et al., 1996). In the human pathogen *Pseudomonas aeruginosa*, about 4% of 6,000 genes are controlled by the quorum sensing mechanism (Schuster et al., 2004). Quorum sensing is also common among plant pathogens. For example, in *Agrobacterium tumefaciens*, which leads to crown gall tumors in plants, quorum sensing controls the conjugation of Ti plasmid, required for the bacteria pathogenicity (Von et al., 2003). In biofilms, quorum sensing enhances the survival of the entire community by establishing a highly collaborative community with individual members having specific duties (Juhas et al., 2005; Rodney, 2002). Therefore, bacteria use quorum sensing to encourage favorable responses (Teresa and Barbaba, 2000).

There are three major types of quorum sensing regulation in bacteria (Bonnie, 1999). Gram-positive bacteria use amino acids and short peptides as the signaling molecules. After these molecules are actively transported out of the cell, they bind with a specific membrane-bound sensor protein and utilize a two-component phosphorelay pathway in the process of signal transduction, which then activates a DNA binding protein to control the transcription of target genes (Bassler, 2002; Whitehead et al., 2001; Winans and Bassler, 2002). The second type is among many Gram-negative bacteria in which the fatty acid derivatives, N-acyl homoserine lactone, act as the signaling molecules in the cell-cell communication (Fuqua and Greenberg, 1998; Kleerebezem et al., 1997; Whitehead et al., 2001). Although these molecules all contain a common homoserine lactone ring, they differ on the chain length (from C4 to C14). Furthermore, the third carbon may be a carbonyl group or have a hydroxyl group substitution. Specific autoinducers are precisely recognized by specific sensors (Gray et al., 1994; Parsek et al., 1999; Taga and Bassler, 2003). The third type of quorum sensing is shared by both Gram-negative and Gram-positive bacteria, and the signaling molecule is a furanosyl borae diester, which is synthesized by protein LuxS and detected by a periplasmic protein LuxP (Federle and Bassler, 2003).

1.1.2 *Vibrio fischeri*

Vibrio fischeri is a marine bioluminescent Gram-negative bacterium. It belongs to genus *Vibrionaceae*, and has a slightly curved rod form. *V. fischeri* has been extensively studied in the field of quorum sensing. It is also the organism in which quorum sensing was first characterized (Fuqua et al., 2001). *V. fischeri* live naturally in different niches within the marine environment. Some strains of *V. fischeri*, like ES114, live in the light organs of the squid *Euprymna scolopes* in an environmentally transmitted symbiotic relationship (Nyholm and McFall-Ngai, 2004). Another strain, MJ-1, lives in the light organs of the Japanese fish *Monocentris japonica* (Ruby and Nealson, 1976). In the light organs, the bacteria reach extremely high cell densities (10^{10}- 10^{11} cells per ml) and luminescent with a light that matches ambient moonlight (Fuqua et al., 1996). Therefore, the luminescence actually fills in the shades of the hosts (i.e. marine fishes and squids)

caused by the cast of moonlight. This function is very important for these marine animals to avoid nocturnal detection by prey and predators. Some strains of *V. fischeri* are free-living in seawater, like ATCC7744, WH1, and MDR7 (Nishiguchi and Nair, 2003). Under this situation, the typical cell densities are less than 100 cells per mL and should not result in luminescence (Fuqua et al., 1996).

1.2 The motivations to study the quorum sensing system in *Vibrio fischeri*

The LuxI/LuxR system of *V. fischeri* is the prototypical quorum sensing regulation module, and over 70 species having *V. fischeri* LuxI/LuxR homologs have been recognized in Gram-negative bacteria (Federle and Bassler, 2003). Examples of the homologs include the LasR/LasI in *P. aeruginosa*, the TraI/TraR in *A. tumefaciens*, the RhiI/RhiR in *Rhizobium leguminosarum*, etc. (Luo and Farrand, 1999; Miller and Bassler, 2001; Wisniewski-Dye and Downie, 2002). In these systems, the LuxI-like proteins are responsible for the synthesis of the signaling molecules, and the LuxR-like receptor proteins form complexes with the autoinducer, which in turn can bind to certain regulatory loci on DNA to induce the transcription of target genes (Freeman and Bassler, 1999b). Therefore, understanding the mechanism in *V. fischeri* can provide physical, chemical, and molecular genetic insights on the homologous quorum sensing systems.

Certain strains of *V. fischeri* can serve as the detective strains for the presence of acute and chronic toxic chemicals because of their high sensitivities to a broad range of chemicals (Aelion and Davis, 2007; Parves et al., 2006; Vosahlikova et al., 2006; Wright et al., 2007). For example, *V. fischeri* NRRL B-11177 can be used to measure the toxicity of environmental samples. The inhibition of toxic chemicals leads to a decrease of the bacterial bioluminescence, a by-product of the important life activity respiration; furthermore, the light reduction from the test suspension of the strain increases with the toxicity (Jennigs et al., 2000).

The bioluminescence character of *V. fischeri* is very useful for screening bacteria strains in Microbiology. Usually, after the *luxCDABEG* gene of *V. fischeri* was fused into different promoters, the luminescence strength from the engineered cell can be used to quantitatively and qualitatively study the expression of target genes (Kaiser, 1998).

Quorum sensing may influence the formation of biofilm, a group of bacteria attaching on a surface by synthesized extracellular polysaccharide (Juhas et al., 2005; McLean et al., 1997; Shiner et al., 2005). Biofilm processes are often used in secondary wastewater treatment (Odegaard, 2006; Shin et al., 2006). There are several types of biofilm reactors, like static biofilms (e.g. in trickling filters), particulate biofilms (e.g. in biofilm fluidized bed reactors, upflow anaerobic sludge blanket reactors and biofilm airlift suspension reactors), and flocs (in activated sludge processes) (Nicolella et al., 2000). Compared with most other bioprocesses, biofilm reactors can hold higher biomass concentrations; therefore, they can handle heavier loads and variable conditions (Nicolella et al., 2000). The degradation of the organic materials in wastewater accompanies the metabolism activities of the bacteria, so the water quality of the waste stream can be improved by oxidation of the Biochemical Oxygen Demand (BOD). In addition, the nitrogen and phosphorus levels can also be improved during the process.

In this study, computational biological techniques were used to investigate the quorum sensing system in *V. fischeri*. Several characteristics of the *V.* fischeri system make it a good candidate for study using this technique. First, the system displays a rich diversity of phenotypes under various environmental and genetic conditions. Second, many regulatory interactions in the system have been identified; yet the details of certain interactions remain unknown, thereby providing a foundation for model development while still affording opportunity for new scientific insight. Third, the entire genome of strain ES114 and important regulatory regions of other strains have been sequenced; thereby facilitating the application of bioinformatic tools to lend evidence to various proposed regulatory mechanisms.

1.3 Research objectives

The mathematical models of *V. fischeri* quorum sensing formulated to date only consider the regulation of bioluminescence through the interaction of the *luxR* and *luxI* genes. However in recent years, *ainS*, *ainR*, *luxO*, and *litR* genes have been found to play important roles in the regulation. It has been speculated, but not confirmed, that certain small RNAs provide the negative link between the LuxO protein and the messenger RNA of LitR.

The objectives of this research are:

To suggest possible regulatory mechanisms by analyzing the promoter regions of the above quorum sensing related genes and the conserved sequences among different strains of *V. fischeri* bacteria.

To develop a quantitative method of 3-oxo-C6-HSL (quorum sensing signaling molecules) detection, and use it to measure the concentrations of this autoinducer during the growth process of *V. fischeri* ATCC7744.

To develop a comprehensive mathematical model, which encompasses all of the above-listed genes. The goal of the model is to be able to qualitatively describe several types of behavior of the wild type and the genetically modified *V. fischeri* strains under various environmental conditions, and to quantitatively describe the measured messenger RNAs and autoinducer levels during a growth experiment.

1.4 Research overview

This research applies computational biology to analyze the quorum sensing regulation in *V. fischeri*.

Chapter 2 reviews the comprehensive quorum sensing signaling regulation in *V. fischeri*. This regulatory network centers on the intracellular homoserine lactones (AI-1), and also involves the intercellular signaling molecules (AI-2) as well as other regulatory

factors, which participate at the transcriptional, post-transcriptional, and translational levels.

Chapter 3 presents the sequence analysis of the important genes (e.g. *luxIR*, *ainS*, *ainR*, and *litR*) in the regulatory network. Bioinformatic tools are used in the comparison of various strains of *V. fischeri* and cross-referencing of the homologous bacteria.

Chapter 4 describes a whole cell method of quantitatively analyzing the autoinducer (3-oxo-C6-HSL) concentrations during the growth process.

Chapter 5 combines all the information to construct a comprehensive quorum sensing signaling regulatory model in *V. fischeri*. The simulated annealing method is used to calibrate the kinetic constants to a group of experiments in which the 3-oxo-C6-HSL concentrations and the messenger RNA levels of several important quorum sensing regulatory genes are measured.

Chapter 2. The Quorum Sensing Regulatory System in *Vibrio fischeri* (Literature Review)

The quorum sensing signaling regulation in *V. fischeri* consists of interlinked intraspecies homoserine lactones (AI-1), interspecies signaling regulation (AI-2), as well as other regulatory factors affecting the regulations at transcriptional, post-transcriptional, and translational levels.

2.1 AI-1 signaling molecules and intracellular signaling regulation

There are at least two different intraspecies homoserine lactone molecules detected by the receptor proteins in this bacterium. One of the molecules is N-(3-oxo-hexanoyl)-L-homoserine lactone, or N-β-ketocaproyl-L-homoserine lactone (3-oxo-C6-HSL), and the other is N-octanoyl-L-homoserine lactone (C8-HSL) (Fuqua et al., 1996). The chemical structures, synthases, and receptors for each molecule are presented in Table 2-1 (Fuqua et al., 2001; Kuo et al., 1994).

2.1.1 *lux* Operon and 3-oxo-C6-HSL signaling regulation

The *lux* operon in *V. fischeri*, composed of *luxI*, *luxR* and *luxCDABEG* genes, plays an important role in the quorum sensing mechanism (Kaplan and Greenberg, 1985).

The transcriptional regulator *luxR* gene is transcribed leftward. The LuxR protein encoded by the *luxR* gene is a 250-amino-acid polypeptide consisting of two distinct domains: C-terminal domain (terminated by an amino acid with a free carboxyl group) and N-terminal domain (terminated by an amino acid with a free amine group) (Figure 2-1) (Egland and Greenberg, 1999; Trott et al., 2001). The N-terminal domain contains a 3-oxo-C6-HSL binding site, and the C-terminal domain has a helix-turn-helix motif and functions ambidextrously by having multiple contact sites with the RNA polymerase (Devine et al., 1988; Egland and Greenberg, 2001). In addition, the protein acts as a

Table 2-1. Chemical structures and regulators of the AI-1 signaling molecules in *V. fischeri*

Signaling Molecule	Chemical Structure	β-R (alkyl) Group	Synthase	Receptor
3-oxo-C6-HSL	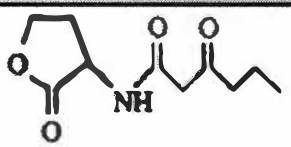	=O	LuxI	LuxR
C8-HSL	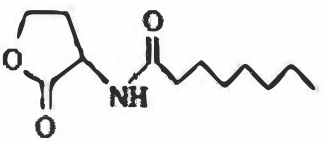	–H	AinS	AinR

N-terminal domain C-terminal domain

Figure 2-1. LuxR domains

(Retrieved from NCBI Conserved Domain Database)

dimer with one signaling molecular per monomer (Choi and Greenberg, 1992). The N-terminal domain of LuxR is bound to the cytoplasmic membrane while the C-terminal domain extends into the cytoplasm (Kolibachuk and Greenberg, 1993).

Both the *luxI* and *luxCDABEG* genes are in the rightward operon (Shadel et al., 1990). The *luxI* gene codes the LuxI protein, an autoinducer synthase, which directly catalyzes the acylation and lactonization reaction between the substrates SAM (S-adenosyl-L-methionine) and specific acylated acyl carrier proteins (Acyl-ACPs). SAM is an activated methyl donor, and synthesized by the transfer of an adenosyl group from ATP to the sulfur atom of methionine. This reaction produces 3-oxo-C6-HSL and MTA (Schaefer et al., 1996; Watson et al., 2002). MTA is unstable and further processed by the Pfs (5'methylthioadenosine) enzyme, which hydrolyzes adenine in MTA to form MTR (Figure 2-2) (Xavier and Bassler, 2003).

The luciferase, a heterodimer with a molecular weight of about 80,000 Daltons, is encoded by the rightward *luxCDABEG* operon (Meighan, 1988). The genes *luxA* and *luxB* separate *luxCD* and *luxEG*, and are responsible for encoding the α (about 42,000 daltons) and β subunits (about 38,000 daltons) of the luciferase, respectively. The active site of the enzyme is on the α subunit, but the β subunit is also required for the catalyst to function. This luciferase catalyzes the oxidation reaction between reduced favomononucleotide ($FMNH_2$) and a fatty aldehyde, and the products of the reaction are oxidized flavomononucleotide (FMN), aliphatic acid, water, and blue green light (Eberhard et al., 1981; Lupp et al., 2003). The *luxC*, *luxD*, and *luxE* genes encode the acyl-reductase, acyl-transferase, and acyl-protein synthase respectively, and these compounds act as aliphatic acid reductase to generate the long chain aldehyde required for the reaction of light production (Figure 2-3). The *luxG* gene encodes the NAD (P) H-dependent FMN reductase (Dunlap, 1999; Ruby et al., 2005). In the bioluminescence formation process, iron in the growth environment may repress the activity of the luciferase (Haygoodt and Nealson, 1985).

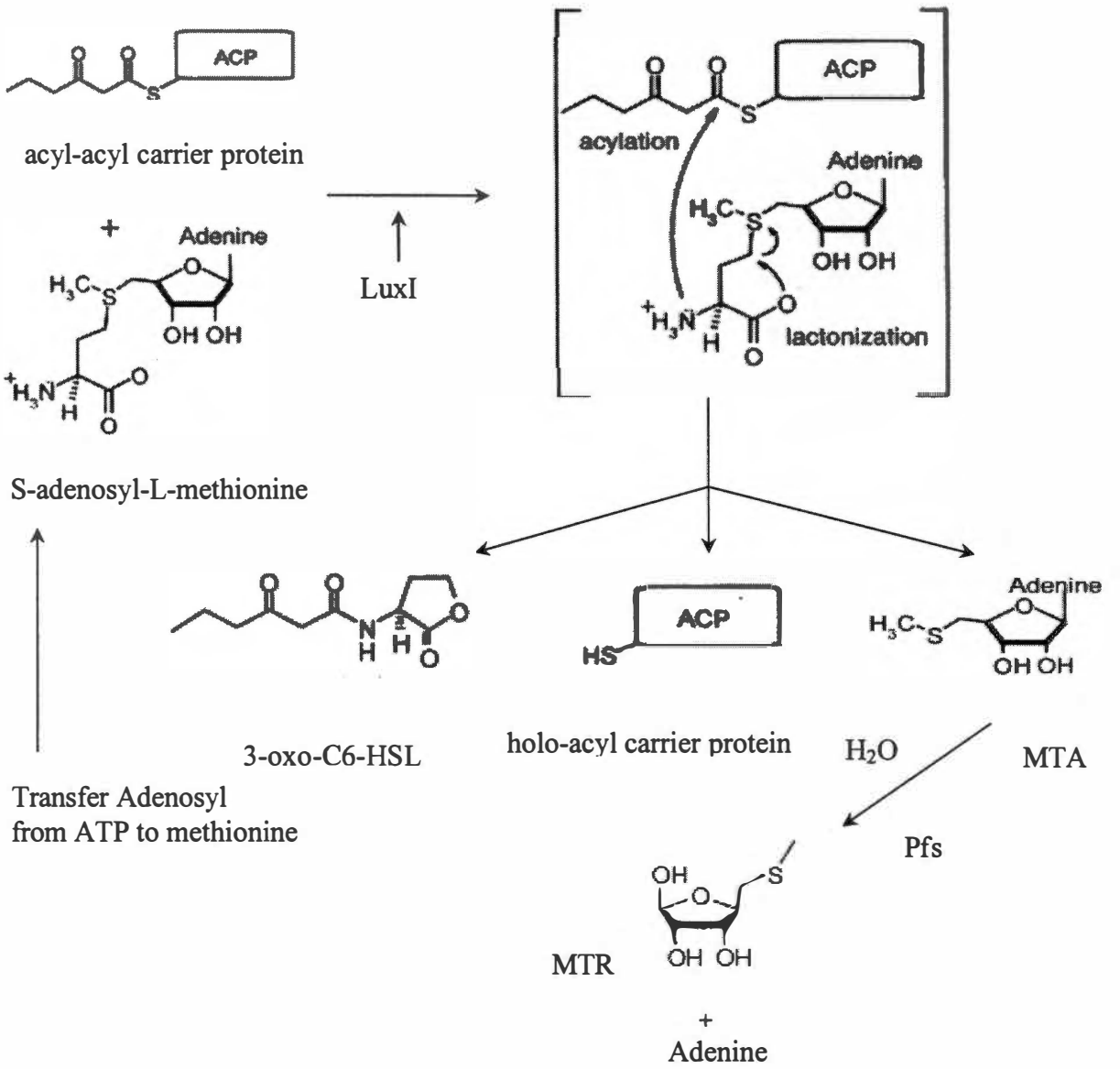

Figure 2-2. 3-oxo-C6-HSL synthesis pathway in *V. fischeri*

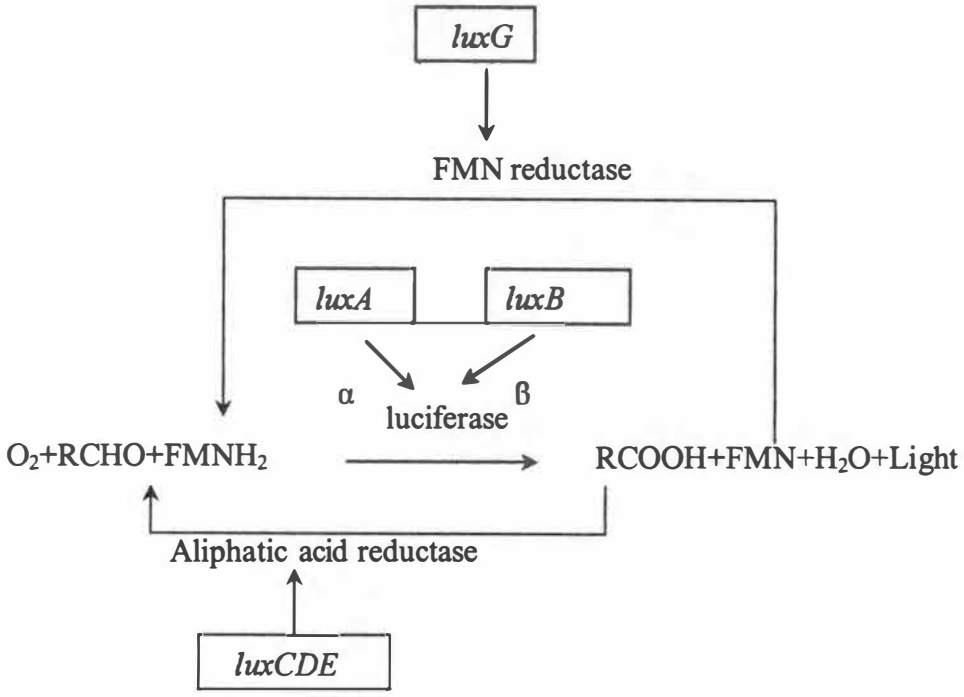

Figure 2-3. *luxCDABEG* genes and the production of bioluminescence

The region between the *luxR* and *luxICDABEG* is comprised of two closely linked *luxI* and *luxR* promoters (Engebrecht and Silverman, 1987). The *luxR* promoter contains regions similar to the RNAP σ^{70} –10 and –35 consensus-binding sites in *E. coli* (Dunlap, 1999). In addition, the binding sequence of a fumarate and nitrate reduction regulatory protein (FNR), the global transcriptional regulation protein, lies between the CAP binding site and the *luxR* transcriptional start site (Meighan, 1994; Rouault and Klausner, 1996; Sawer et al., 1997; Sitnikov et al., 1995). The CAP binding site connects the *lux* operon with the global metabolic regulation. In a glucose rich environment, the level of cAMP, the molecule that signals for glucose starvation, is low, resulting in repression of the LuxR protein, and hence, bioluminescence. The cAMP concentrations increase in the absence of glucose, and the molecule then binds to CAP and functions as an activator. The CAP-cAMP complex can bind to the CAP binding site, which is centered about 60 bp before the *luxR* transcription start site, leading to the stimulation of the leftward *luxR* transcription rate (Dunlap and Greenberg, 1985; Dunlap and Greenberg, 1988). The LuxR protein complexes with the autoinducer to induce the

rightward *luxICDABEG* operon, leading to the induction of luminescence. The *luxR* gene can also negatively auto-regulate its transcription via an autoinducer-dependent mechanism (Dunlap and Ray, 1989). The binding site, related to this regulation, is located in the *luxD* gene and has high fidelity to the *lux* box (11 of 20 base pairs for MJ1), but lower affinity with LuxR than the *lux* box (Shadel and Baldwin, 1992, Sitnikov, et al., 1995).

The promoter region of *luxI* has only a –10 region but no similar –35 *E. coli* sigma-70 region. A 20-bp palindrome sequence (*lux* box) is centered about 40 bp upstream of the transcription start site of the rightward *luxICDABEG* operon (Devine et al., 1989; Dunlap, 1999; Fuqua et al., 1996; Shadel et al., 1990). The binding of LuxR-3-oxo-C6-HSL complex to *lux* box can increase the affinity between RNA polymerase and the promoter region of the *luxICDABEG*, but this binding is not very tight, and can be reversibly inactivated by dilution (Urbanowski et al., 2004). The *lux* box sequence is very similar to the sequence recognized by a repressor protein LexA, which is controlled by the SOS activities, and probably a competitor of LuxR protein (Devine et al., 1989; Sitnikov et al., 1995).

When the cell population is low, the genes in the *lux* operon are transcribed at basal levels. With an increase of cell density, the newly synthetical 3-oxo-C6-HSL molecule diffuses freely out of the cell membrane and is detected by the same cell and the neighboring cells. When the concentration of the autoinducer reaches a threshold level, it binds to the N-terminal domain and activates the C-terminal domain to bind to *lux* box, and stimulates the transcription of *luxICDABEG*, thereby leading to the generation of an intense bioluminescence (Figure 2-4) (Brian and Greenberg, 1994; Egland and Greenberg, 1999; Schaefer et al., 1996b). Since both *luxI* and *luxCDABEG* are in the same operon, the bioluminescence level can indicate the transcriptional activation of the rightward operon.

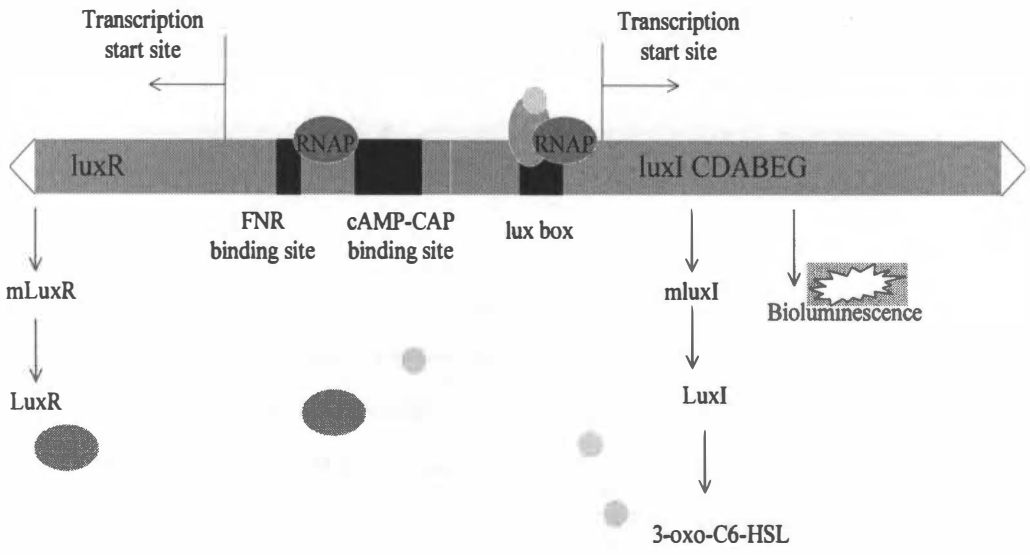

Figure 2-4. The lux operon and the 3-oxo-C6-HSL molecules regulation

2.1.2 *ain* genes and C8-HSL signaling regulation

The C8-HSL signaling molecules and the *ain* genes (including *ainS* and *ainR*) constitute a second autoinduction system in *V. fischeri*. The *ainS* gene encodes the AinS protein, which is a second *V. fischeri* acyl-HSL synthase, and is responsible for the generation of C8-HSL (Gilson et al., 1995). The synthesis activity of C8-HSL from AinS is similar to that of 3-oxo-C6-HSL from LuxI via the reaction between SAM and octanoyl-ACP (Hanzelka et al., 1999). C8-HSL has been shown to link with AinR, which is encoded by the *ainR* gene located on the same operon and downstream of *ainS*. A 20-bp palindrome *lux* box-like region (TAATGAGTTA|TCAATCAATA) is centered at the -35 promoter site of *ainS* (Gilson et al., 1995).

The AinS protein does not show significant amino acid similarities to the LuxI protein, but the C-terminal of AinS shows homology to LuxM of *V. harveyi* (34% identity) (Gilson et al., 1995, Kuo et al., 1996). *lux*M and its upstream *luxL* gene are required for the synthesis of a bioluminescent autoinducer in *V. harveyi* (Bassler et al., 1993). AinR also shows homology to LuxN of *V. harveyi*, which is encoded downstream

of LuxM in that bacterium and has sensor and regulator functions in the bioluminescence response system (Gilson et al., 1995). These similarities suggest the *ain* genes and C8-HSL regulation in *V. fischeri* could be analogous to the autoinducer regulation found in *V. harveyi* (Kuo et al., 1996), and AinR could act as a two-component sensor-kinase protein in *V. fischeri* (Lupp and Ruby, 2004). The *ain* genes system can relieve the negative regulation of gene expression of the *lux* system by inactivating LuxO, because LuxO is the transcriptional activator of certain small RNAs (sRNAs), which act as repressors of LitR. LitR can increase bioluminescence by activating the transcription of LuxR (Miyamoto et al., 2000). If cell density is low, LuxO is phosphorylated, and the transcription of sRNAs is activated. Otherwise, LuxO is dephosphorylated, and the transcription of sRNAs is at basal level.

C8-HSL also interferes with the *lux* operon regulation directly. The autoinducer C8-HSL binds with LuxR in a similar manner as the primary autoinducer 3-oxo-C6-HSL (Callahan and Dunlap, 2000; Miyamoto et al., 2000; Kuo et al., 1996). However, the LuxR-C8-HSL complex has lower activity for the induction of the *lux* operon than that of the LuxR-3-oxo-C6-HSL complex; therefore the binding of C8-HSL and LuxR actually leads to a delay of the expression of the *lux* operon and the accumulation of 3-oxo-C6-HSL (Figure 2-5) (Callahan and Dunlap, 2000; Kuo et al., 1996).

Environmental factors such as culture carbohydrates, oxygen concentration, cyclic nucleotides, temperature, salt concentration, and some specific amino acids are able to affect the activity of the *lux* operon (Brelles-Marino and Bedmar, 2001; Boettcher and Ruby, 1995; Dunlap and Kuo, 1992; Eberhard et al., 1981; Leaderbetter and Greenberg, 2000). These environmental factors also influence the actions of C8-HSL (Kaplan and Greenberg, 1985).

2.1.3 LuxO regulation

As in *V. harveyi*, LuxO in *V. fischeri* can also function as a quorum sensing regulator (Miyamoto et al., 2000). The sequence and functions of the *luxO* in *V. fischeri* are very similar to that in *V. harveyi*. These similarities suggest the LuxO regulatory

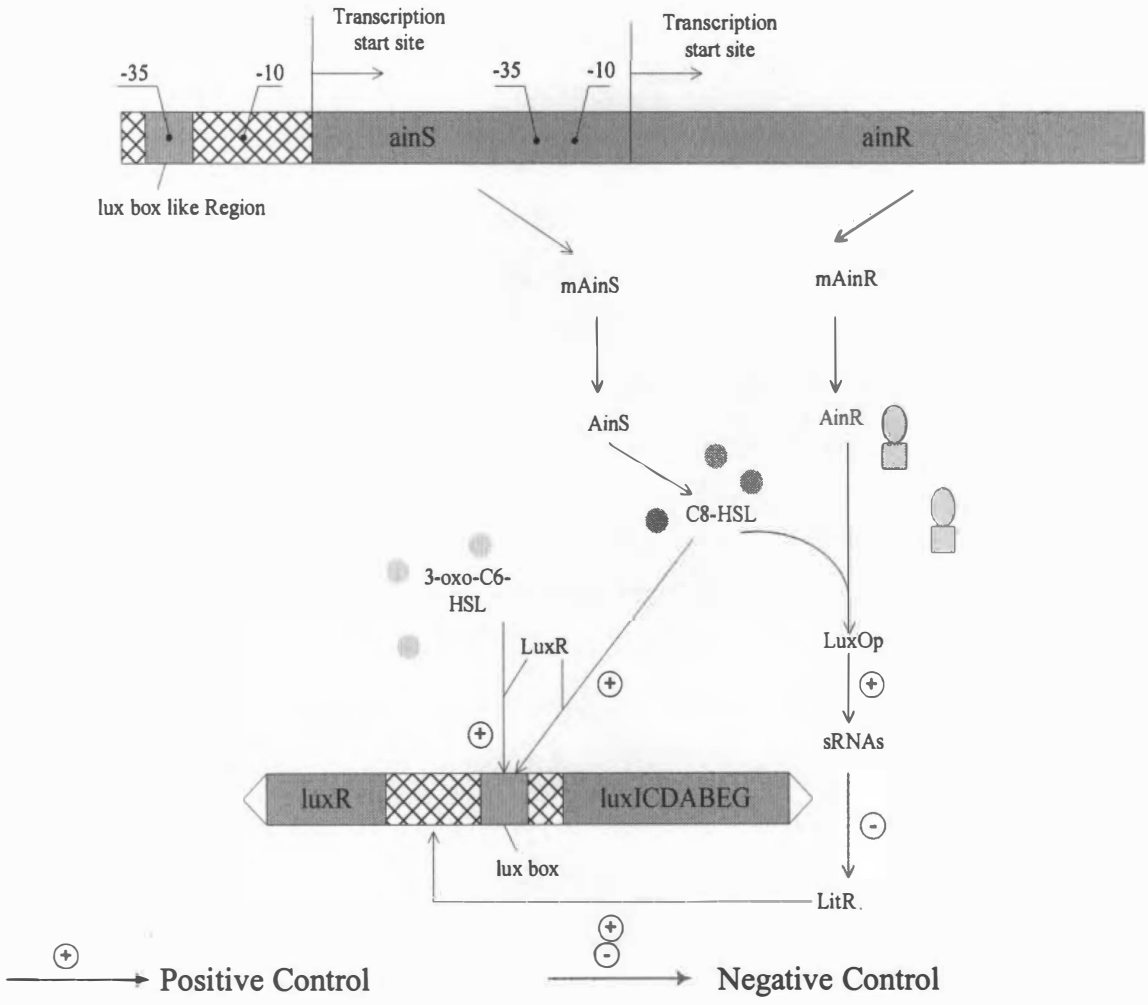

Figure 2-5. The *ainS*, *ainR* genes and the C8-HSL signaling molecules regulation

system may have a common mechanism in *V. fischeri* and *V. harveyi* (Miyamoto et al., 2000).

LuxO regulation in *Vibrio harveyi*

V. harveyi, a bacterium related to *V. fischeri*, also uses quorum sensing to control bioluminescence (Jennifer and Bonnie, 2004). The autoinducer N-3-hydroxybutanoyl homoserine lactone (3-OH-C4-HSL) of *V. harveyi* is synthesized by *luxM* (Cao and Meighen, 1989). However, the regulatory mechanism of luminescence in *V. harveyi* differs substantially from that of the LuxI/LuxR and 3-oxo-C6-HSL regulations in *V. fischeri*, despite the similar structures of their autoinducers (Miyamoto et al., 2000).

The LuxO protein in *V. harveyi* contains an important Aspartate residue (D) (Asp-47), which can be either phosphorylated or dephosphorylated according to different cell densities (Freeman and Bassler, 1999b). In the environment with low autoinducer levels (Figure 2-6 A), the sensor LuxN (H_1 and D_1) functions as a kinase, and transports the phosphoryl groups via LuxU (H_2), a phosphorelay protein, to LuxO (D_2). The phosphorylated form of LuxO is thought to stimulate the transcription of a σ^{54}-dependent small RNAs (Visick, 2005; Visick and Fuqua, 2005). These small regulatory RNAs, upon binding together with the Hfq (chaperone) decrease the transcription of the messenger RNA from LuxR. LuxR in *V. harveyi*, not homologous to the LuxR in *Vibrio fischeri*, is a transcriptional regulator of luminescence genes (Lenz et al., 2004; Visick, 2005). Therefore, the expression level of the *luxCDABEG* operon is low when LuxR is repressed (Pappas et al., 2004). A similar small RNAs regulation phenomenon occurs with the mRNAs of *hapR* in *V. cholerae* (Lenz et al., 2004; Miller et al., 2002).

When the autoinducer concentration achieves a critical level (Figure 2-6 B), LuxN switches from a kinase to a phosphatase (Freeman et al., 2000). LuxU inactivates the repressor, phosphorylated LuxO, and the phosphate is transferred from LuxO through LuxU to LuxN (Freeman and Bassler, 1999a). The transcription of these QS regulatory sRNAs is deactivated, resulting in the increase of the transcription of *luxR*, and

A: At low cell density

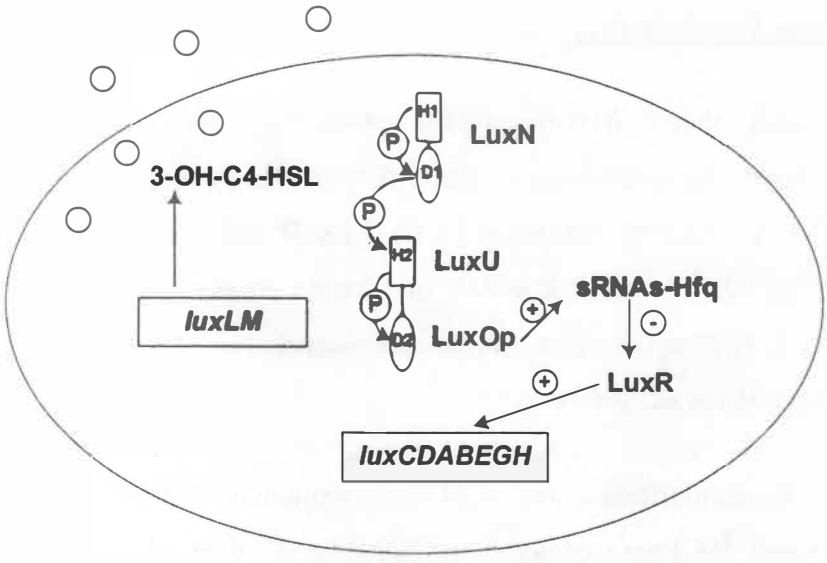

B: At high cell density

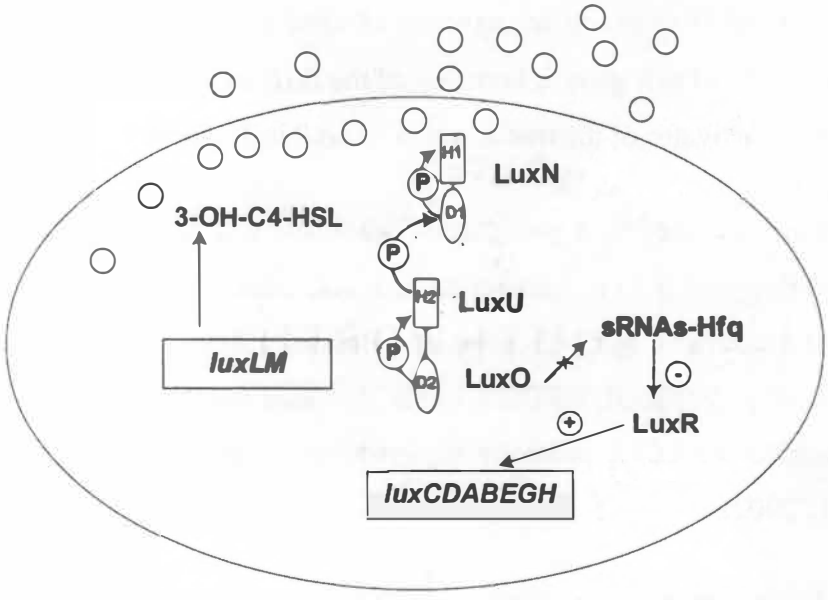

Positive Control Negative Control

Blocked Reaction

Figure 2-6. *Vibrio harveyi* signaling regulation

thus the transcription of *luxI* and luminescence (Visick, 2005).

LuxO regulation in *Vibrio fischeri*

Besides LuxO, other *V. harveyi* quorum sensing regulatory components are also identified in *V. fischeri*. All these suggest that *V. fischeri* has a similar second regulatory mechanism. Therefore, although regulation by LuxI-LuxR and 3-oxo-C6-HSL functions independently of LuxO, the AinR, C8-HSL and LuxO cooperation pathway may be similar to the LuxN, N-(3-hydroxybutanoyl)-L-homoserine lactone, and LuxO pathway in *V. harveyi* (Miyamoto et al., 2000).

By noting the similarities of the regulatory components between *V. harveyi* and *V. fischeri*, a scheme for LuxO centered-regulation in *V. fischeri* can be inferred as shown in Figure 2-7: when the cell-density is low, AinR can function as a kinase by autophosphorylation, and the signal is transferred to the regulator LuxO through LuxU. The phosphorylated LuxO works as an activator of some σ^{54}-dependent sRNAs, which repress the transcription of *litR* gene, a homolog of the *luxR* in *V. harveyi*. LitR encoded by the *litR* gene is an activator of the transcription of *luxR* in *V. fischeri*.

AinR protein switches to a phosphatase when the cell-density is high, and the unphosphorylated form of LuxO is inactive. At high cell density, most LuxO exists as the unphosphorylated deactivated form (Freeman and Bassler, 1999b; Freeman et al., 2000). The level of sRNAs is decreased, resulting in the increased translation of *litR* gene, and LitR protein binds to the LuxR promoter region to activate the transcription of *luxR* (Fidopiastis et al., 2002).

2.2 AI-2 and intercellular regulation

The quorum sensing mechanisms discussed thus far have been for intraspecies communication. Recently, a possible interspecies communication mechanism has been studied that operates through the signaling molecule AI-2, a furanosyl borate diester (Chen et al., 2002). AI-2 was originally found as an extracellular signaling molecule

LuxO regulation at low cell density in *V. fischeri*

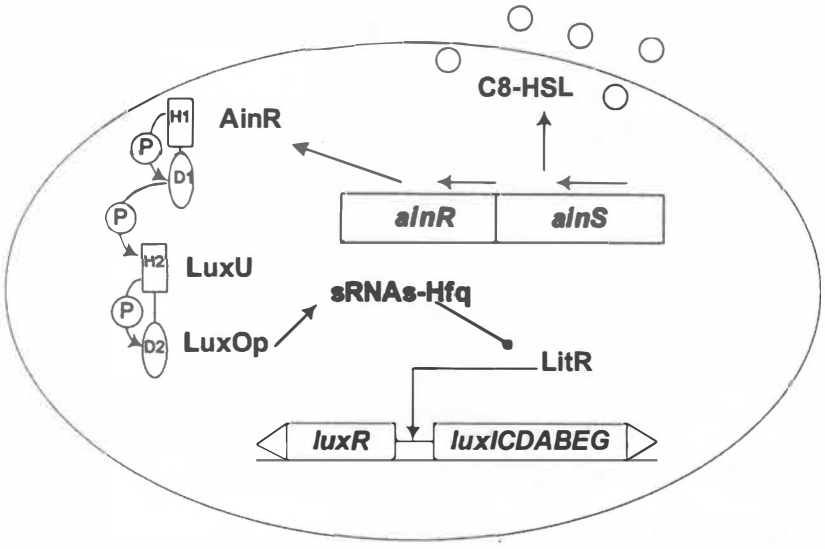

LuxO regulation at high cell density in *V. fischeri*

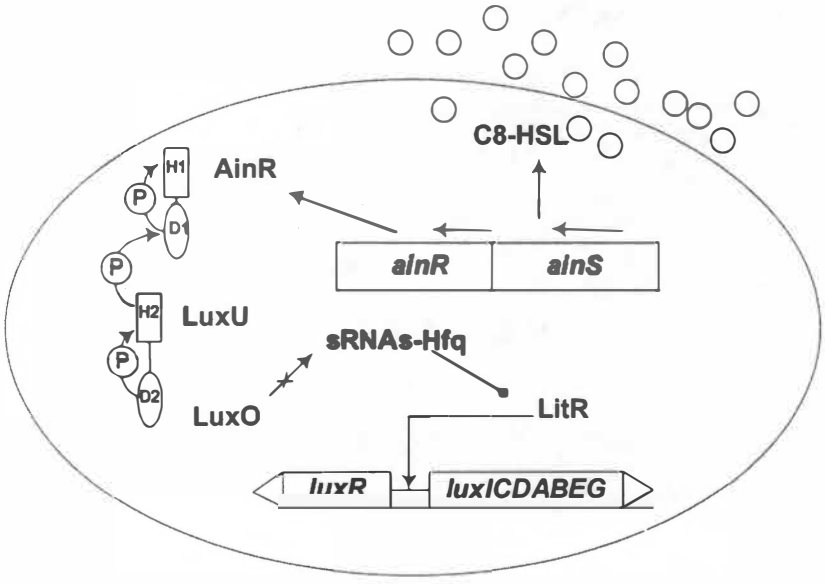

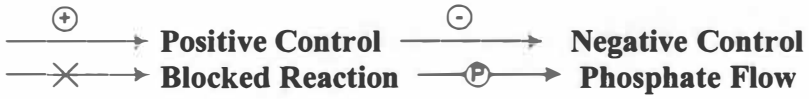

Figure 2-7. LuxO centered regulation in *V. fischeri*

produced by *Vibrio harveyi* and distinct from previously found autoinducers (Table 2-2) (Bassler et al., 1997; Chen et al., 2002; Xavier and Bassler, 2003). The production of AI-2 depends on the synthase LuxS (Schauder et al., 2001), which has been found among a large number of bacteria. AI-2 is synthesized from adenosylmethionine (SAM) through three enzymatic steps (Figure 2-8). In the first reaction, SAM, which serves as a methyl donor in metabolic processes, combines with methylacceptor to yield the toxic intermediate S-adenosylhomocysteine (SAH). Next, SAH is hydrolyzed to S-ribosylhomocysteine (SRH) and adenine by the nucleosidase enzyme Pfs. Then, SRH is cleaved and forms unstable 4, 5-dihydroxy-2, 3-pentanedione (DPD) and homocysteine by the catalyzation of LuxS (Federle and Bassler, 2003; Hanzelka et al., 1996; Xavier and Bassler, 2003; Bassler et al., 1997). DPD can spontaneously form different but inter-convertible derivatives (Xavier and Bassler, 2005a). The families of the derivatives are referred to as AI-2. Different bacteria recognize distinct DPD derivatives. However, the inter-convertible nature of these molecules allows bacteria to respond to AI-2 both from themselves and produced by other bacterial species, suggesting that AI-2 is a universal communication language of interspecies bacterial (Xavier and Bassler, 2005a).

The synthesis process and transportation of AI-2 is different from that of AI-1 molecules. The substrate required for the synthesis of AI-2 is from the process of cell growth; while the synthesis of AI-1 uses SAM directly as a substrate. The accumulation of extracellular AI-2 stimulates the expression of genes encoding an ABC transporter Lsr, which transports AI-2 into the cells (Taga et al., 2001; Wang et al., 2005; Xavier and Bassler, 2005b); while C6-HSL is freely diffusible through the cell membrane.

AI-2 signaling regulation is related to cell densities (Figure 2-9). At low cell density or in the absence of AI-1, LuxP, as a homologue of the soluble and periplasmic ribose-binding proteins, binds with AI-2 (Neiditch et al., 2005). The LuxP-AI-2 complex interacts with the two-component regulator protein LuxQ containing both sensor kinase and response regulator (Freeman and Bassler, 1999a; Neiditch et al., 2005). In this system, the sensor kinase phosphorylates itself on the conserved His residues responding to the environmental signal, and then transfers the phosphoryl group to the conserved

Table 2-2. AI-2 structure

Signaling Molecule	Chemical Structure [b]	Sensor	Synthase
AI-2	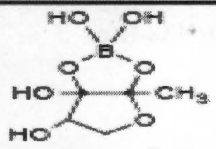	LuxPQ	LuxS

[b] from Xavier and Bassler, 2003

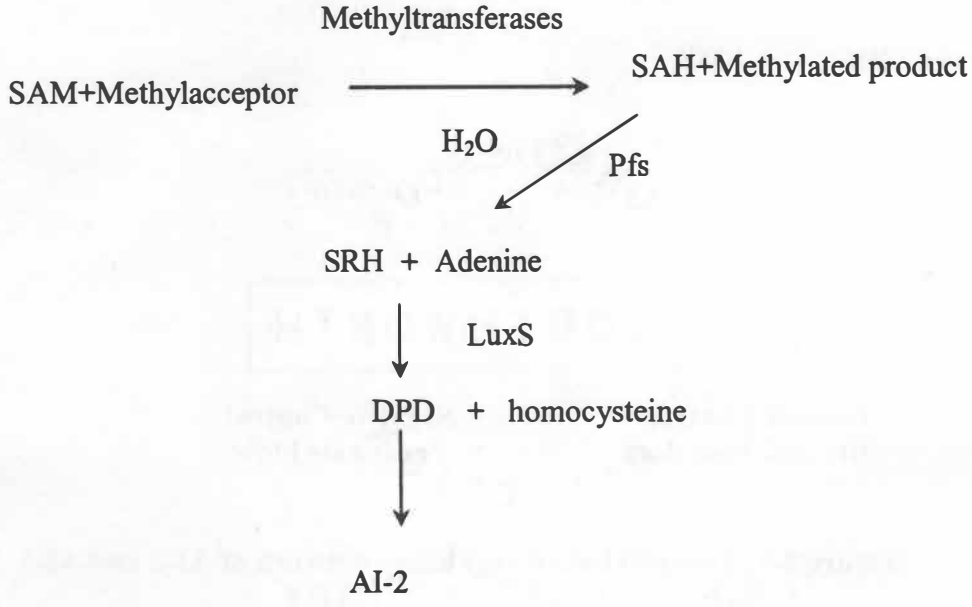

Figure 2-8. Synthesis process of AI-2

At low cell density:

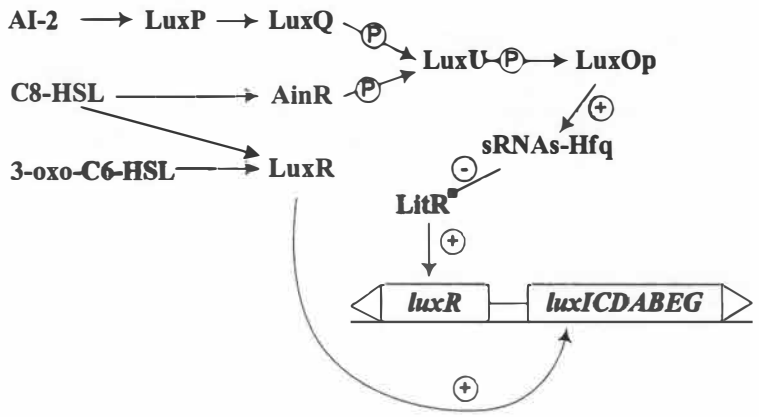

At high cell density:

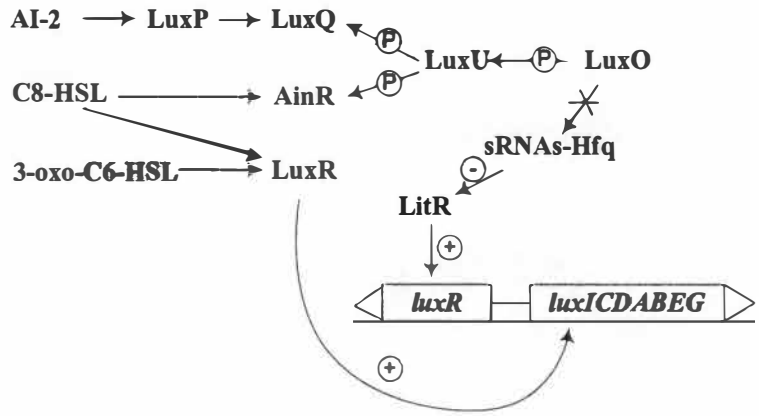

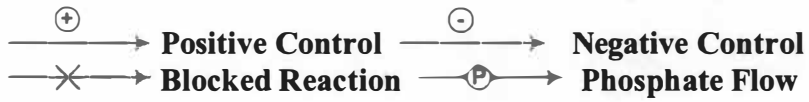

Figure 2-9. The interlinked regulatory network of AI-2 and AI-1

Asp residue of its response regulator domain. Then, the phosphoryl group is transduced to the phosphotransferase sensor protein LuxU, and finally transferred to the conserved Asp residue of the downstream response regulator LuxO. Therefore, LuxU and LuxO connect the homoserine lactone controlled intracellular quorum sensing regulation network with the AI-2 intercellular signal communication. Because phosphorylated LuxO can indirectly inhibit the transcription of *luxCDABEG* by activating the expression of sRNAs to repress the production of the LitR protein, which positively regulates the transcription of the *luxR* (Fidopiastis et al., 2002), the presence of AI-2 signal results in the decrease of bioluminescence (Dove et al., 2003; Federle and Bassler, 2003; Lilley and Bassler, 2000). But at high cell density and with the presence of AI-1 signaling molecules, LuxQ switches from being a sensor kinase to a phosphatase, which can remove the phosphate group, and lead to a rapid elimination of LuxO-phosphate, so the LuxO is inactive and cannot repress the *luxCDABEG* operon to reduce the emission of bioluminescence (Figure 2-9) (Lilley and Bassler, 2000). Although LuxS and AI-2 in *V. fischeri* affect the luminescence, the influence is smaller compared to that of AinS and C8-HSL (Lupp and Ruby, 2004).

AI-2 is hypothesized to be a signaling molecule carrying information concerning the fitness of the population to the environment (Lupp and Ruby, 2004; Xavier and Bassler, 2003). For most of the studied bacterial species, the extracellular AI-2 activity peaks in mid-late exponential phase with the presence of certain preferred carbon sources, and then decreases in stationary phase, suggesting the production and the degradation of AI-2 are connected to the physiological and metabolic activities of bacteria communities (Xavier and Bassler, 2003). During the rapid-growth logarithmic phase, and with the presence of preferred carbon sources, as well as low pH, and/or high osmolarity, the production of AI-2 is induced; however, during stationary phase, with the lack of preferred carbon sources, neutral pH, and low osmolarity, the degradation of AI-2 is induced (Chen et al., 2002; Winzer, 2002).

Chapter 3. Bioinformatics Analysis of the Quorum Sensing Regulatory Network in *Vibrio fischeri*

3.1 Introduction

3.1.1 Motivation to use bioinformatics tools

Bioinformatics has become an essential tool for the analysis of the information content encoded within genomes (Mount, 2004). Proteins, RNAs, and DNAs are some of the essential macromolecules of life. Of these, proteins comprise the largest fraction of the cell mass and function as structural components, catalysts and regulators. The RNA content of cells is second only to proteins in concentration. The three major types of RNA (messenger RNA, transfer RNA, and ribosomal RNA) play an important role in the protein translation. DNA molecules semi-conservatively replicate themselves and pass on the cell's genetic information to its decedents. Together, these macromolecules form the pathway through which information flows in living cells: DNAs are transcribed into RNAs, which can then be translated to proteins. In certain situations, RNAs can be reversibly transcribed to DNAs. This information is encoded in the sequences of the nucleotides within the DNA (A, T, G and C) and RNA (A, U, G and C) molecules and in the sequences of the 20 amino acids in proteins. Although the most reliable approach to determine the structure and function of these macromolecules is still through hypothesis-driven experiments, the knowledge of bioinformatics can guide this bench work through the study of homologies (Lupp et al., 2003). With the completion of the genomic DNA sequence of *V. fischeri* ES114 and partial sequences of other *V. fischeri* strains, bioinformatics tools have become very useful in the analysis of sequences involved in the quorum sensing regulatory network in the bacteria.

3.1.2 The genomic properties of *Vibrio fischeri* ES114

The V. fischeri ES114 bacterium has two chromosomes (Chromosome I and II) and one plasmid (pES100). The total length of the genome is around 4.2 M base pairs

with the lowest GC content (about 38%) among the 27 species of *Vibrionaceae* (Table 3-1) (Ruby et al., 2005). Both of the two chromosomes have 25 classes of genes responsible for the basic bacteria mechanisms and functions (Ruby et al., 2005). The known quorum sensing related genes of *V. fischeri* are located in the two chromosomes (Table 3-2). Chromosome I contains the genes that encode LuxS, LuxP, and LuxQ, which are the AI-2 synthase, detector and responder, respectively. It also contains the genes that encode AinS and AinR, which are the C8-HSL synthase and detector, as well as the genes that encode for proteins involved in the signal transduction (LuxO, LuxU, LitR, and Hfq) from the AinR receptor protein to LuxR regulator protein. The *luxR* and *luxICDABEG* genes are in chromosome II and are transcribed divergently.

3.1.3 The important components involved in the dynamic quorum sensing regulatory process

The quorum sensing regulation in *V. fischeri* is a cell-density dependent process, and the known components involved in the process are the signaling molecules and the gene products of the *lux* operon (*luxI* and *luxR*), the *ain* genes (*ainR* and *ainS*), the *litR*, *luxO, luxU, hfq gene*, and certain small regulatory RNAs. At low cell densities, the predominant signaling molecules are C8-HSL, which bind with LuxR and form a LuxR-C8-HSL complex. This complex has a lower induction activity for the *lux* operon than that of the LuxR-3-oxo-C6-HSL complex, resulting in a low level of luminescence (Callahan and Dunlap, 2000; Kuo et al., 1996). AinR functions as a kinase by autophosphorylation, which in turn catalyzes the phosphorylation of the regulator LuxO

Table 3-1. *Vibrio fischeri* ES 114 genome information (Based on Ruby et al., 2005)

Name	GenBank Accession Number	Length (Mbp)	GC content	Annotation Database	
				Proteins	rRNA/ tRNA
Chromosome I	CP000020	2.90618	38%	2575	141
Chromosome II	CP000021	1.33202	37%	1172	14
Plasmid pES100	CP000022	0.045849	38%	55	----

Table 3-2. Quorum sensing genes and proteins

Chromosome I

Location	Strand[a]	Length	Protein ID	Locus_tag	Product
594358..594876	+	172	59711152	VF0545	autoinducer-2 production protein LuxS
774175..775293	+	372	59711314	VF0707	LuxP protein precursor
775296..777530	+	744	59711315	VF0708	sensor protein LuxQ
1033942..1035372	+	476	59711544	VF0937	repressor protein LuxO
1035362..1035718	+	119	59711545	VF0938	LuxU[b]
1143189..1145648	-	819	59711643	VF1036	autoinducer regulatory protein AinR
1145660..1146802	-	380	59711644	VF1037	autoinducer synthase AinS
1449566..1451644	-	692	59711903	VF1296	sensor protein LuxQ
2452212..2452817	+	201	59712784	VF2177	LitR, transcriptional regulator
2617346..2617612	-	88	59712930	VF2323	Hfq protein

Chromosome II

Location	Strand[a]	Length	Protein ID	Locus_tag	Product
1043727..1044437	-	236	59714101	VFA0918	LuxG, NAD(P)H-dependent FMN reductase
1044447..1045577	-	376	59714102	VFA0919	LuxE, long-chain-fatty-acid ligase
1045656..1046636	-	326	59714103	VFA0920	LuxB, luciferase beta chain
1046647..1047714	-	355	59714104	VFA0921	LuxA, luciferase alpha chain
1047737..1048660	-	307	59714105	VFA0922	LuxD, acyl transferase
1048676..1050115	-	479	59714106	VFA0923	LuxC, acyl-CoA reductase
1050153..1050725	-	190	59714107	VFA0924	LuxI, autoinducer synthesis protein
1050941..1051693	+	250	59714108	VFA0925	LuxR, transcriptional regulator

[a]: Negative strand denotes the complementary strand of the gene.

[b]: This protein is annotated as a hypothetical protein in the ES 114 genomic project at W.M. Keck Microbial Communities and Cell-signaling Program, but it matches the LuxU sequence of *V. fischeri* (accession number: AAF66012) at a significant E-value (1e-35) and has 41 % identity with the LuxU protein of *V. harveyi*; therefore, it is marked as the phosphorelay protein LuxU in this table.

to LuxOp. Phosphorylated LuxO activates the transcription of certain small regulatory RNAs, which bind to the mRNAs of *litR*, thereby preventing their translation and making them for rapid biodegradation. The LitR protein, encoded by the *litR* gene, is an activator of the transcription of *luxR* and *ainS* genes (Fidopiastis et al., 2002; Lupp and Ruby, 2004); therefore, the phosphorylated LuxO protein indirectly represses the production of the LuxR protein and the C8-HSL molecules, leading to a low level of bioluminescence. Under these conditions, the transcription activity of the *lux* operon is "off" or at a basal level.

With the increase of cell density, AinR switches to a phosphatase, and the dephosphorylated form of LuxO protein loses the ability to indirectly repress the transcription of *litR* gene through certain small RNA. Therefore, the transcriptions of *luxR* and *ainS* gene are induced by the protein LitR. As more 3-oxo-C6-HSL molecules are produced, they diffuse freely between cells and environment. When the concentration of the signal molecules' level reaches a threshold point, they bind to the N-terminal domain of the LuxR protein and activate the C-terminal domain to bind with *lux* box, stimulating the transcription of the *luxICDABEG* by facilitating the binding between RNA polymerase and the promoter region, and thereby enabling a cascade activation of the luminescent gene's transcription, leading to the generation of intense bioluminescence (Brian and Greenberg, 1994; Egland and Greenberg, 1999; Schaefer et al., 1996b; Ulitzur, 1998). At this time, the *lux* operon is "on".

3.2 Important sequences in the quorum sensing regulatory network

The different strains of *V. fischeri* bacteria in Table 3-3 were isolated from either seawater or the light organs of marine animals (Nishiguchi and Nair, 2003).

3.2.1 The regulatory region between the LuxI and LuxR coding sequences

Section Summary: Various *V. fischeri* strains can be categorized as belonging to one of two groups based on the similarities in the sequence of the regulatory region between the coding sequences of LuxI and LuxR. The characterization of the regulatory

Table 3-3. The characteristics of different *V. fisheri* strains

Vibrio fischeri Strain	Isolate Environment	Luminescent Characteristics[b]	*luxIR* Accession Number[a]	*16s RNA* Accession Number[a]
ATCC7744	Free-living	Bright	AY292977	AY341436
WH1	Free-living Massachusetts, USA (Woods Hole)		AY292973	AY292930
SR5	Sepiola robusta France (Banyuls sur Mer)	Bright (Nishiguchi et al., 1998)	AY292972	AY292926
EB12	Euprymna berryi Japan (Tosa Bay)		AY292968	AY292921
SL518	Sepiola ligulata France (Banyuls sur Mer)		AY292985	AY292950
MJ101	Monocentrus japonicus Japan	Bright (Boettcher and Ruby, 1995)	AY292982	AY292946
SI1D	Sepiola intermedia France (Banyuls sur Mer)	Bright (Nishiguchi et al., 1998)	AY292984	AY292948
SA1	Sepiola affinis France (Banyuls sur Mer)	Bright (Nishiguchi et al., 1998)	AY292971	AY292924
CG101	Cleidopus gloriamaris Australia (Townsville)		AY292978	AY292939
ES114	Euprymna scolopes Hawaii, USA (Kaneohe Bay)	Dim (Boettcher and Ruby, 1995)	NC_006841	CP000020
ESP915	Euprymna scolopes Hawaii, USA (Paiko)		AY292967	AY292920 (ESPaiko)
ET401	Euprymna tasmanica Australia (Townsville)		AY292980	AY292943
ET301	Euprymna tasmanica Australia (Sydney)		AY292979	AY292942
EM17	Euprymna morsei Japan (Tokyo Bay)		AY292969	AY292922
ET101	Euprymna tasmanica Australia (Melbourne)	Dim (Nishiguchi et al., 1998)	AY292970	AY292923

[a]: The sequence information was obtained from GenBank.

[b]: The luminescence descriptions are based on different sources; therefore, only two levels are used here: dim and bright.

regions is consistent with the Partial coDing Sequence (PDS) of the LuxI and LuxR proteins. Strains in the first group (including *Vibrio fischeri* ATCC7744, WH1, CG101, SL518, SR5, SI1D, MJ101, EB12 and SA1) tend to luminescent brighter under laboratory conditions than strains in the second group (including *Vibrio fischeri* ES114, ESP915, EM17, ET401, ET301 and ET101), indicating that the differences in phenotype may be related to the types of the regulatory regions.

The *luxR* and *luxI* genes are transcribed divergently, and the region between the two ORFs includes the promoter regions, the ribosomal binding sites (RBS), and the regulatory sites (Figure 3-1). The sites for the *luxR* gene (RBS, -10, -35, FNR binding site and CAP binding site) are located on the complementary strand of the marked places (red dashed line in Figure 3-1). There are several known regulatory sites in the *luxR* promoter region. A CRP-binding site is located close to the -35 promoter site, and the consensus sequence was reported as TGTGA-N6-TCACA (where N is any nucleotide) (Spiro and Guest, 1990). A potential FNR (fumarate and nitrate reduction regulatory protein)-binding site sequence has been recognized between the CRP-binding site and the LuxR transcription start site with the core consensus sequence TTGAT-N4-ATCAA (Spiro and Guest, 1990). This suggests that LuxR may be under positive transcriptional control by an FNR-like protein. As opposed to the *luxR* gene, the *luxI* gene only has a -10 binding site (TATAGT) (Egland and Greenberg, 1999). The *lux* box (ACCTGTAGGA/TCGTACAGGT) palindrome sequence is centered at around –42.5 bp from the *luxI* start site (Egland and Greenberg, 1999).

According to the sequence characteristics of the regulatory regions between the CDS (CoDing Sequence) of LuxI and LuxR, the *V. fischeri* strains in Table 3-3 can be separated into two groups. Group 1 contains the strains ATCC7744, WH1, CG101, SR5, EB12, SL518 SI1D, SA1 and MJ101; Group 2 contains the strains ES114, ESP915, ET401, ET301 EM17 and ET101. The similarity of the regulatory regions between the CDS of LuxR and LuxI to ATCC7744 (Group 1) and ES114 (Group 2) are in Table 3-4.

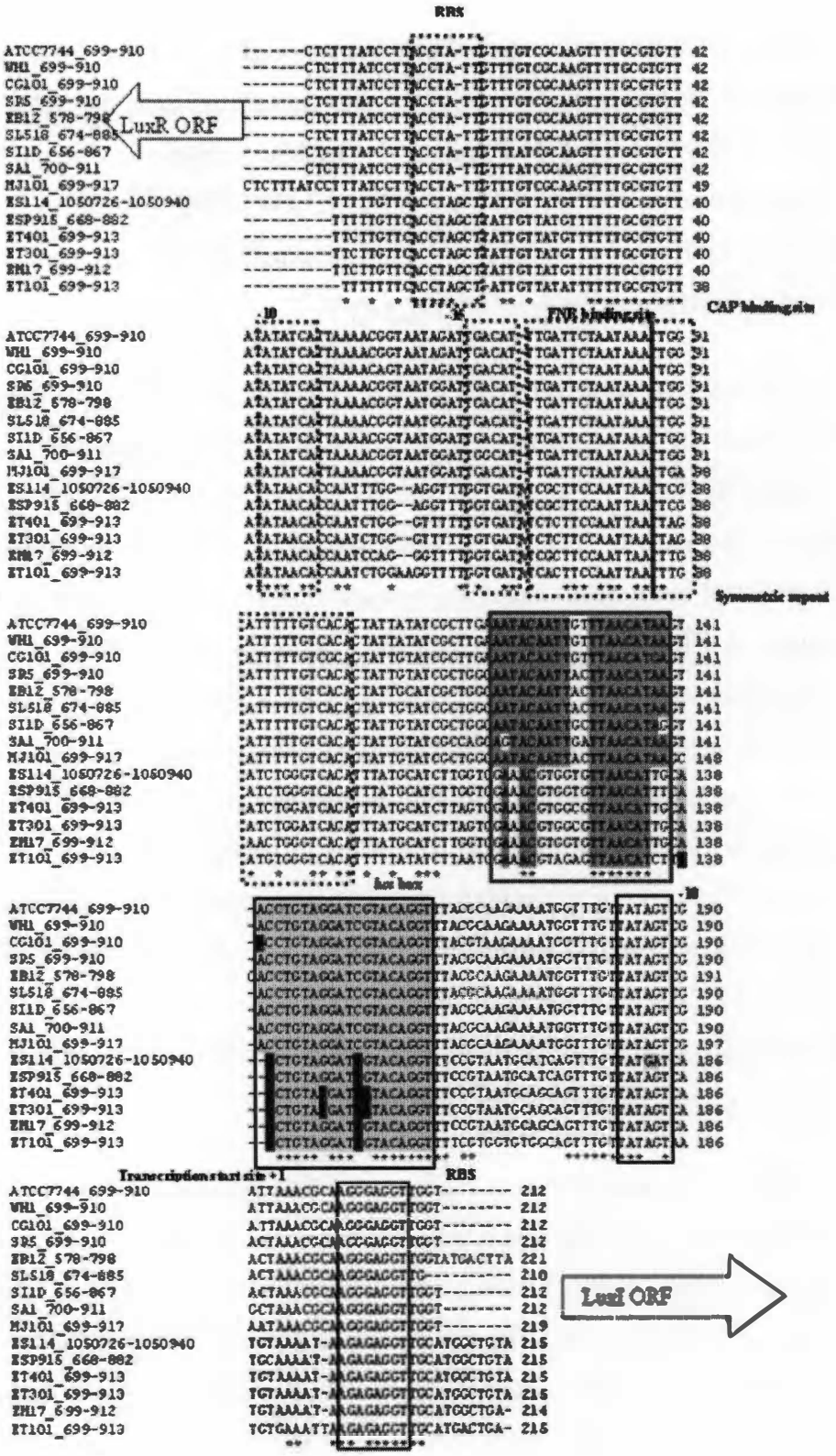

Figure 3-1. The alignment of the regulatory regions between the coding sequences of LuxI and LuxR for different strains of *V. fischeri*

Table 3-4. The similarity of the regulatory region between the CDS of LuxI and LuxR by BLAST

Group	*V. fischeri* strains	Similarity
1	ATCC7744	The comparison standard for Group 1
	WH1	100%
	CG101	97%
	SL518	96%
	SR5	96%
	SI1D	96%
	MJ101	95%
	EB12	95%
	SA1	94%
2	ES 114	The comparison standard for Group 2
	ESP 915	98%
	EM 17	94%
	ET401	92%
	ET301	92%
	ET101	83%

* The similarity of the regulatory regions between ATCC7744 and ES1 14 is very low.

There are several characteristics that distinguish the two groups of bacteria. The *lux* box sequence for the strains in Group 1 are completely conserved with the exception of CG101, which has one mismatch. In contrast, the strains in Group 2 have two to four mismatched nucleotides compared to the consensus sequence, suggesting a possible weaker binding of the luminescent activator in these bacteria. There is also a very conserved symmetric repeat located immediately upstream of the *lux* box with sequence (AATACAATT-N_2-TTAACATAA) for all the strains in Group 1 that was identified through application of the Oligonucleotides Repeats Finder (http://wwwmgs.bionet.nsc.ru/mgs/programs/OligoRep/InpForm.htm). This symmetric repeat is less conserved in the Group 2 strains. No information about it has been reported; however, its conservation in Group 1 strains and its proximity to the *lux* box suggests a possible function of stabilizing the binding of LuxR-autoinducer to the *lux* box. Additional evidence for this hypothesis is provided by the fact that both half-sites of the *lux* box are needed for the LuxR activity (Egland and Greenberg, 1999). The *Vibrio logei* strain 15382 (AN: AY292974) has an identical sequence, and *Vibrio mimicus* (AN: AY292976) has a very similar sequence in the regulatory region of the *luxR*-like and *luxI*-like genes with only one mismatch (AATACAATT-N_2-TTAACAT[redacted]A).

The characteristics of the PDS (Partial coDing Sequence) of the LuxI and LuxR proteins also support the grouping approach. Because the complete coding sequences of the two proteins are not available for most of the *V. fischeri* strains in Table 3-3, only the PDS are chosen to construct the phylogenetic trees (Figure 3-2). The amino acid sequences of the LuxI and LuxR proteins, as well as the regions between the two proteins were drawn by ClustalW using the neighbor-joining (NJ) method and viewed by TreeView (Nishiguchi and Nair, 2003). The NJ method is the most common distance-based method, which computes pair-wise distances, and then derives the trees by repeating the process of inserting branches between a pair of closest neighbors and the remaining terminals in the tree (Baxevanis and Ouellette, 2005; Chenna et al., 2003).

LuxR(partial CDS)

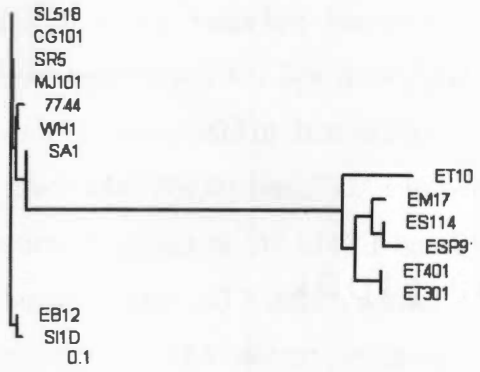

Regulatory Regions between LuxI and LuxR

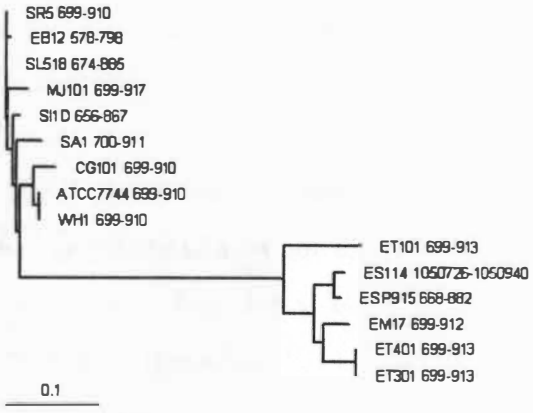

LuxI(partial CDS)

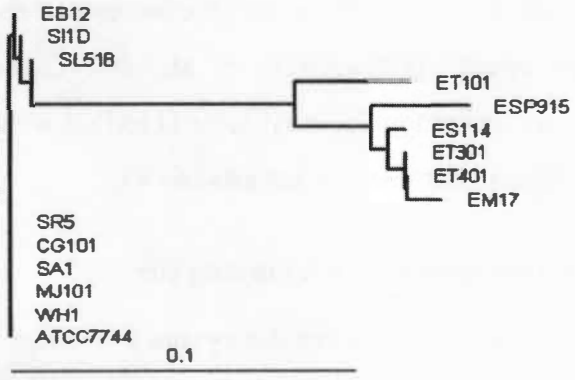

Figure 3-2. Phylogram trees of the partial CDS of LuxI, LuxR and the regulatory region by ClustalW and TreeView

The calculated evolutionary distances are based on the proportion of pair-wise differences (p-distance). The bars indicate a p-distance of 0.1.

The available luminescence information suggests the *V. fischeri* strains in Group 1 may produce more light than those in Group 2. The *V. fischeri* strains ATCC7744 and MJ1 (both are in Group 1) are known as the bright strains, and share almost 98% DNA sequence identity for the region including the *luxR*, *luxI*, and the intervening sequence (Gray and Greenberg, 1992b). However, ES114 is almost dark in laboratory cultures, and the luminescence is about 10-fold lower than that of EM17, and 10,000-fold lower than that of MJ1 (Boettcher and Ruby, 1995). EM17 and ES114 are in Group 2, and share 94% identity for the regulatory region, and 96% for the partial CDS, which include the partial CDS of LuxI and LuxR and the regulatory region (AN: AY292969.1). Furthermore, ET101 (in Group 2) was reported as a dim strain, and SR5, SA1, and SI1D (in Group 1) luminesce with moderate intensity (Nishiguchi et al., 1998).

No significant difference in membrane permeability between ES114 (in Group 2) and MJ1 (in Group 1) has been found (Boettcher and Ruby, 1995). The reason for the lower luminescent activity for ES114 in laboratory was attributed to a low concentration of autoinducer (Boettcher and Ruby, 1990; Boettcher and Ruby, 1995; Gray and Greenberg, 1992). Since luminescence depends on the reversible binding of the LuxR-3-oxo-C6-HSL complex to the *lux* operon (Urbanowski et al., 2004), the reduced luminescence could be caused by a weaker autoinducer synthase (LuxI), a weaker LuxR-autoinducer binding site, or a less efficient autoinducer sensor (LuxR).

3.2.2 The litR promoter region and the possible LitR binding site

Section summary: A possible autonegative regulatory site is located in the *litR* promoter region. The FNR-CAP binding site could be part of the LitR binding site in *V. fischeri*.

LitR in *V. fischeri* shares about 59% identity with *Vibrio cholerae* HapR, *Vibrio harveyi* LuxR, *Vibrio parahaemolyticus* OpaR, and *Vibrio vulnificus* SmcR. The -35 and -10 promoter sites of the *litR* gene do not match very well with the homologous bacteria, which have consensus promoter sequences located at the –35 (TTGACC) and –10 (TACACT) sites (Shao and Hor, 2001). The suggested –35 and –10 sites in Figure 3-3

A: The promoter region of the *litR* gene

```
>gi|21464735|gb|AF378100.1| Vibrio fischeri luminescence regulator LitR gene,
complete cds
        1 gattaaggaa gagctgttaa cggatttata gtgacataaa aagatcatca acacttggca

       61 atactacatt caaaatgtaa acttcacttt ctatttattg cgtaaatata tgcaatactg

                                                  -35
      121 aaaaaaattc tttaagttcg tcataaattt ca[      ]ag ctgaataact gttgaata[ ]  -10
                                  Possible autoregulatory site
      181 [      ]agcct tatgtaaagt tattgagaat aataataata aaaccctata taaaataata
                  RBS
      241 atttgttggc [      ]tataa atata
                                  LitR CDS
```

B: Sequence alignment of the promoter regions of *smcR*, *opaR*, *luxR*, *hapR*, and *litR*

```
                -35                          -10
smcR-p          TTGACCCAATGCATA-TGCACCAT-TACACTCATGGA-GCTAAAAGCAATTA- 49
opaR-p          TTGACCTTGTGCATA-TGCACCAT-TACACTCATCACTGCTTAAAGCAATTA- 50
luxR-p          TTGACCTCGCACATA-TGCACCAT-TACACTCATCAGTGCTTTAAGCAACTA- 50
hapR-p          TTGACCTTGAATATA-TGCACCAT-TACACTCATAGG-GCTTTAAGTAGCAAA 50
litR-p          TTGATCAGCTGAATAACTGTTGAATATATAAGCAGCCTTATGTAAAGTTATTGA 54
                **** *       *** **     ** ** *  **          ***
```

The –35 and –10 sites are decided according to the consensus sequence of *smcR*, *opaR*, *luxR* and *hapR*.

C: A possible LitR autonegatively regulatory site:

```
LitR_promoter              AATTTCATTGATCAG 15
TetR_operatorregion        TCTATCATTGATAGG 15        (Identity: 10/15)
                             * ********  *
```

Figure 3-3.The promoter site of the litR gene

(A) were chosen based on sequence similarity (Figure 3-3(B)), a spacing of 20 base pairs between the two sites, and the similarity of the position of the sites in comparison to homologous bacteria. The -35 promoter site shows significant conservation with the other homologous sequences compared to the -10 promoter site. There is a possible LitR autoregulatory site located around the -35 promoter site, which was identified through the consensus binding sequence of the TetR proteins operator site (Ramos et al., 2005), suggesting LitR could negatively autoregulate its own production. The alignment of the possible autoregulatory site and the TetR protein consensus-binding site is shown in Figure 3-3(C). Although LitR has been described as a positive regulator of the luxR gene and a indirect positive regulator for the ainS genes in V. fischeri, it could also act as a repressor consistent with most of the other known tetR family proteins, and the homologous LuxR protein in *V. harveyi*, which was reported as an autonegative regulator (Chatterjee et al., 1996; Lupp and Ruby, 2004).

LitR is able to bind to a DNA region in *luxR* promoter to activate the transcription of *luxR* (Fidopiastis et al., 2002). Mobility shift analysis was used to locate the binding site within a 427 bp BstBI–PvuII restriction region that includes the 5' end of *luxR* gene and part of the regulatory region between *luxR* and *luxI* (Fidopiastis et al., 2002). Restriction site analysis using NEBcutter V2.0 (Figure 3-4(A)) identified the PvuII site to be within the *lux* box. Within this restriction region, sequenced bases conserved among different *V. fischeri* strains were considered to precisely locate the binding site. The conserved sequence between the –10 and –35 promoter sites of the *luxR* gene (Figure 3-1) was eliminated from consideration since LitR acts as an activator instead of a repressor for the *luxR* gene. However, within the FNR binding site there is a sequence that matches 10 of the 15 bases in the TetR operator sequence (Figure 3-4 (B)); therefore, it appears that the part of the FNR-CAP binding site is a strong candidate to be the LitR binding site in *V. fischeri*.

A: Restriction enzymes analysis of the ES114 *luxR* and *luxI* sequence (AN: AY292966) by NEBCutter

	Enzyme	Specificity	Cuts	Sites & flanks	Cut positions (blunt - 5' ext. - 3' ext.)
1	BstBI	TT CG▲AA	1	389 TTGTTTTTTT TT CG▲AA TACGTTCCAA	400/402
2	PvuII	CAG▲CTG	1	819 GTTAACATTG CAG▲CTG TAGGATGGTA	831

B: Alignment of the FNR-CAP binding site and the TetR operator region

```
CLUSTAL W (1.83) multiple sequence alignment


TetR            -------TCTATC--ATTGATAGG------ 15
FNR-CAP         TGTGACCCAGATCGAATTAATTGGAAGCGA 30        Local identity: 10/15
                        ***  *** ** **
```

Figure 3-4. LitR binding site analysis

3.2.3 *ain* Genes

Section summary: The LitR protein could positively regulate the transcriptions of the *ainS gene* according to the similarities between the promoter site of gene *ainS* and gene *luxR*.

The *ainR* gene is located immediately downstream of the *ainS* gene. The regulatory regions for these genes in ES114 and MJ1 are nearly identical. The potential -10, -35, and Shine-Dalgarno (SD) sequences are shown in Figure 3-5(A) (Gilson et al., 1995). A *lux*-box like palindrome region (TAATGAGTTA|TCAATCAATA) was found centered at the –35-site of *ainS*, suggesting another interaction between the *ain* and *lux* systems via the LuxR protein (Gilson et al., 1995).

The promoter region of the *ainS* (MJ1) is similar to that of the *luxR* promoter (ATCC7744) (Figure 3-5(B)). The CAP and FNR binding sites of *luxR* are close to the consensus sequences TGTGA-N6-TCACA (CAP binding site) and TTGAT-N4-ATCAA (FNR binding site), with three and one mismatch, respectively. In comparison, the sequence of the *ainS* promoter has four and five mismatches for those sequences at the equivalent positions of the *luxR* promoter region. Another possible FNR putative sequence is located around the –35 promoter site (TT[redacted]AT[redacted]ATCAA). This sequence has only one mismatch with the FNR consensus sequence, but has five instead of four nucleotides located between the two ends of the FNR consensus binding sequence. These similarities between the promoter region of *ainS* and *luxR* suggest that LitR could positively regulate the transcription of the *ainS* gene. This hypothesis agrees with the experimental observations that a *litR* mutant strain produced lower transcription levels of the gene *ainS* (Lupp and Ruby, 2004). However, the promoter region of *ainR* is greatly different from that of *luxR*, except that it has a possible FNR binding site ([redacted]TG[redacted]T(TTCA)ATCAA), which is located before the –35 promoter site of the *ainR* (Figure 3-5(A)).

A: The promoter region of *ains* and *ainR*

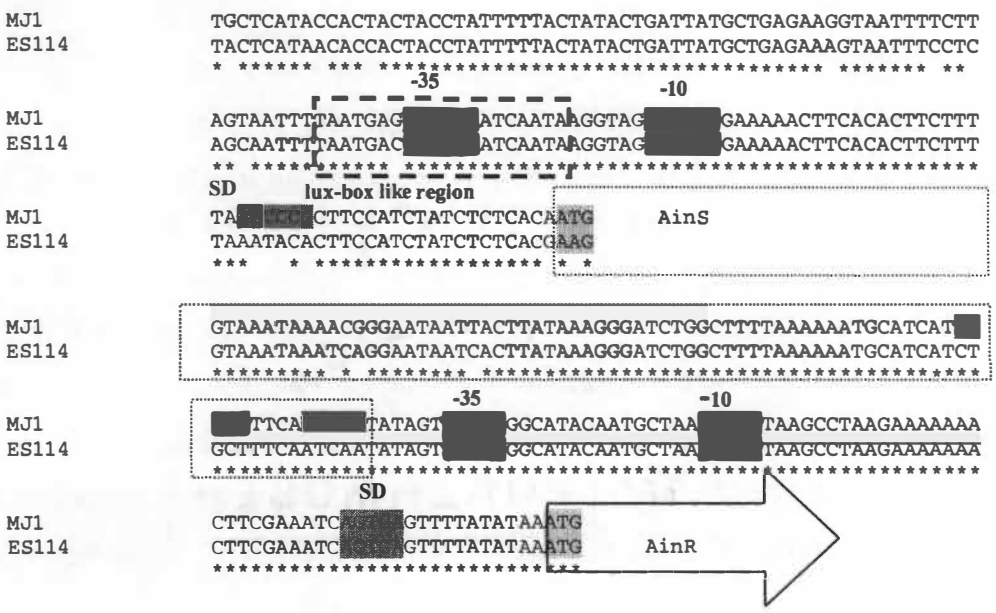

B: Comparison of the promoter region of *luxR* and *ainS*

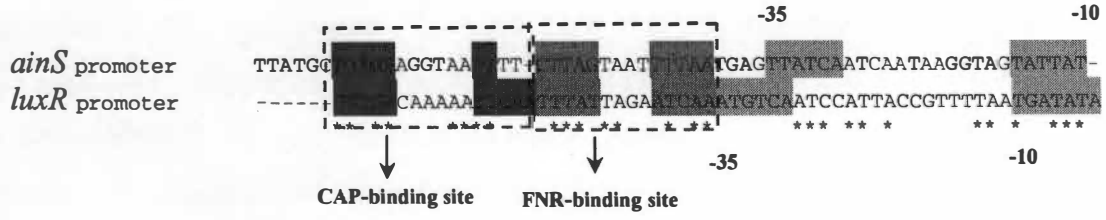

Figure 3-5. The important sequences of the *ainS* and *ainR genes*

3.2.4 Sigma-54 dependent sRNAs

Section summary: The section pursued the prediction process of the possible small quorum sensing regulatory RNAs, and the analysis of a hypothetical small regulatory RNA sequence, which is conserved in several different strains of *V. fischeri*.

Small RNAs can regulate protein synthesis at the post-transcription level or interact with proteins. Like other regulatory responses, they are involved in cell physiology and its adaptation to the environment (Argaman et al., 2001). However, these small RNAs are usually very difficult to detect by traditional experimental procedures; therefore, discovery of new small RNA molecules is often achieved by comparisons to consensus sequences of closely related species (Argaman et al., 2001; Hershberg et al., 2003).

A promoter is the DNA region where the transcriptional initiation takes place. In prokaryotes, the sequence of a promoter is recognized by different sigma factors of the RNA polymerase (Appendix A: Table A-1). Sigma-54, encoded by *rpoN*, binds to the –31 to –5 positions of DNA, although specific protein-DNA interactions have only been identified at GG and GC dinucleotides located at positions –24 and –12 (Burrows et al., 2003). Sigma-54 dependent gene activation also depends on activator proteins. For example, NtrC acts as the activator protein during the process of nitrogen assimilation, a common function of sigma-54 dependent genes (Reitzer and Schneider, 2001). In the *V. fischeri* quorum sensing circuit, LuxO, a homolog of the NtrC activator family, could act as a transcriptional activator for certain small quorum sensing regulatory RNAs when it is phosphorylated (Lenz et al., 2004). These sRNAs, together with the important chaperon protein Hfq, could degrade the mLitR, and thus influence the luminescence. This hypothesis was constructed based on the homologies between *V. fischeri* and *V. harveyi* (Miyamoto et al., 2000).

Hfq, a conserved and abundant protein, was originally discovered as a host factor for RNA phage QB replicase in *E. coli*, and plays an essential role in post-transcriptional regulation of mRNAs (Masse et al., 2003). Both the sequences and structures of the Hfq proteins are very similar to the eukaryotic Sm proteins, which are also involved in other RNA metabolic steps. The majority of the Hfq proteins are associated with ribosomes, while a minor fraction is associated with the nucleoid (Zhang, et al., 2002). As a chaperone protein of certain regulatory sRNAs, the Hfq protein can stabilize these RNAs by binding single-stranded AU-rich regions located near the stem-loop structure, which are commonly the cleavage site of the endoribonuclease RNase E (Gottesman, 2004; Wilusz and Wilusz, 2005). The Hfq protein can also stimulate the activity of poly (A) polymerase and bind the poly (A) tail at the 3' end of RNAs, leading to the stabilization of mRNAs. In addition, Hfq can bind both sRNAs and their targets to facilitate the pairing between sRNAs and their targets (Gottesman, 2004; Masse, et al., 2003; Wilusz and Wilusz, 2005). However, whether multiple Hfq hexamers are involved in bringing two RNAs together or a single hexamer recognizes both the sRNA and its target still remains unclear.

Prediction of the sigma-54 dependent quorum sensing regulation sRNAs in *V. fischeri*

The following criterions were used to identify possible sequences of sRNA involved in the quorum sensing regulation in *V. fischeri*:

1. The upstream region of the candidate sRNAs should contain a sigma-54 binding site, because the phosphorylated LuxO protein with the help of sigma-54, can activate the transcription of these RNAs (Lenz et al., 2004). Based on the consensus DNA sequence recognized by sigma-54 from 186 compiled promoters, the sequence 5' TGGCACGA/GNNNTTGCA/T 3' was used in this study (Barrios et al., 1999).

2. The small RNAs are assumed to be located in intergenetic regions and the distance between the predicted promoter and terminator is between 50 and 400 bps (Argaman et al., 2001). This method excludes the cis-encoding sRNAs.

3. Only the small RNAs with Rho-independent terminators are considered here, because the Rho-dependent terminators lack a consensus-binding site (Lewin, 1994). The sequence with a stem-loop structure followed by a U-rich unpaired region at the 3' end of the RNA can be a Rho-independent terminator (Christie et al., 1981; Farnham and Platt, 1981).

4. Other approaches can also be used to select sRNAs candidates. For example, the sRNA sequence candidate should not have a possible ribosome-binding site (RBS). An idealized RBS sequence of AGGAGG located 7-11 bases upstream of the start codon, and followed by at least 15 coding triplets was used in this criterion. (Chen et al., 2002).

A weighted matrix based on the consensus information of the sigma-54 dependent promoter sequences, was input into PATSER (Barrios et al., 1999; Hertz and Stormo, 1999) to scan the σ^{54} binding sites. A threshold was chosen to obtain possible sigma-54 binding sites with no more than four mismatches compared with the consensus sequence. In addition, all the intergenetic regions were analyzed.

Consensus standards

Based on the homology of LuxR/HapR/SmcR/OpaR, LuxO, LuxU and Hfq in *V. harveyi*, *V. cholerae*, *V. vulnificus* and *V. parahaemolyticus* (Table 3-5), the sequence of sRNA is hypothesized to be highly conserved among these species (Chen et al., 2002). The consensus sequence of the quorum sensing regulatory small RNAs (qrr) among *V. cholerae, V. parahaemolyticus, V. vulnificus, and V. harveyi*, is GGGTC ACCTA GCCAA CTGAC GTTGT TAGTG AA (Lenz et al., 2004). BLAST (www.ncbi.nih.gov/blast) was used to identify exact matches to this sequence in *V. fischeri* ES114 (Figure 3-6 (A)). The sequence is found in one of the putative sRNA sequences that satisfy all the above-mentioned sRNA identification criterions. Based on

Table 3-5. ***Vibrio fischeri*** **AinS-AinR homologous system**

Bacterium		**Identity**			
		LuxO		**LitR**	
Vibrio fischeri	***Protein*** **AN**	**LuxU** **YP_204320**	**YP_204321**	**YP_205560**	**Hfq** **YP_205706**
Vibrio harveyi		69%	41%	59%	93%
Vibrio cholerae		68%	36%	59%	90%
Vibrio vulnificus		68%	36%	59%	86%
Vibrio parahaemolyticus		69%	39%	59%	93%

A: BLAST(Altschul, et al., 1997) the qrr consensus sequence

```
>  gi|59478708|gb|CP000020.1|  Vibrio fischeri ES114 chromosome I,
 complete sequence
Length=2906179

 Features flanking this part of subject sequence:
   77 bp at 5' side: excinuclease ABC subunit B
   186 bp at 3' side: repressor protein LuxO

 Score = 63.9 bits (32),  Expect = 1e-08
 Identities = 32/32 (100%), Gaps = 0/32 (0%)
 Strand=Plus/Minus

Query  1        GGGTCACCTAGCCAACTGACGTTGTTAGTGAA  32
               ||||||||||||||||||||||||||||||||
Sbjct  1033756  GGGTCACCTAGCCAACTGACGTTGTTAGTGAA  1033725
```

B: The putative qrr1 sequence in ES114

>gi|59478708:1033799-1033667 *Vibrio fischeri* ES114 chromosome I, complete sequence Complement sequence:

-24 -12 +1

5' GCTCC ATAGGTATATT TTTAAGCCAAA

G ATTTA TGAACAATAAA CCGGGATATTGC

GG CTTC TTTTT 3'

Figure 3-6. The sequence of the putative sRNA

these criterions, this sequence is suggested to be the homologous small quorum sensing regulatory RNA (qrr) in *V. fischeri* (Figure 3-6 (B)). *V. fischeri* ES114 has only one region having the conserved sequence, in contrast to the homologous bacteria (*V. harveyi*, *V. cholerae*, *V. vulnificus* and *V. parahaemolyticus*), which has multiple copies of the sequence.

The characteristics of the putative Qrr1 in *V. fischeri*

The putative qrr1 in *V. fischeri* is located immediately upstream of *luxO* (Figure 3-7 (A)) like the qrr1s predicted in *Vibrio cholerae* and *Vibrio harveyi* (Lenz et al., 2004). The predicted RNA secondary structure of *V. fischeri* based on a minimum free energy configuration was obtained using the program RNAFOLD (Zuker and Stiegler, 1981) and is shown in Figure 3-7 (B). The alignment of the reverse complement sequence of the untranslated upstream region of mLitR and the putative sRNA is shown in Figure 3-8. The sRNA, when annealed to the 5' end of the *litR* mRNA, would block the ribosome binding site, thereby preventing its translation.

This putative sequence is conserved across several *Vibrio fischeri* strains, including ATCC7744, ES114, EB12 and ET 301. The experimental procedures for DNA sequencing are listed in Appendix B. Since the regulatory regions of the *ainSR* genes and the DNA sequence of the putative sRNA have high similarity among different *V. fischeri* strains of the categorized group 1 and group 2, they are probably not the major factors for the differences on luminescent strength.

The qrr1 of *V. cholerae* and the qrr1 of *V. harveyi*, which are also located in the upstream of the LuxOs of the species, could not be detected by Northern Blot, but the qrr4 of *V. cholerae* and *V. harveyi*, which have very similar sequences were detected successfully by Northern Blot (Lenz et al., 2004). The instability of the qrr1 sRNAs and insensitivity of the Northern Blot could be the possible reason leading to the inability to detect the sRNAs (Lenz et al., 2004). In order to improve the sensitivity of the detection method, the RT-PCR (reverse transcriptase polymerase chain reaction) technique may be

A: Location in the genome

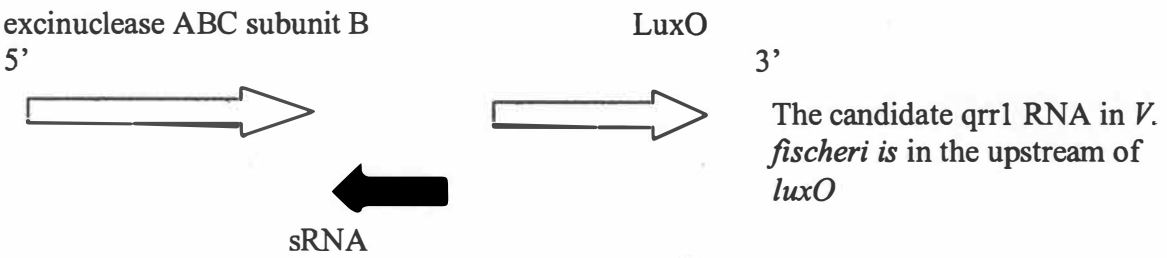

B: Secondary structure

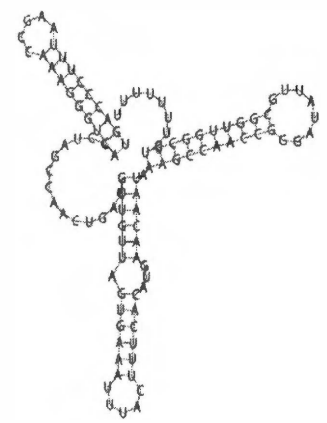

The free energy of the thermodynamic ensemble for *V. fischeri* qrr1 is -38.48 kcal/mol.

Figure 3-7. The characteristics of the qrr1 in *V. fischeri*

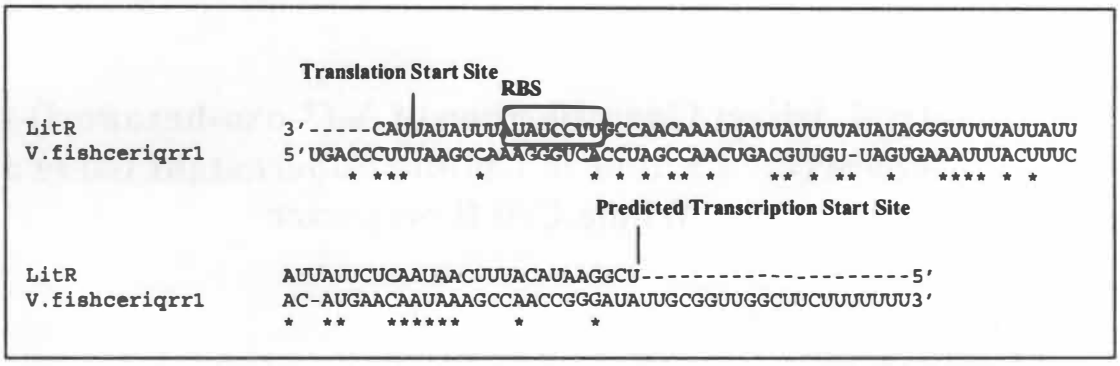

Figure 3-8. The possible sRNA binding site on mLitR

a good choice to validate the small RNA sequence. As the most sensitive technique to date for mRNA quantification, RT-PCR can also tolerate partially degraded RNA. The parallel experiment of detecting the qrr4 in V. harveyi could be used as a control to test the feasibility of the approach. Samples from different growth phases (early, middle, and late log phase) could be used to get the optimal level of this small RNA.

Chapter 4. Direct Quantification of *N*-(3-oxo-hexanoyl)-*L*-Homoserine Lactone in Culture Supernatant Using a Whole-Cell Bioreporter

4.1 Introduction

Many Gram-negative bacteria use acylated homoserine lactone molecules to sense and respond to their own cell density in a process known as quorum sensing (Fuqua et al., 1994). This process, first described for the marine bacterium *Vibrio fischeri*, has been extensively studied as a model of density-dependent gene regulation (Nealson and Hastings, 1979). The autoinducer N-(3-oxo-hexanoyl)-L-homoserine lactone (3-oxo-C6-HSL) was identified as one of the quorum signaling molecules for *V. fischeri* (Eberhard et al., 1981). This molecule is the product of the LuxI autoinducer synthase, which catalyzes the reaction between S-adenosylmethionine and acylated-acyl carrier proteins (Acyl-ACPs) to produce 3-oxo-C6-HSL (Schaefer et al., 1996; Watson et al., 2002). The LuxI gene resides in the rightward portion of the bidirectional *lux* operon (*luxICDABEG*) containing both LuxI and the genes encoding the proteins involved in bioluminescence (Kaplan and Greenberg, 1985; Shadel et al., 1990). The *luxR gene*, which encodes the 3-oxo-C6-HSL-dependent response regulator, is encoded in the left operon (Egland and Greenberg, 1999). The *lux*A and *lux*B genes encode the α and β subunits of the luciferase enzyme, which catalyzes the reaction among reduced flavomononucleotide ($FMNH_2$), fatty aldehyde and oxygen to produce oxidized FMN, aliphatic acid, water and blue green light (Eberhard et al., 1981; Lupp et al., 2003). The *lux*C, *lux*D, and *lux*E genes encode the aliphatic acid reductase that regenerates the substrate, and *lux*G encodes an $FMNH_2$ reductase (Dunlap, 1999; Eberhard et al., 1981; Lupp et al., 2003). When the level of the freely diffusible 3-oxo-C6-HSL reaches a threshold concentration, this molecule binds to the N-terminal domain of the LuxR protein and activates the C-terminal domain of the protein to bind with *lux* box (Brian

and Greenberg, 1994; Schaefer et al., 1996b). The *lux* box is a 20-bp region of DNA in the promoter region having dyad symmetry and is centered upstream of the transcriptional start site of the *luxICDABEG* operon (Devine et al., 1989; Fuqua et al., 1996; Shadel et al., 1990). The binding of the LuxR-3-oxo-C6-HSL complex to the *lux* box facilitates the binding between RNA polymerase and the promoter region of *luxICDABEG*, leading to increased transcription and the production of bioluminescence (Brian and Greenberg, 1994; Egland and Greenberg, 1999).

A second autoinducer, N-octanoyl-L-homoserine lactone (C8-HSL), has been reported to influence bioluminescence in *V. fischeri* by two mechanisms. In one mechanism, thought to be most relevant at low cell densities, C8-HSL forms a complex with LuxR protein and induces bioluminescence via interaction with the *lux* box (Callahan and Dunlap, 2000; Kuo et al., 1996; Miyamoto et al., 2000). C8-HSL may also regulate the activity of *luxR* through a pathway that is analogous to the LuxLM-LuxN-LuxU-LuxO-LuxR system in *Vibrio Harveyi* (Miyamoto et al., 2003).

A number of methods have been described to assay bacteria for HSL production or to screen environmental samples for the presence of HSL. Most of these methods use various bioreporters because of their greater sensitivity compared to conventional analytical methods (Brelles-Marino and Bedmar, 2001). Bioassays based on reporter systems such as *luxCDABE* (Boettcher and Ruby, 1995; Watson et al., 2002), green fluorescent protein (Andersen et al., 2001), violacein production (Blosser and Gray, 2000; Ravn et al., 2001), and lacZ-ß-galactosidase (Winson et al., 1998) have been used. Bioreporters can be selected to respond specifically to a particular HSL (Boettcher and Ruby, 1995), or to a broad range of homologies (Shaw et al., 1997). HSL concentrations may be quantified using a calibration curve with standards of known concentration.

Prior to detection, the HSL is often extracted from the samples using organic solvents (e.g. dichloromethane, ethyl acetate or chloroform). The extraction process improves the sensitivity of detection by removing the background effects caused by the complex sample matrix. Following extraction, high-pressure liquid chromatography

(Boettcher and Ruby, 1995) or thin-layer chromatography (Shaw et al., 1997) is frequently used to separate various homologies and to further purify the HSL from interfering impurities that may have been coextracted by the organic solvent. A recent study used solid phase extraction as an alternative means of separation and sample purification for environmental samples (Schupp et al., 2005).

In order to quantitatively study the quorum sensing mechanism in *V. fischeri*, it is necessary to evaluate the concentration of the signaling molecule present at various stages in the growth process. Here we present a simplified method of quantifying concentrations of a known HSL that may be particularly advantageous when a series of samples must be taken. A bioreporter strain with a high specificity to 3-oxo-C6-HSL was employed. A linear response between the peak biomass-normalized bioluminescence and 3-oxo-C6-HSL was found in the physiologically relevant concentration range of 3 to 390 nM. Further, a standard additions method was developed that effectively circumvented artifacts related to the sample supernatant. Although specifically applied in this case, the methodology presented here may be adaptable to other systems using bioreporters for the detection of target analytes.

4.2 Materials and methods

4.2.1 Bioreporter strain and its cultivation

The bioreporter *E. coli* RO*lux*2 (Perry, et al., 2005) was used for the quantification of 3-oxo-C6-HSL. This strain carries the *luxR* gene and bidirectional promoter (containing the *lux* box) of *Vibrio fischeri* MJ1, as well as the *luxCDABE* cassette from *Photorhabdus luminescens* cloned into the rightward operon. Because it contains no *luxI*, the strain does not produce 3-oxo-C6-HSL. RO*lux*2 was cultivated overnight at 37°C in 20 ml LB broth (10 g NaCl/L, 10 g Tryptone/L, 5 g Yeast Extract/L, adjusted to pH 7.5) containing 50 μg/ml Kanamycin. The following day, 1 ml of the overnight cell culture was inoculated into 20 ml of fresh media and grown to an optical density at 600 nm (OD_{600}) of about 0.3.

4.2.2 Bioreporter detection of HSLs

Both 3-oxo-C6 (sold as N-β-ketocaproyl-L-homoserine lactone) and C8 (available only as a D/L mixture) HSLs were purchased from Sigma Chemical Co. A 4.69 mM stock solution of 3-oxo-C6-HSL was made by dissolving it directly into 1 ml sterile distilled water. A 4.4 mM stock solution of C8-HSL was made by first dissolving 1 mg of the compound completely in 100 µl ethanol, and then adding 900 µl of sterile distilled water.

A specific amount of HSL stock solution was added to a well of 96-well, black, clear-bottom plates (COSTAR). The well was then filled with sterile distilled water to make a 100 µl solution at a concentration of 100 µM. Serial dilutions (1:1) with sterilized distilled water were made to obtain wells containing test solutions ranging in concentration from 50 µM to 3 nM. The final dilution for each concentration was made by the addition of RO*lux*2 cell culture instead of distilled water. The effect of cell supernatant on HSL measurement was determined by a similar method, except filtered (Pall, 0.2 µm) supernatant from a culture of *V. fischeri* KV240 (LuxI⁻) (Visick et al., 2000) was used to dilute the HSL stock solutions, instead of distilled water. All samples were prepared in triplicate.

4.2.3 Data reading and processing

The 96-well plates were sealed using sealing films (Perkin Elmer) and read in a Wallac 1420 Multilabel Counter. The plates were read 45 times at a nominal sampling interval of 20 minutes. At each time point, the optical density (450 nm) and bioluminescence were read sequentially, with a 10-second shaking period prior to each measurement. Triplicate measurements were taken at each time point.

4.3 Results and discussion

Figures 4-1 and 4-2 show the time dependent change in biomass-normalized bioluminescence produced by ROlux2 under different concentrations of synthetic 3-oxo-C6 and C8-HSL, respectively. The detection limit of the bioreporter to 3-oxo-C6-HSL

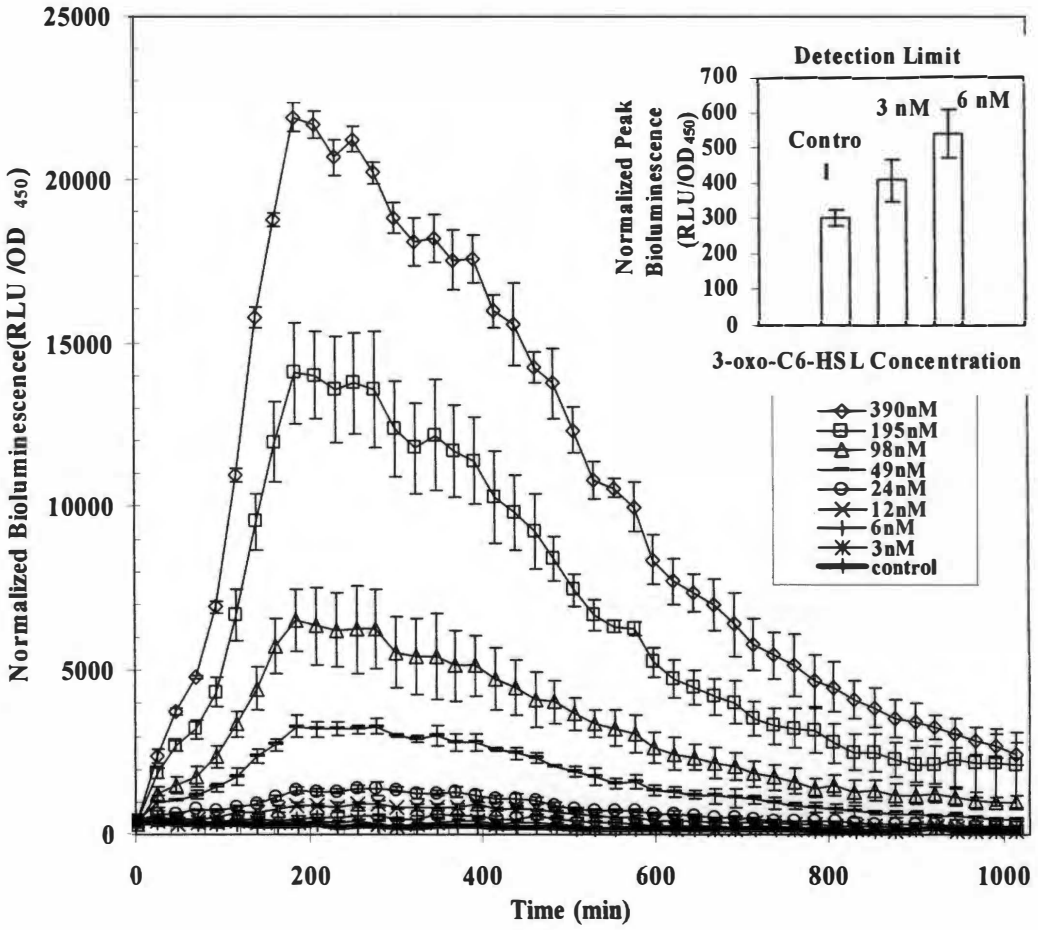

Figure 4-1. Bioreporter detection of synthetic 3-oxo-C6-HSL in fresh medium

All the data points and error bars represent the average and standard deviation of triplicates.

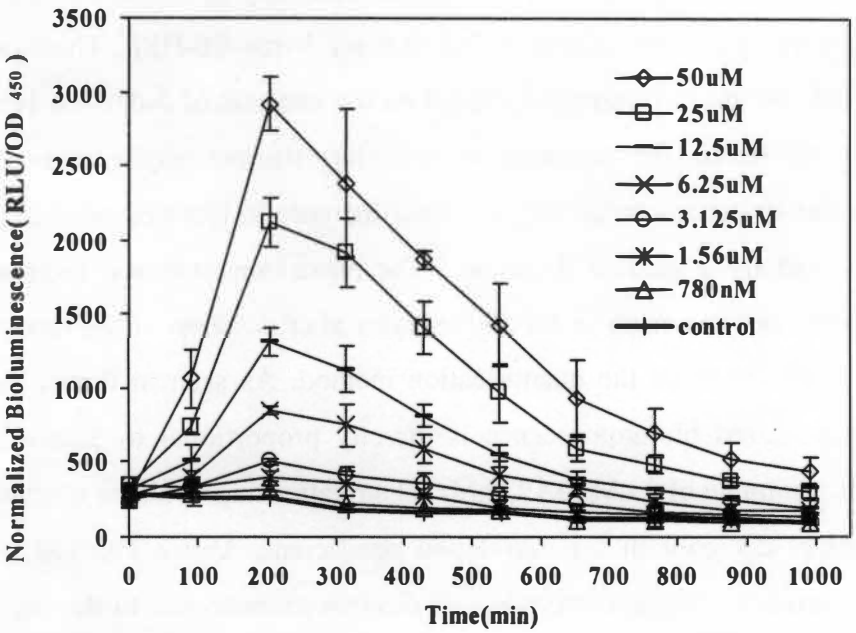

Figure 4-2. Bioreporter detection of synthetic C8-HSL in fresh medium

All the data points and error bars represent the average and standard deviation of triplicates. The detection limit is about 780 nM.

was about 3 nM (Figure 4-1, inset). By comparison, the sensitivity to C8-HSL is about 780 nM (Figure 4-2); a value 260 times greater than that for 3-oxo-C6-HSL. Therefore, the presence of C8-HSL should have minimal impact on the analysis of 3-oxo-C6-HSL. In the experimental range tested, the response curves under different concentrations of autoinducer were similar and characterized by an initial increase in biomass-normalized bioluminescence followed by a gradual decrease. The maximum observed biomass-normalized bioluminescence, occurring about 200 minutes after addition of the reporter strain, was selected as the basis of the quantification method. As seen in Figure 4-3, maximum biomass-normalized bioluminescence is directly proportional to 3-oxo-C6-HSL concentrations in the range of 3 nM to 195 nM. The relationship could be extended to 390 nM with a slight decrease in the correlation coefficient. Above 195 nM, the maximum biomass-normalized bioluminescence was directly proportional to the log of the 3-oxo-C6-HSL concentration (Figure 4-4). These relationships demonstrate that the maximum biomass-normalized bioluminescence from the reporter strain ROlux2 can be used to quantify the 3-oxo-C6-HSL in solution over a large range of concentrations.

The LuxI⁻ strain *V. fischeri* KV240 (Visick et al., 2000) was used to investigate the effect of the culture supernatant on the quantification of 3-oxo-C6-HSL by RO*lux*2. Known concentrations of synthetic 3-oxo-C6-HSL were added to supernatant samples collected from cultures of *V. fischeri* KV240 grown to different ODs and assayed with RO*lux*2. The maximum biomass-normalized bioluminescence was observed to be inversely proportional to the OD of the culture (Figure 4-5). However, for a given *V. fischeri* KV240 OD, the linear relationship between 3-oxo-C6-HSL concentration and maximum biomass-normalized bioluminescence of RO*lux*2 was still apparent.

The method of standard additions is commonly used to overcome matrix effects. Here, we exogenously added known amounts of synthetic 3-oxo-C6-HSL to supernatant culture samples, measured the resulting luminescence, and back extrapolated to zero luminescence to determine the concentration of HSL in the initial solution. To test the method, we prepared samples of known 3-oxo-C6-HSL concentration (50 and 100 nM) in supernatant from *V. fischeri* KV240 cultures. Standard additions of exogenous

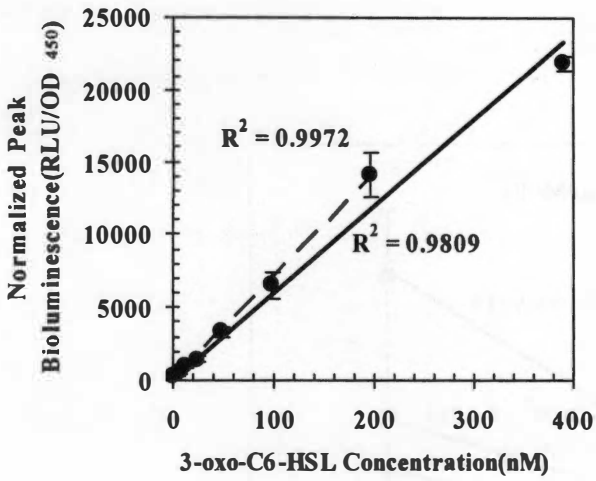

Figure 4-3. Normalized peak bioluminescence at various 3-oxo-C6-HSL concentrations (3~390nM)

The solid line is the regression line for all concentrations in the range, R^2=0.981; Dashed line represents the regression line excluding the highest concentration, R^2=0.997.

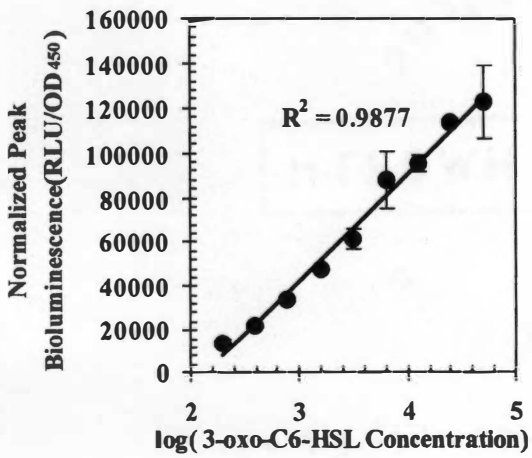

Figure 4-4. 3-oxo-C6-HSLconcentration (195nM~50uM) and normalized peak bioluminescence

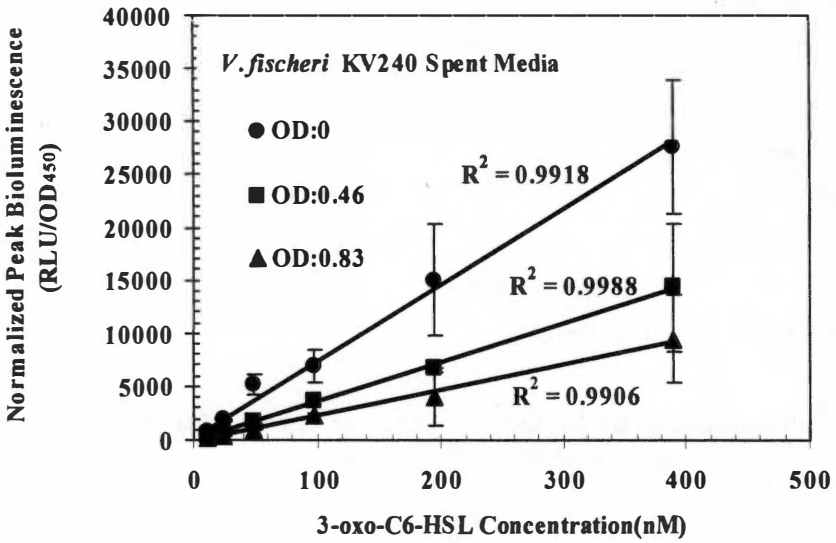

Figure 4-5. Bioreporter detection of 3-oxo-C6-HSL added to KV240 culture supernatant

synthetic 3-oxo-C6-HSL were added, corresponding to concentrations of 0, 12.5, 25, 50 and 100 nM. The bioluminescence was measured and the concentration of 3-oxo-C6-HSL in the sample without standard additions was determined by extrapolating to zero bioluminescence (Figure 4-6). The measured concentrations of 3-oxo-C6-HSL of the 50 and 100 nM samples were determined to be 44.5 and 107 nM, respectively, for OD600 0.29. Repeats of the experiment using spent KV 240 culture with different ODs yielded measured concentrations of 51 and 105, as well as 63 and 127 nM (data not shown).

Therefore, when a known concentration 3-oxo-C6-HSL (ca. 50 nM) is added to the sterile supernatant of a wild type V. fischeri growth culture, the incremental increase of the normalized peak bioluminescence can be determined, and the concentration of 3-oxo-C6-HSL in the unknown sample mixture could be directly calculated using the slope of the normalized peak bioluminescent responses between the samples with and without the addition of synthetic 3-oxo-C6-HSL. The advantages of the quantitative approach described here are that it requires neither concentration nor extraction of the signaling molecules, can be used with small-volumes samples, and accounts for variations in bioreporter performance caused by matrix effects. While the set of problems addressed here are specific to quantification of homoserine lactone molecules in spent media, the approach can be adapted to an array of bioreporter applications used for the detection of analytes in samples of varying consistency.

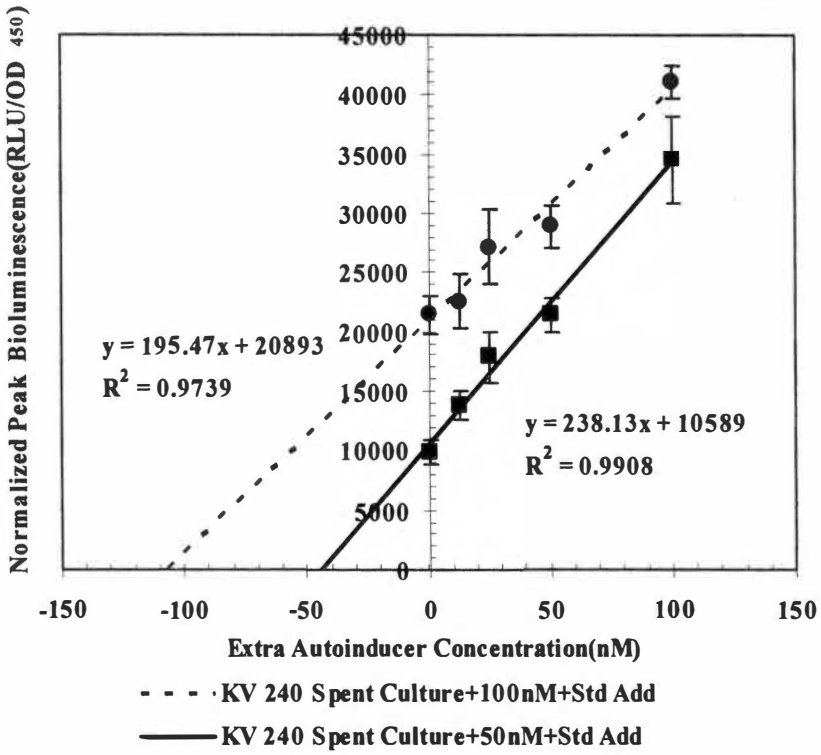

Figure 4-6. Standard additions for detection of AHL in complex supernatants

Chapter 5. Modeling and Simulation of Quorum Sensing Regulation in *Vibrio fishceri*

5.1 Introduction

Bacteria are "social" populations. In a process called quorum sensing (QS), bacteria can sense the levels of the signaling molecules excreted by either themselves or neighbor cells, and then respond by controlling the expression levels of target genes, resulting in a population dependent response (Fuqua et al., 1994). The active signaling molecules for cell-cell communication among many Gram-negative bacteria are homoserine lactones, which consist of a conserved homoserine lactone ring and a species-specific acyl side chain (Brelles-Marino and Bedmar, 2001; Parsek et al., 1999; Taga and Bassler, 2003). The LuxI/R system in the marine bioluminescent organism, *Vibrio fischeri*, has been extensively studied as a model for the QS mechanism in Gram-negative bacteria. There are dozens of known analogous quorum sensing systems in the fields of plant and animal pathogenesis, biofilm metabolism, and microbial-host interactions (Brelles-Marino and Bedmar, 2001; Collins et al., 2005). Therefore, the study of the QS regulatory system in *V. fischeri* can benefit the understanding of the other homologous systems. Mathematical models are useful for studying the dynamics of quorum sensing; however, the models published to date have only considered the induction of bioluminescence through the interaction of the LuxR-autoinducer (3-oxo-C6-HSL) complex to the *lux* box (eg. Alur et al., 2001; Belta et al., 2001; Cox et al., 2003; James et al., 1999). A comprehensive model that considers additional interactions among the regulatory elements in the circuit is expected to enrich the understanding to the typical QS regulatory network. In this study, we combined existing knowledge of QS mechanisms with dynamic measurements of the level of signaling molecules and mRNAs of the known important QS genes in growing cultures to quantitatively model the QS regulatory network in *V. fischeri*.

In this paper, the molecular biology of the regulatory process of the QS regulatory network is first reviewed. The results of growth experiments are then reported in which the expression levels of the QS genes (*luxR*, *luxI*, *ainS* and *litR)* and the concentrations of the important signaling molecules (3-oxo-C6-HSL) are measured. Next, a conceptual model of the QS system is created, which in turn is formulated into chemical reactions with assumed initial kinetic parameters. These parameters are then calibrated using the simulated annealing method to minimize the weighted least squares of the discrepancy between the simulation result and the experimental data. The behavior of the model is then compared to various experimental observations in the literature.

5.2 The quorum sensing regulatory network in *Vibrio fischeri*

5.2.1 Important components of the network

At least two different intraspecies homoserine lactones have been reported in the QS regulatory network of *V. fischeri*: 3-oxo-C6-HSL (N-(3-oxo-hexanoyl)-L-homoserine lactone, or N-β-ketocaproyl-L-homoserine lactone) and C8-HSL (N-octanoyl-L-homoserine lactone) (Fuqua et al., 1996). The QS network both controls the synthesis of these molecules and receives and processes their associated signals. The genes associated with both signaling molecules and their interactions are described below.

5.2.2 The components in the *lux* operon- 3-oxo-C6-HSL system

The *lux* operon in *V. fischeri*, composed of the *luxI*, *luxR* and *luxCDABEG* genes, plays a significant role in the QS mechanism (Kaplan and Greenberg, 1985; Dunlap, 1999). The *luxR* gene is transcribed leftward. The LuxR protein encoded by the *luxR* gene is a 250-amino-acid polypeptide consisting of two distinct domains: C-terminal and N-terminal domains (Egland and Greenberg, 1999). The N-terminal domain contains a 3-oxo-C6-HSL binding site (Ulitzur, 1998). The C-terminal domain has a helix-turn-helix motif and contains the site through which the LuxR-3-oxo-C6-HSL complex binds to the *lux* box, the regulatory region for the activation of the *luxI* gene. The *lux* box is a 20-bp sequence with dyad symmetry and is located in the regulatory region between *luxI* and *luxR* (Sitnikov et al., 1995; Devine et al., 1989). Both the *luxI* and the *luxCDABEG* genes

are in the same rightward operon (Shadel et al., 1990). The *luxI* gene encodes LuxI, a synthase that catalyzes the reaction between S-adenosylmethionine (SAM) and specific acyl-acyl carrier proteins (Acyl-ACPs) to produce the 3-oxo-C6-HSL molecules (Kaplan and Greenberg, 1985). The *lux*A and *lux*B genes are responsible for encoding the α and β subunits of the luciferase, which catalyzes the oxidation reaction of reduced favomononucleotide ($FMNH_2$) and an aldehyde to produce oxidized flavomononuckeotide (FMN), aliphatic acid, water and blue green light (Eberhard et al., 1981; Lupp et al., 2003). The *luxC*, *luxD*, and *luxE* genes encode the aliphatic acid reductase complex to recycle aldehyde for the light production reaction (Finney et al., 2002). The *luxG* gene encodes the NAD (P) H-dependent FMN reductase (Dunlap, 1999; Ruby et al., 2005).

5.2.3 The components in the *ain* genes- C8-HSL system

A second QS regulatory system in *V. fischeri* is centered on the C8-HSL signaling molecule. The *ainS gene* encodes the AinS protein, which is the second synthase of C8-HSL. AinS synthesizes C8-HSL by catalyzing the reaction between SAM and octanoyl-ACP (Hanzelka et al., 1999). The synthesized C8-HSL binds to AinR, which is encoded by the *ainR* gene, located immediately downstream of *ainS* (Gilson et al., 1995). The AinS-AinR system in *V. fischeri* is homologous to the LuxM-LuxN QS system in *Vibrio harveyi.* The C-terminal domain of the AinS protein is homologous to the C-terminal domain of the autoinducer synthase protein LuxM in *Vibrio harveyi.* Further, the AinR protein is homologous to the LuxN protein, which is similarly encoded downstream of the LuxM protein in *V. harveyi* and has sensor and regulator functions in the bioluminescence response system (Gilson et al., 1995). The LuxO protein in *V. harveyi* contains an important conserved aspartate residue, which can be either phosphorylated or dephosphorylated in response to different cell densities. Because the sequence and function of the LuxO protein in *V. fischeri* are very similar to those in *V. harveyi*, the LuxO protein in *V. fischeri* is also likely to function as a QS regulator (Freeman and Bassler, 1999b; Lin et al., 2000; Miyamoto, 2000). The open reading frames (ORF) of other known QS components in *V. harveyi*, which include LuxU, LuxR

(a homology of LitR in *V. fischeri*), and Hfq (a small QS regulatory chaperon protein), have also been found in *V. fischeri* (Ruby et al., 2005). These similarities suggest that the *ain* system and the C8-HSL regulation in *V. fischeri* are likely to be analogous to the principal QS system in *V. harveyi* (Kuo et al., 1996). In this context, AinR would act as a two-component sensor-kinase protein in *V. fischeri* (Lupp and Ruby, 2004). However, the LuxI-LuxR and 3-oxo-C6-HSL regulations work independently on LuxO (Miyamoto, 2003).

5.2.4 The cell-density dependent dynamic regulatory process

The QS regulatory process in *V. fischeri* is a complex multiple-signal circuit by which *V. fischeri* bacteria "make decisions" based on the cell-density of the population. The QS regulation of bioluminescence is dependent upon the levels of both the C8-HSL and 3-oxo-C6-HSL signaling molecules. At low cell densities, the predominant signaling molecule C8-HSL binds with the LuxR proteins; however, the LuxR-C8-HSL complex has a lower induction activity for the *lux* operon than that of the LuxR-3-oxo-C6-HSL complex, resulting in a lower level of luminescence (Callahan and Dunlap, 2000; Kuo et al., 1996). AinR functions as a kinase by autophosphorylation, and the signal is then transferred to the regulator LuxO by changing it to the phosphorylated form (LuxOp). The phosphorylated LuxO can activate the transcription of certain small regulatory RNAs, which bind to the mRNA of *litR* and facilitate its degradation, thereby preventing its translation to LitR protein. The LitR protein, encoded by the *litR* gene, is an activator of the transcription of *luxR* and *ainS* genes (Fidopiastis et al., 2002; Lupp and Ruby, 2004); therefore, the phosphorylated LuxO protein indirectly represses the production of the LuxR protein and the C8-HSL molecules, and leads to a lower level of bioluminescence. At this time, the transcription activity of the *lux* operon is "off" or at basal levels. With the increase of cell density, the AinR protein switches to phosphatase, and the dephosphorylated form of LuxO protein loses the ability of indirectly repressing the transcription of *litR* gene through certain small RNAs; therefore, the transcriptions of the *luxR* and *ainS* gene are induced. More and more 3-oxo-C6-HSL is produced and diffuses freely between cells and environment. When the concentration of the signal

molecules level reaches a threshold point, they bind to the N-terminal domain of the LuxR protein and activate the C-terminal domain to bind with *lux* box, stimulating the transcription of the *luxICDABEG* by facilitating the binding between RNA polymerase and the promoter region, and thereby enable a cascade activation of the luminescent gene's transcription, leading to the generation of intense bioluminescence (Brian and Greenberg, 1994; Egland and Greenberg, 1999; Schaefer et al., 1996b; Ulitzur, 1998). At this time, the *lux* operon is "on" or at induced levels.

5.3 Experimental methods and data analysis

Growth Experiments and Sample Collection

Stock cultures of *V. fischeri* ATCC7744 were cultivated to an OD_{600} of about 0.3. One mL of this culture was reinoculated into 2 L flasks containing 1 L filtered marine broth (DIFCO 279110). The temperature was controlled at 26±0.5°C. Cultures were shaken vigorously at 180 rpm. One 8-mL aliquot was harvested per hour until the culture arrived at a stationary stage. The aliquot was subdivided as follows: 0.5 mL was immediately stabilized by RNAprotect Bacteria Reagent (Qiagen, Valencia, CA). Two mL of the aliquot was used to measure the optical density at 600 nM with Beckman DUR 640B spectrophotometer. The remaining volume was passed through a 0.2μm Pall syringe filter, and then refrigerated for later measurement of 3-oxo-C6-HSL.

Cell number counting

A calibration curve was developed to relate cell numbers to OD measurements. Fifty microliters of 50% glutaraldehyde (0.22 μm filtered) was added to each mL of a *V. fischeri* ATCC7744 cell culture with known OD_{600}, and then the cell culture was stained by addition of 10 μL of 1% (w/v) acridine orange (0.2 μm filtered), and left in the dark for 10-15 min. After staining, 950 μL of each sample was filtered through a 0.45 μm MF-Millipore Membrane covered by a 0.22 μm Micron polycarbonate black membrane, 25 mm in diameter (Osmonics). Filters were mounted on microscope slides using type FF immersion oil and were examined by a ×100 oil immersion lens on a fluorescent microscope with a 420 nm UV filter. Cell concentration was calculated as follows:

number of cells per milliliter = (Average number of cells per square) × (Number squares per filter) × 1000 μL /950μL × Dilution factor.

Quantification of 3-oxo-C6-HSL

The bioreporter *E. coli* RO*lux*2 was used for the quantification of 3-oxo-C6-HSL. This strain carries the *luxR* gene and bidirectional promoter (containing the *lux* box) of *V. fischeri* MJ1, as well as the *luxCDABE* cassette from *Photorhabdus luminescens* cloned into the rightward operon. RO*lux*2 was cultivated overnight at 37°C in 20 ml LB broth (10 g NaCl/L, 10 g Tryptone/L, 5 g Yeast Extract/L, adjusted to pH 7.5) containing 50 μg/ml Kanamycin. The following day, 1 mL of the cell culture was inoculated into 20 mL of fresh media and grown to an OD_{600} of about 0.3. Cell-free filtrate samples (0.95 μL) collected from the ATCC7744 growth experiments were added into 6 wells of a COSTAR 96-well clear-bottom plate. Then, 5 μL of synthetic 3-oxo-C6-HSL (concentration: 2 μM) was added into one of the triplicate wells (final total volume 200 μL) to yield a concentration of 50 nM, and 5 μL dH_2O was added into another triplicate well as a control. Finally, 100 μL *E. coli* Ro*lux*2 cell culture was added into all of the wells. The resulting peak bioluminescence was measured using a Wallac1420 Counter for the wells (Figure 5-1-A). The concentration of 3-oxo-C6-HSL in samples was determined from the linear correlation between the 3-oxo-C6-HSL concentrations and the induced normalized bioluminescent peak under a common background (Yan et al., 2007). The 3-oxo-C6-HSL concentrations by cell numbers were calculated according to Eq.1.

$$Cell\ \ density\ \ normalized\ \ 3-oxo-C6-HSL\ \ concentraton(molecules/cell)$$
$$=\mathrm{X(nM)}\times\frac{10^{-9}\,mol}{nmol}\times\frac{6.02\times10^{23}\,molecules}{mol}\times\frac{10^{3}\,L}{m^{3}}\times V_{cell}(m^{3}/cell)$$

$$\mathrm{X(nM)}=\mathrm{B_{Sample}}\times\frac{50(nM)}{(\mathrm{B_{Sample+50nM}}-\mathrm{B_{Sample}})} \qquad (1)$$

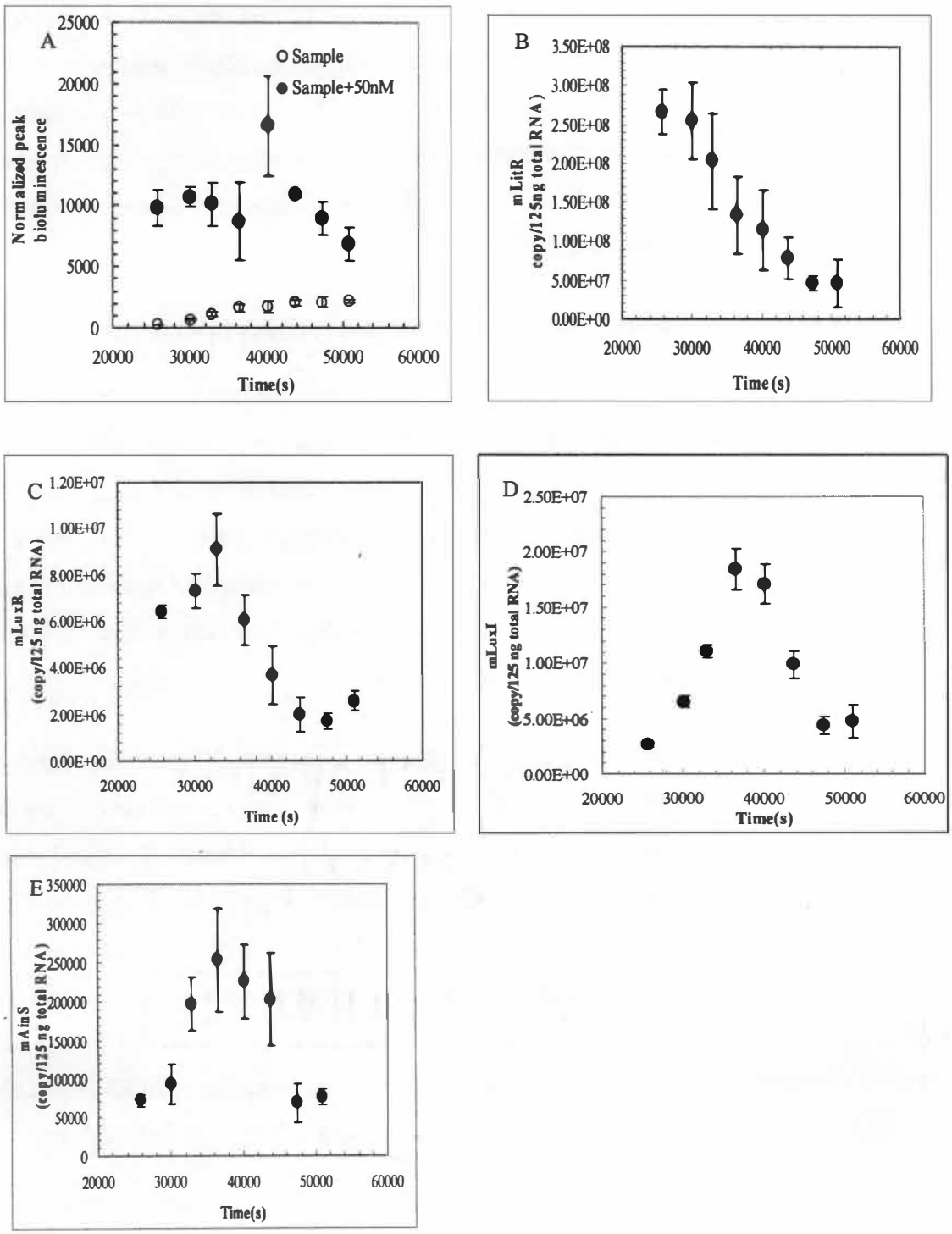

Figure 5-1. The experimental measurements of the levels of m*litR*, m*luxR*, m*luxI* m*ainS*, and 3-oxo-C6-HSL

Here, X denotes the measured 3-oxo-C6-HSL concentrations (nM) in the sample, and B_{sample} and $B_{sample+50nM}$ represent the peak bioluminescence produced by the bioreporter strain under the induction of the 3-oxo-C6-HSL in the unknown sample and the mixture of sample and 50nM synthetic 3-oxo-C6-HSL, respectively. V_{cell} represents cell volume (m^3/cell) ($1.13x10^{-19}$ m^3 was used here because the diameter of the *V. fischeri* cells is about 0.6 μm (Ruby, 1996)).

Quantitative reverse transcriptase polymerase chain reaction (qRT-PCR)

The transcription levels of *ainS*, *luxR*, *luxI* and *litR* messenger RNAs in *V. fischeri*7744 were measured by quantitative reverse transcriptase polymerase chain reaction (qRT-PCR). The mRNA samples were first stabilized by adding 0.5 mL cell suspension to 1.0 mL RNA Protect™ bacteria reagent (Qiagen, Valencia, CA), mixed by vortex for 30s and incubated at room temperature for 5 min. Samples were subsequently pelleted by centrifugation at 13,000 rpm in a bench top microfuge (Eppendorf, Westbury, NY), decanted, and frozen at -20°C prior to extraction.

RNA was extracted from culture samples using the RNeasy kit (Qiagen, Valencia, CA) with on-column DNase digestion using the RNase-free DNase set (Qiagen, Valencia, CA) and eluted in diethyl pyrocarbonate-treated deionized water (DEPC water). Total RNA in each sample was quantified using the Ribogreen RNA Quantification Kit (Molecular Probes, Eugene, OR) following the manufacturer's protocol. Sample fluorescence was measured in Versafluor cuvettes (BioRad, Hercules, CA) using a VersaFluor Fluorometer (BioRad, Hercules, CA). A standard curve was generated using known quantities of ribosomal RNA. The extracted total RNA samples were quantified relative to the standard curve and subsequently diluted in DEPC water to a final concentration of total RNA of 25 ng/μL.

For positive control RNA, all the four genes were independently cloned into pCR4.0 or pCR2.1 vectors (Invitrogen, Carlsbad, CA). Plasmids were isolated, verified by sequence, linearized by digestion using either PmeI or EcoRV, and *in vitro* transcribed from the T7 promoter using the Ribomax *in vitro* Transcription Kit

(Promega, Madison, WI) following the manufacturer's instructions. In the *in vitro* transcription reaction, only one type of mRNA of a known size was made and subsequently purified. The produced mRNA served as a stock solution and was quantified independently. The copy number of the target mRNA in the stock solution was calculated based on the molarity of the solution and the Avogadro's number: [target mRNA(g / uL)/(size in base pair × avg mol weight of bp 340 g/base pair)] × 6.02 ×10^{23} copy/mole= copy / uL].

Quantification of gene-specific mRNA in samples by qRT-PCR was performed in triplicate using the QuaniTect Probe RT-PCR kit (Qiagen, Valencia, CA) following the manufacturer's instructions using an Opticon DNA Engine (MJ Research, Waltham, MA). Each sample contained 125 ng total RNA (5 μL) per 25-μL reaction in Microseal 96 Polypropylene microplates (MJ research, Waltham, MA). The final sequences for qRTPCR primers and probes are as in Table 5-1. TaqMan-style probes (Biosearch Technologies, Novato, CA) were labeled on the 5' end with 6-carboxyfluorescein-aminohexyl amidite (6-FAM) and on the 3' end with Black Hole Quencher (BHQ). The qRT-PCR protocol was as follows: 50°C RT reaction for 30 min., 95°C RT inactivation for 15 min., followed by 41 cycles of 95°C denaturation for 15 sec, 58°C annealing/extension for 30 sec, and a fluorescence measurement, except for ainS, which used a 56°C annealing/extension temperature for 40 sec and 55 cycles. Samples were quantified based on the standard curve containing series dilutions of *in vitro* transcribed target mRNA for each experiment. The transcription levels of *litR*, *luxR*, *luxI*, and *ainS* are ploted in Figure 5-1 (B, C, D, and E). The target mRNA level by cell number was calculated according to Eq. 2, where M represents the target mRNA level (copy/125 ng total RNA), R denotes the total RNA concentration in the sample (ng total RNA /mL sample), and N stands for the cell number (cell/mL sample).

$$Target\ \ mRNA(copy/cell) = M\left(\frac{copy}{125ng\ \ total\ \ RNA}\right) \times \frac{R(ng\ \ total\ \ RNA/mL\ \ sample)}{N(cell/mL\ \ sample)} \quad (2)$$

Table 5-1. Primers and probe sequences

	qRT Primer Sequences		qRT Probe
	Left	Right	
ainS	tggctcttctttgacggttt	taaacgaattgcttcgcatatc	ataccaaatggaaaccaaatcttgaaaccga
litR	atctccagaaaagcgcaaag	ttggtgaaattcgttttcaact	tacttgatatcgcaattgaagtgttttcacaacg
luxR	ttctaactccaatcattcaccaa	ctaagcattccgaagccatt	agtatgaatagggaaactaaacccagtgataaga
luxI	gcaattccatcggaggagta	aaacgccagcatccacttac	aggtattctaagtcttcgttatcaagtgtttaag

Data analysis

For each target time point, copies were normalized by dividing each value by the sample with the highest copies. This allowed direct comparison of the trends between the mRNA levels and 3-oxo-C6-HSL.The levels of mLitR, mLuxR, mLuxI, mAinS, and the 3-oxo-C6-HSL, normalized to the maximum observed levels are plotted in Figure 5-2. The change of mLitR is very close to that of mLuxR (correlation r=0.94), while the trend of mAinS is similar to mLuxI (correlation r=0.94). The 3-ox-C6-HSL concentrations arrived at a maximum value before decreasing slightly at the end of the experiment. With the increase of the 3-oxo-C6-HSL concentrations, mLitR and mLuxR went down earlier than mAinS and mLuxI. The same trend was found in three repeated experiments.

Earlier studies of quorum sensing have focused only on increases of gene expression level with time. This is the first data to demonstrate that the expression level of various genes decrease during later stages of the quorum sensing process. Conceivably, once the quorum has been sensed through out the population, high expression levels of these genes are no longer needed and the cell diverts resources to more critical functions. The reaction mechanisms described in the literature to date cannot explain the decreases in expression level; hence in our model we have included various reactions based on speculative mechanisms that could potentially give rise to the observed expression levels. Whenever possible we have selected reactions that have certain support from bioinformatic analysis of the sequence. Experimental investigation

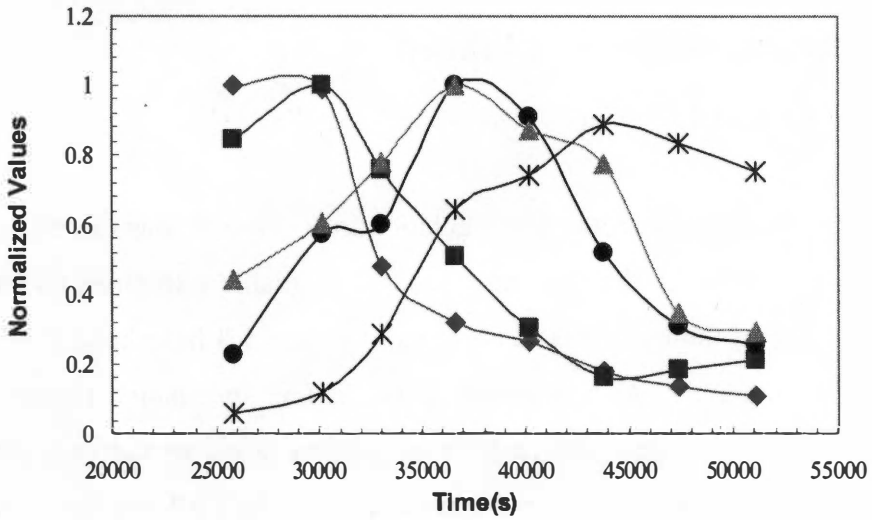

Figure 5-2. Experimental data normalized to peak values

Messenger RNA levels of *litR* (diamond), *luxR*(square), *luxI* (triangle), *ainS*(circle), and 3-oxo-C6-HSL(asterisks). All the values are normalized to the maximum value of each set of data.

of the molecular mechanisms was beyond the scope of this study.

5.4 Model formulation and calibration

5.4.1 Conceptual model

A conceptual model of the QS regulation in *V. fischeri* was developed based on the known interactions in the literature and the available experimental observations (Figure 5-3). Most of the mechanisms depicted in Figure 5-3 have been described in the quorum sensing literature. As mentioned above, a few speculative mechanisms were added to account for the decrease in gene expression levels in the later stages of the quorum sensing mechanism. The positive regulation by the LitR protein is probably not the controlling factor for the expression of *ainS*, or the time difference between the transcriptional levels of *ainS* and *litR* in the experimental data (Figure 5-2) is difficult to achieve. A 20-bp palindrome *lux* box-like region (TAATGAGTTA|TCAATCAATA) is located at the -35 promote site of the promoter region of *ainS* (Gilson et al., 1995). The conserved autoinducible sequence suggests the transcription of *ainS*, like that of *luxICDABEG*, may be controlled by the complexes formed by LuxR and autoinducers (Gilson et al., 1995). AinR was assumed to detect, either directly or indirectly, the signaling molecule 3-oxo-C6-HSL, and change the protein LuxO to the phosphorylated status in order to make the messenger *litR* level decrease. In addition, certain assumptions were made according to the similarities between the 3-oxo-C6-HSL and the C8-HSL signaling molecules, and the LuxO-centered signaling regulatory system between *V. fischeri* and *V. harveyi*. For the reason of simplification, the cells are assumed to be homogenous.

5.4.2 Mathematical model

The conceptual model was further characterized into a mathematical model containing 61 reactions with 37 species. Characteristic reaction types are summarized in

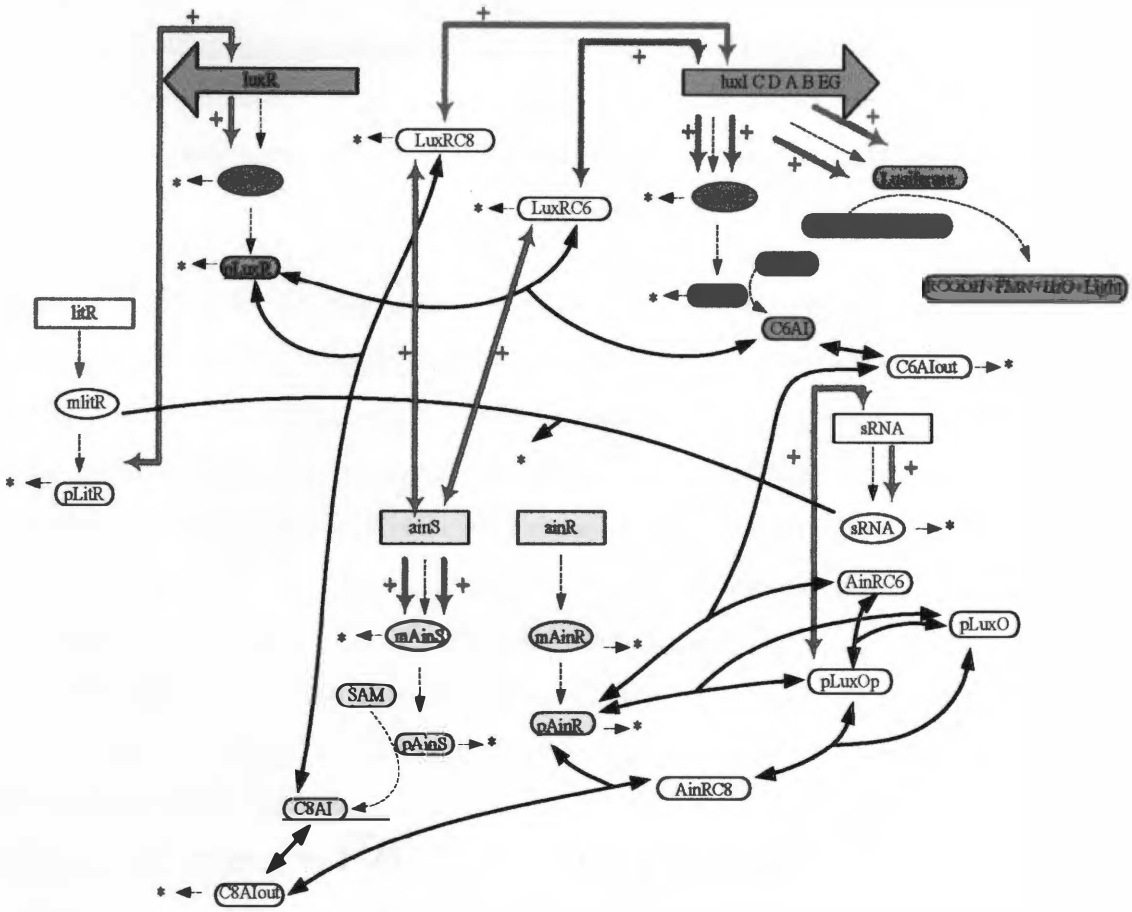

Figure 5-3. Conception model of *V. fischeri* quorum sensing regulation

The major components in the *lux* operon- 3-oxo-C6-HSL system and the components in the *ain* genes-C8-HSL system are shown in blue and yellow, respectively. The asterisks (*) denote degradation, rectangles (▭) indicate the genes, ellipses (⬭) represent mRNA species, all the other species including the proteins, signaling molecules, and the complexes formed by them are represented by flattened circles (▭). The dashed lines represent the basic reactions including transcriptions, translations, decay of the proteins, mRNAs, signaling molecules, generation of the bioluminescence, as well as the generation of the signaling molecules. The solid lines depict the signaling molecules related regulatory process, and the red solid lines represent the activated (+) or repressed (-) regulatory reactions.

Table 5-2. The definition of the parameters and the reactions are denoted in Table 5-3 and Table 5-4, respectively. The reaction rates of the species were decided according to the mass action law. Therefore, 37 ordinary differential equations (ODEs) were constructed with the independent variable (time) and the dependent variables (the concentrations of the species at that moment).

The initial concentrations of many of the species and the values of the reaction rate constants were unknown, but required to solve the system of ODEs. Considering the scale of one cell, the initial values for all basal level of genes (gbAinS, gbAinR, gbLitR, gbLuxI, gbLuxR, and gbsRNA) were set as one copy/cell. The concentrations of the messenger RNAs were assumed as 0s because their short half-life will allow steady-state levels to be achieved rapidly by solution of the ODEs. Certain proteins were set to different values in order to initiate the related reactions. All of the initial concentration values are listed in Table 5-3.The model was not very sensitive to moderate changes in the assumed values of the initial species concentrations, so no further adjustments of the initial species levels were made. The values of certain reaction rate constants were constrained according to the published data for *V. fischeri* or other prokaryotes when available, as follows. The rate constants of all the decay reactions were decided according to the half-lives. A typical mRNA half-life is assumed as 2 min (Gregory et al., 1998). Proteins are usually more stable than the mRNAs that code for them (Appendix C)(Dockery and Keener, 2000; Karlsson et al., 2006); therefore, the decay reaction constants of the proteins were initially set equal to the dilution rate as determined by cell growth rate. In this model, a half-life of 2.5 hours was used to decide the initial decay constants of proteins; in some cases, it was necessary to increase this rate in order to obtain a good fit to the data. The maximum production rate constant of the autoinducer 3-oxo-C6-HSL is 0.018 mol-homoserine lactone/s-mol LuxI (Schaefer et al., 1996a). The translation reaction constant was decided according to the burst rate (the average number of transcripts produced during a mRNA molecule's lifetime, calculated as the ratio of the

Table 5-2. The transformational rule between the conceptual and the mathematical models

Formation	Description
aA+bB ==>cC+dD	A general reaction in which reactants A and B react to give product C and D
Gene ==> Gene+mRNA	Transcription for mRNAs
mRNA ==> mRNA+Protein	Translation for proteins
D ==> *	Decay, applicable to mRNA and proteins
Gene+TF ⇔ Gene-TF ==>Gene-TF+mRNA	Gene regulation (TF can be regulatory proteins or complexes formed by reactions of proteins and the signaling molecules.)
D1 ⇔ D2	Diffusion

Table 5-3. Initial concentrations of the parameters

No.	Parameter	Description	Value (copies/cell)	No.	Parameter	Description	Value (copies/cell)
1	gbLuxR	Basal level *luxR* gene	1	19	giLuxIC6	Induced *luxI* gene by 3-oxo-HSL	0
2	gbLuxI	Basal level *luxI* gene	1	20	giLuxIC8	Induced *luxI* gene by C8-HSL	0
3	gbAinS	Basal level *ainS* gene	1	21	gisRNA	Induced sRNA gene	0
4	gbAinR	*ainR* gene	1	22	C6AIout	Environmental 3-oxo-C6-HSL concentration	10^4
5	gbLitR	*litR* gene	1	23	C8AIout	Environmental C8-HSL concentration	1500
6	gbsRNA	Basal level sRNA gene	1	24	Biomass	Cells	1
7	mLuxR	messenger RNA of LuxR	0	25	Substrate	All the nutrients for cells to grow	2500
8	mLuxI	messenger RNA of LuxI	0	26	GC	Middle products	0
9	mAinS	messenger RNA of AinS	0	27	C6AI	3-oxo-C6-HSL concentration in a cell	0
10	mAinR	messenger RNA of AinR	0	28	C8AI	C8-HSL concentration in a cell	0
11	mLitR	messenger RNA of LitR	0	29	LuxRC6	LuxR-3-oxo-C6-HSL complex	0
12	sRNA	Small messenger RNA	0	30	LuxRC8	LuxR-C8-HSL complex	0
13	pLuxR	Protein LuxR	100	31	AinRC6	The product of AinR detecting of 3-oxo-C6-HSL	0
14	pLuxI	Protein LuxI	0	32	giAinSC6	Induced ainS gene by LuxRC6	0
15	pAinS	Protein AinS	0	33	pLuxOp	Phosphorylated LuxO	1000
16	pAinR	Protein AinR	100	34	pLuxO	LuxO protein	0
17	pLitR	Protein LitR	10	35	AinRC8	The product of AinR detecting of C8-HSL	0
18	giLuxR	Induced *luxR* gene by LitR	0	36	Nil	Degradation product	0
				37	giAinSC8	Induced ainS gene by LuxRC8	0

Table 5-4. The reactions and the rates in the model

Reactions	Kinetic constant	Estimated value
Substrate+Biomass==>GC	k1	1.00E-04
GC==>Substrate+Biomass	k2	6.67E-01
GC==>2Biomass	k3	9.00E-04
C6AI==>C6AIout	k4	3.92E+08
C6AIout==>C6AI	k5	1.9132
Biomass+pLuxI==>pLuxI+Biomass+C6AIout	k6	8.30E-02
pAinR+2C6AIout==>AinRC6	k7	2.48E-06
AinRC6==>pAinR+2C6AIout	k8	4.1251
mLuxI==>mLuxI+pLuxI	k9	7.80E-01
pLuxI==>*	k10	5.76E-03
C8AI==>C8AIout	k11	3.92E+08
C8AIout==>C8AI	k12	1.91
Biomass+pAinS==>pAinS+Biomass+C8AIout	k13	10
pAinR+2C8AIout==>AinRC8	k14	9.41E-06
AinRC8==>AinR+2C8AIout	k15	1.8824
mAinS==>mAinS+pAinS	k16	8.20E-02
pAinS==>*	k17	5.76E-03
pLuxO+pAinR==>pLuxOp+pAinR	k18	35.659
pLuxO+AinRC6==>pLuxOp+AinRC6	k19	1000
pLuxOp+AinRC8==>AinRC8+pLuxO	k20	100
pLuxOp+gbsRNA==>gisRNA	k21	7.62E-02
gisRNA==>pLuxOp+gbsRNA	k22	108.83
gisRNA==>gisRNA+sRNA	k23	1
sRNA+mLitR==>*	k24	1
sRNA==>*	k25	0.00577
gbLitR==>gbLitR+mLitR	k26	0.6
mLitR==>mLitR+pLitR	k27	1.16E-01
pLitR==>*	k28	1.52E-04
2LuxRC6+gbAinS==>giAinSC6	k29	1.00E-06
giAinSC6==>2LuxRC6+gbAinS	k30	1
giAinSC6==>giAinSC6+mAinS	k31	1.20E-03
gbAinS==>gbAinS+mAinS	k32	5.00E-05
mAinS==>*	k33	5.77E-03
2pLitR+gbLuxR==>giLuxR	k34	9.21E-11
giLuxR==>giLuxR+2pLitR	k35	0.64459
giluxR==>giLuxR+mLuxR	k36	0.0338
mLuxR==>*	k37	5.77E-03

Table 5-4 continue

Reactions	Kinetic constant	Estimated value
pLuxR+C6AI==>LuxRC6	k38	1.20E+01
LuxRC6==>pLuxR+C6AI	k39	1.00E+00
LuxRC6==>*	k40	2.46E-04
pLuxR+C8AI==>LuxRC8	k41	3.00E+00
LuxRC8==>pLuxR+C8AI	k42	1
LuxRC8==>*	k43	2.46E-04
pLuxR==>*	k44	2.46E-04
mLuxR==>mLuxR+pLuxR	k45	1.16E-01
2(LuxRC6)+gbluxI==>giLuxIC6	k46	2.00E-06
giLuxIC6==>2(LuxRC6)+gbLuxI	k47	1.00E+00
giLuxIC6==>giLuxIC6+mLuxI	k48	0.038
2(LuxRC8)+gluxI==>giLuxIC8	k49	2.00E-06
giLuxIC8==>2(LuxRC8)+gbLuxI	k50	1
giLuxIC8==>giLuxIC8+mLuxI	k51	1.84E-02
mLuxI==>*	k52	3.78E-03
mLitR==>*	k53	5.78E-03
GC+pLuxI==>pLuxI+GC+C6AIout	k54	8..30E02
GC+pAinS==>pAinS+GC+C8AIout	k55	10
2LuxRC8+gbAinS==>giAinSC8	k56	2.00E-03
giAinSC8==>2LuxRC8+gbAinS	k57	1
giAinSC8==>mAinS+giAinSC8	k58	1.80E-04
C6AIout==>*	k59	6.93E-05
C8AIout==>*	k60	6.93E-05
gbLuxI==>gbLuxI+mLuxI	k61	1.00E-04

translation rate to the mRNA decay rate), which is about 5-40 in prokaryotes (Thattai and Oudenaarden, 2001). The induced (or repressed) transcription rates were assumed at least 100 times above (or below) the basal levels to reflect the "on" (or off) status except the gene *ainS*. In this case, a larger basal rate was needed to produce sufficient C8-HSL autoinducer to initiate all other quorum sensing systems. Finally, rate constants of all reversible reactions were set so that their kinetics would be fast in comparison to transcription and translation reactions.

The mathematical model was analyzed using a custom software package written in Fortran 77 (Appendix D). The double precision edition of the LSODE (Livermore Solver for Ordinary Differential Equation) was used to solve the system of ODEs (Heath, 2002). A custom full Jacobian and the backward differentiation formula (BDF) method were employed. The time step Δt is an important factor for the implicit linear multi-step process. A smaller step size yields better approximation, but also means more computation time and roundoff errors; however, larger step size could lead to no solution for the ODE system. A value of $\Delta t=100$ seconds was used for this case. In order to calibrate the model to our experimental observations, we first calibrated the relatively independent biomass growth process (reaction 1-3) based on the experimental observations through a trial and error process (supporting information). Next, the Simulated Annealing method (Corana et al., 1987; Goffe et al., 1994), a global optimization approach, was used to select the optimum kinetic constants by minimizing the differences between the model simulation outputs and the experimental data (Kirkpatrick S. et al., 1983; Vicente J.D. et al., 2003). Considering that the experimental data span several magnitudes, the error function (or cost function) was set as a weighted summation of all the errors between the experimental and model output items.

The weight factors were calculated according to Eq. 3, and the error function calculation is shown in Eq. 4. The flow chart of the model calibration program is showed in Figure 5-4.

$$Weight \quad factor_i = \frac{\sum_{j=1}^{n} \max_j}{\max_i} \tag{3}$$

$$Error = \sum_{i=1}^{n}((weight \quad factor_i \times \sum_{t=1}^{s}(experimental \quad data_{t,i} - model \quad output_{t,i}))^2 \tag{4}$$

Here, n represents the number of experimental variables to which the model is calibrated, s expresses the number of the experimental data points for each variable, and max_i represents the maximum value of variable i (i=1, 2... n). The calibrated model parameters are given in Table 5-4.

5.5 Discussion

The simulation of the cell density is shown in Figure 5-5-A. The simulations of the 3-oxo-C6-HSL concentrations (Figure 5-5-B) and the transcriptional levels of *luxI* (Figure 5-5-C), *ainS* (Figure 5-5-D), *litR* (Figure 5-5-E), *luxR* (Figure 5-5-F) per cell display a cell-density dependent QS status. The correlations (r) between the experimental data points and the model are: Biomass (0.99), 3-oxo-C6-HSL (0.98), mLuxI (0.85), mAinS (0.94), mLitR (0.90), and mLuxR (0.98). Therefore, the mathematical model describes the basic trends of the experimental data.

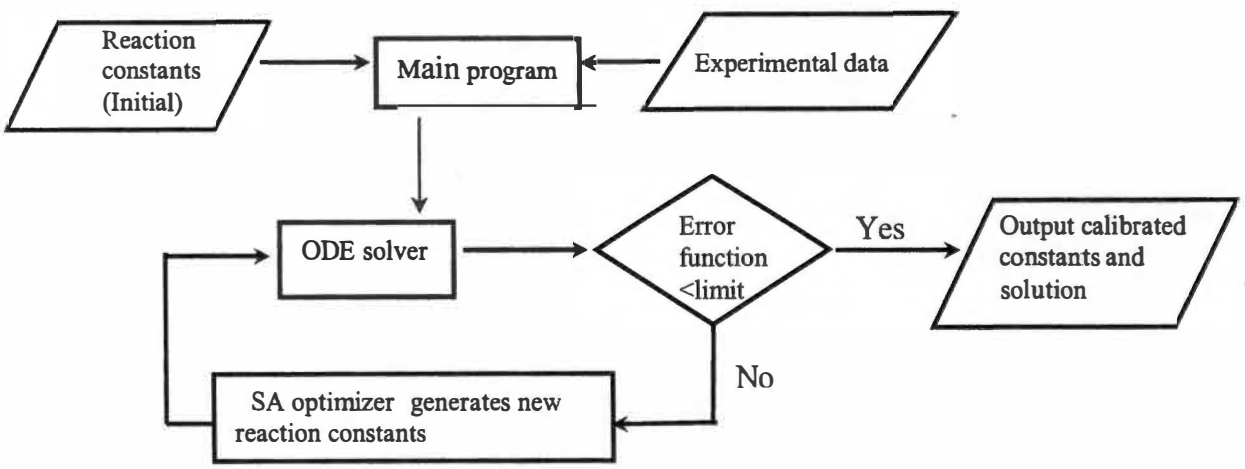

Figure 5-4. Flow chart of the model calibration program

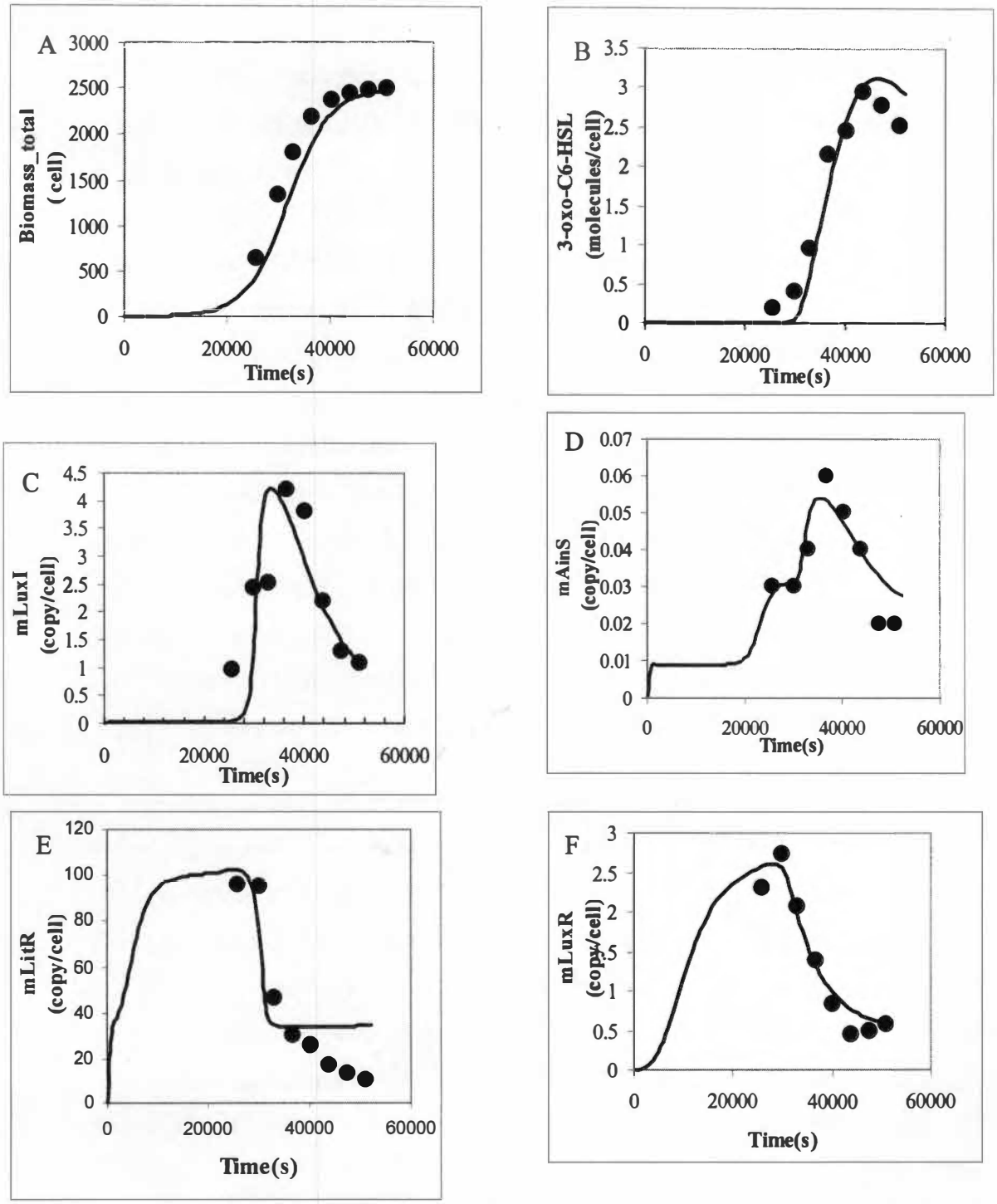

Figure 5-5. The comparison of simulation results and experimental data
The solid points represent experimental data, and the lines denote the model simulation output.

To facilitate comparison with the results of other experiments reported in the literature, we assumed that luminescence is qualitatively related to the transcriptional level of *luxI* in this study, because the *luxI* gene is located in the same operon as the luminescent genes. The regulation of the rightward *luxICDABEG* operon could be directly related to the complex of the gene products of *ainS* and *luxI*, because the LuxI$^-$ ainS$^-$ *V. fischeri* stain has no luminescence (Kuo et al., 1996). The fact that the genes *luxI* and *ainS* code for the synthases of the two known signaling molecules (3-oxo-C6-HSL and C8-HSL) can also explain why the transcripts of the *ainS* and *luxI* genes increase with the cell-density in this study. In addition, the transcriptional levels of *luxI* are more than 10 times greater than that of *ainS* in this experimental range; therefore, the 3-oxo-C6-HSL concentrations would be much larger than that of C8-HSL if both synthetic systems have similar reaction rates. Furthermore, because the luminescent induction ability of 3-oxo-C6-HSL is stronger than that of C8-HSL (Kuo et al., 1996), the induced gene complex by 3-oxo-C6-HSL was assigned a higher transcriptional rate constant than that by C8-HSL in the model, and the simulation result agrees with these preset values.

The model behaviors were also tested under different biomass growth rates to determine if the quorum sensing mechanism accurately responded to cell concentration under a number of different growth conditions. If the rate constant of the growth reaction 3 in Table 5-4 was increased to 1.2E-3 (faster growth rate) or decreased to 6E-4 (slower growth rate) from 9E-4 (original growth rate), the model prediction in Figure 5-6 suggests the slower growth process takes longer time (about 40000 seconds) to reach a threshold value of mLuxI (0.5 copy/cell) than the faster growth processes. However, in each case, the critical mLuxI level was reached after the initial cell density had increased by a factor of 500 to 1000 from its initial value. The lower critical cell densities were associated with slower growth. Therefore, it appears that the number of cell necessary to achieve a quorum may be dependent on growth rate. Nevertheless, the model of the quorum sensing system does demonstrate good sensitivity to cell biomass, as would be expected.

Other researchers have used a variety of mutant *V. fischeri* strains to test different

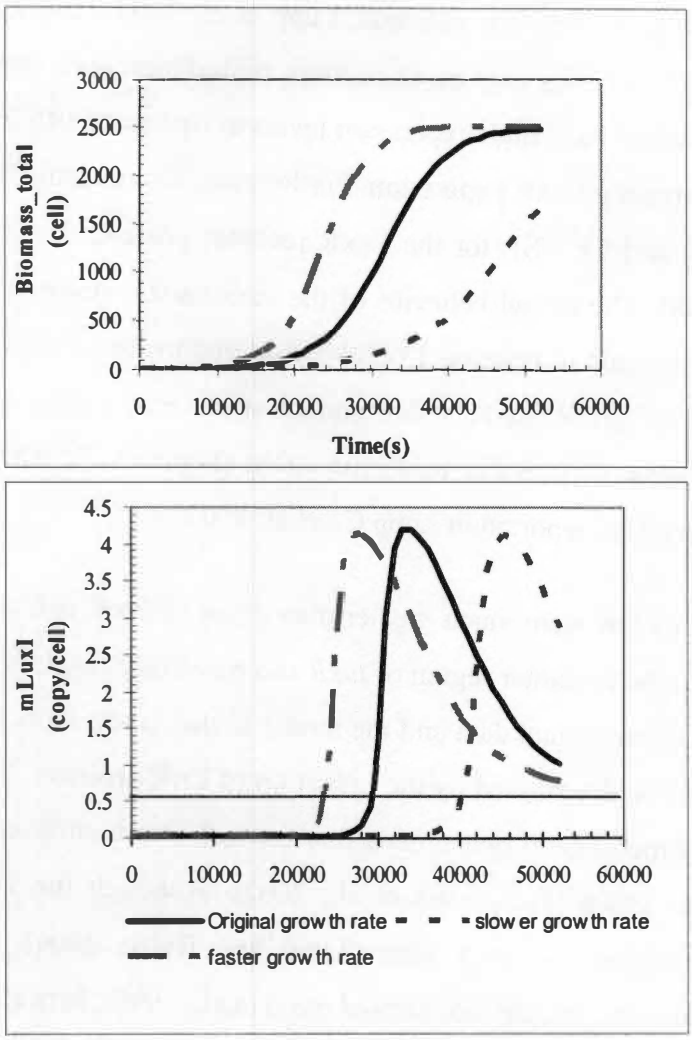

Growth rate	Reach the threshold value (0.5 copy/cell of mLuxI)	
	Time(s)	Biomass(cell)
Slower	40000	500
Original	30000	800
Faster	24000	1000

Figure 5-6. Model prediction the biomass and luminescence under different growth rates

hypotheses about the quorum sensing system. For example, Lupp et al, 2003, reported that a strain deficient in both LuxO and *ainS* may produce more bioluminescence than the wild type strain. Such a strain would have high expression levels of *litR* since sRNAs would not be activated, thereby activating LuxR expression. Furthermore, there would be no competition between 3-oxo-C6 and C8 HSL for the LuxR receptor protein, thereby allowing stronger induction of LuxI. The model behavior of the ainS LuxO- strain was simulated by setting both the rate constant of reaction 13 (Table 5-4) and the initial LuxO protein level (Table 5-3) to 0. The model predicts this mutant strain may produce a higher level of mLuxI (or luminescence) than the wild type strain (Figure 5-7), which agrees with the experimental observation reported in Lupp C., et al, 2003.

The transcriptional levels of *litR* were much greater than those of *luxR*, *luxI* and *ainS*. The LitR protein can bind to the promoter region of *luxR* and positively regulate its transcriptional activity. Both the experimental data and the model in this study show the transcriptional level of *luxR* might be determined by the induction of LitR proteins. This hypothesis also agrees with the experimental phenomena that the *litR*$^-$ strain emits only 20% as much light as its parent strain (Fidopiastis et al., 2002). Although the LitR proteins may also positively regulate the *ainS* gene (Lupp and Ruby, 2004), the bioluminescence of the *ainS*$^-$ strain was actually accelerated (Kuo et al., 1996); hence, the major reason for the decrease of the luminescence for the LitR$^-$ strain could be the decrease of the LuxR protein instead of the increase of the AinS protein.

The model also predicts the possible trends of the AinR complexes, the LuxO protein and the small regulatory RNAs under different cell densities according to the available knowledge (Figure 5-8). At very low cell densities and low signaling molecular concentrations, most of the protein AinR is autophosphorylated and the signal can be transferred to the LuxO protein. Therefore, the LuxOp concentration and certain small regulatory RNAs are relatively high. With the increase of cell density, the protein AinR would detect the signaling C8-HSL molecule and be changed to a phosphatase, leading to the dephosphorylation of LuxOp to LuxO and a decrease in the concentration of small regulatory RNAs. If the cell density continues to increase, more AinR proteins would in

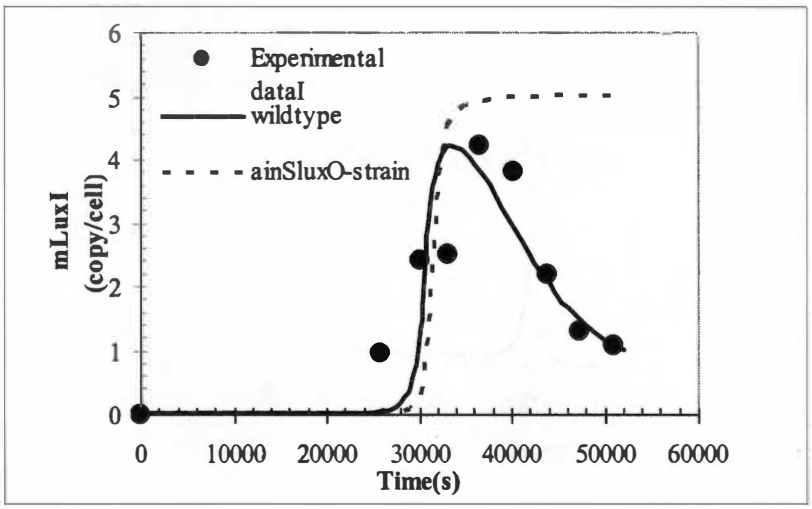

Figure 5-7. The comparison of the experimental observations in Lupp C., et al, 2003, and the model simulation

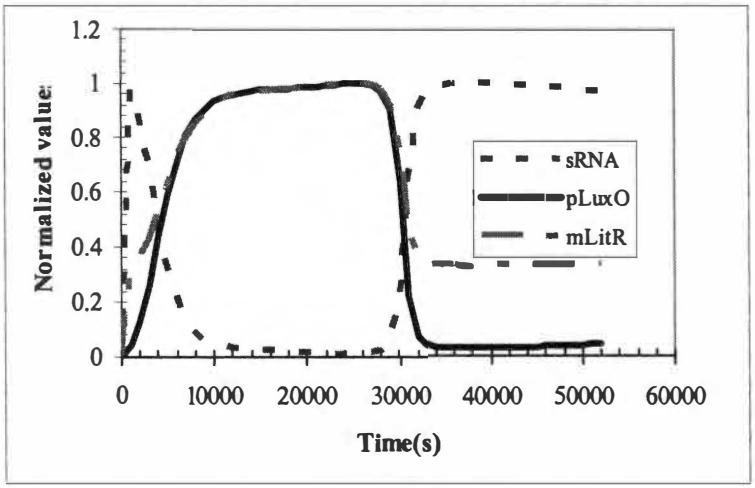

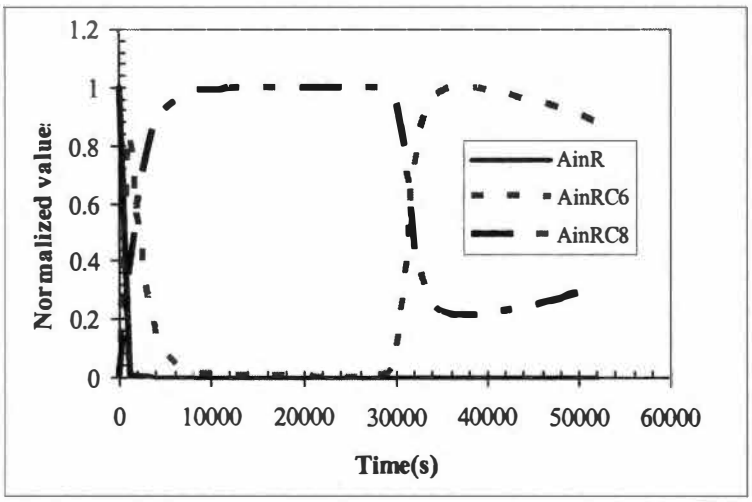

Figure 5-8. Model prediction of the levels of the LuxO protein, small regulatory RNA and the AinR complex.

All the values are normalized based on the maximum values of each species during the period.

the phosphatases form and more LuxO proteins would be in the inactivated status; hence mLitR would keep increasing, which is different from our experimental data in which the transcription of *litR* was turned off when cell density is relatively high (Figure 5-2). One possible explanation is that AinR could also detect, either directly or indirectly, the signaling molecule 3-oxo-C6-HSL, and change the protein LuxO to the phosphorylated status; as a result, the messenger LitR level would decrease.

This study used a continuous deterministic method to model the QS regulatory network in *V. fischeri*; therefore, the discrete nature of molecular components and the stochastic character of their interactions were not considered. While this model reproduces many of the experimental behaviors observed by us and other researchers, many of the molecular mechanism that we have postulated have not been confirmed experimentally. Therefore, the QS regulatory network in *V fischeri* remains to be a system requiring further experimental investigation. In addition, the calibrated rate constants should not be considered to be the actual rate constants of the reactions. However, the combination of the experimental data and modeling techniques demonstrates that the current conceptual model explains most experimental observations to date. It also provides a tool to systematically make predictions of system behaviors to serve as the basis for future studies.

5.6 Supporting information

Approximation of the growth curve ($[Biomass]_{total}$ ~ time)

$$\text{Substrate} + \text{Biomass} \underset{k2}{\overset{k1}{\rightleftharpoons}} GC \xrightarrow{k3} 2\text{Biomass}$$

$$\frac{d[GC]}{dt} = k_1[Biomass][Substrate] - (k_2 + k_3)[GC] \quad \text{(S1)}$$

$$\frac{d[Biomass]}{dt} = -k_1[Substrate][Biomass] + k_2[GC] + 2k_3[GC] \quad \text{(S2)}$$

$$\frac{d[Biomass]_{total}}{dt} = \frac{d([Biomass] + [GC])}{dt} = k_3[GC] \quad \text{(S3)}$$

Obtain [GC]

If k2>>k3, the quasi-steady approximation can be applied to the middle product GC.

$$\frac{d[GC]}{dt} = k_1[Substrate][Biomass] - (k_2 + k_3)[GC] \approx 0 \Rightarrow [Biomass] = \frac{k_2[GC]}{k_1[Substrate]} \quad \text{(S4)}$$

Because different formats of biomass are conserved with the amount of $[Biomass]_{total}$ at time t in the close system:

$$[GC] = [Biomass]_{total} - [Biomass] = [Biomass]_{total} - \frac{k_2[GC]}{k_1[Substrate]} \quad \text{(S5)}$$

[GC] can be solved from Eq.S5

$$[GC] = \frac{[Biomass]_{total}}{1 + \frac{1}{\frac{k_1}{k_2}[Substrate]}} = [Biomass]_{total}\left(1 - \frac{1}{1 + \frac{k_1}{k_2}[Substrate]}\right) \quad \text{(S6)}$$

Obtain [Substrate]

Because different formats of Substrate are equal to the initial amount of substrate provided by the system, and one copy of consumed substrate was assumed to be transformed to one copy of biomass.

$$[Substrate] = [Substrate]_{t=0} - ([Biomass]_{total} - [Biomass]_{t=0}) \quad \text{(S7)}$$

We can obtain the expression of d[Biomass]/dt by substituting Eq. S6 and Eq. S7 into Eq.S3

$$\frac{d[Biomass]_{total}}{dt} = k_3[Biomass]_{total}\left(1 - \frac{1}{1 + \frac{k_1}{k_2}\{[Substrate]_{t=0} - ([Biomass]_{total} - [Biomass]_{t=0})\}}\right)$$

$$= G_1[Biomass]_{total}\left(1 - \frac{1}{1 + G_2\{[Substrate]_{t=0} - ([Biomass]_{total} - [Biomass]_{t=0})\}}\right) \quad \text{(S8)}$$

Therefore, changing the parameters k1/k2, and k3 can approximate the growth process according to the experimental data.

Chapter 6. Conclusion

This study combines techniques from the fields of system biology, bioinformatics, molecular microbiology, and engineering to investigate the quorum sensing signaling regulatory network in the bacteria *Vibrio fischeri*. The conclusions are as follows.

Through consensus sequence analysis among different strains of *Vibrio fischeri* and cross-reference to homologous bacteria, we predict: 1) Various *V. fischeri* strains can be categorized as belonging to one of two groups, which have different luminescent characteristics under experimental conditions, based on the similarities in the sequence of the regulatory region between the coding sequences of LuxI and LuxR. The characterization of the regulatory regions is consistent with the Partial coDing Sequence (PDS) of the LuxI and LuxR proteins, indicating that the differences in phenotype may be related to the types of the regulatory regions. 2) A possible autonegative regulatory site is located in the *litR* promoter region, and the FNR-CAP binding site could be part of the LitR binding site in *V. fischeri*. 3) The LitR protein could positively regulate the transcriptions of the *ainS gene* based on the similarities between the promoter site of gene *ainS* and gene *luxR*. 4) A hypothetical small regulatory RNA sequence was predicted, which is conserved in several different strains of *V. fischeri*.

Many factors can influence the strength of luminescence, an important energy-consuming process. In order to monitor the levels of 3-oxo-C6-HSL signaling molecules during the growth process, a novel approach was developed, which is based on the apparent linear relationship between 3-oxo-C6-HSL concentration and maximum biomass-normalized bioluminescence of a luminescent bioreporter strain *E. coli* RO*lux*2 under the same environmental condition.

This research also combines experimental data and modeling techniques to demonstrate and explain the experimental observations to date. This method provides a tool to systematically make predictions of system behaviors to serve as the basis for

future studies. The study of the QS regulatory system in *V. fischeri* may also benefit the understanding of the other homologous systems, and provide hints for the communication among different species of bacteria, such as biofilm system. Because of the benefits of selectivity, sensitivity, and low cost of using bioluminescence-based biosensors constructed from genetically engineered microorganisms, we certainly can expect a promising future for the study of the bacterium, *Vibrio fischeri*, in the fields related to the protection of the surrounding environment and people's health.

Bibliography

1. Aelion C.M. and Davis H.T. (2007). Use of a general toxicity test to predict heavy metal concentrations in residential soils. *Chemosphere*, 67, P1043-1049

2. Andersen J.B., Heydorn A., Hentzer M., Eberl L., Geisenberger O., Christensen B.B., Molin S., and Givskov M. (2001). gfp-Based N-Acyl Homoserine-Lactone Sensor Systems for detection of Bacterial Communication. *Applied and Environmenatal Microbiology*, 67(2), P 575-585

3. Alur R., Belta C., Ivancic F., Kumar V., Mintz M., Pappas G.J., Rubin H., and Schug J. (2001). Hybrid Modeling and Simulation of Biomolecular Networks Proceedings of the 4th International Workshop on Hybrid Systems: Computation and Control, P 19 - 32

4. Altschul, S. F., Madden T.L., Schäffer A.A., Zhang J., Zhang Z., Miller W., and Lipman D.J. (1997). Gapped BLAST and PSI-BLAST: a new generation of protein database search programs. *Nucleic Acids Res.* 25(17), P 3389-3402

5. Argaman L., Hershberg R., Vogel J., Bejerano G., Wagner E.G., Margalit H., Altuvia S.(2001). Novel small RNA-encoding genes in the intergenic regions of *Escherichia coli. Curr Biol.* 11(12), P 941-950

6. Barrios H., Valderrama B. and Morett E. (1999). Compilation and analysis of sigma(54)-dependent promoter sequences. *Nucleic Acids Research,* 27(22), P 4305-4313

7. Bassler B.L., Wright M., Showalter R.E., and Silverman M.R. (1993). Intercellular signaling in *Vibrio harveyi*, sequence and function ofgenes regulating expression of luminescence. *Mol. Microbiol.*, 9(4), P 773-786

8. Bassler, B.L., Greenberg, E.P., Stevens, A.M. (1997). Cross-species induction of luminescence in the quorum sensing bacteria *Vibrio harveyi. J. Bacteriol.* 179(12), P 4043– 4045

9. Bassler B.L. (2002). Small Talk: Cell-to-Cell Communication in Bacteria. *Cell,* 109(4), P 421–424

10. Baxevanis A.D. and Ouellette B.F.F (2005). Bioinformatics A practical guide to the analysis of genes and proteins. Third edition. A John Wiley & Sons, Inc., P 366-388

11. Belta C., Schug J., Dang T., Kumar V., Pappas G.J., Rubin H. (2001). Stability and reachability analysis of a hybrid model of luminescence in the marine bacterium *Vibrio fischeri.* Proceedings of the 40th IEEE Conference on Decision and Control Orlando, Florida USA

12. Blosser R.S. and Gray K.M. (2000). Extraction of violacein from Chromobacterium violaceum provides a new quantitative bioassay for N-acyl homoserine lactone autoinducers. *J. Microbiol. Methods,* 40(1), P 47-55

13. Boettcher, K.J., and Ruby E.G. (1990). Depressed light emission by symbiotic *Vibrio fischeri* of the sepiolid squid *Euprymna scolopes. J. Bacteriol.*, 172(7), P 3701–3706

14. Boettcher K.J., and Ruby E.G. (1995). Detection and quantification of *Vibrio fischeri* autoinducer from symbiotic squid light organs. *J. Bacteriol.*, 177(4), P 1053-1058

15. Bonnie L Bassler (1999). How bacteria talk to each other: regulation of gene expression by quorum sensing. *Current Opinion in Microbiology*, 2(6), P 582-587

16. Brelles-Marino G., Bedmar E.J. (2001). Detection, purification and characterisation of quorum-sensing signal molecules in plant-associated bacteria. *J. Biotechnol.,* 91(2-3), P 197-209

17. Brian L.H. and Greenberg E.P. (1994). Evidence that the N-terminal region of the *Vibrio fischeri* LuxR Protein constitutes an autoinducer-binding domain. *J. Bacteriol.*, 177(3), P 815-817

18. Burrows P.C., Severinov K., Ishihama A., Buck M. and Wigneshweraraj S.R. (2003). Mapping σ54-RNA Polymerase Interactions at the –24 Consensus Promoter Element. *J. Biol. Chem.*, 278(32), P 29728-29743

19. Callahan S.M. and Dunlap P.V. (2000). LuxR- and acyl-homoserine-lactone-controlled non-*lux* genes define a quorum-sensing regulon in *Vibrio fischeri. J. Bacteriol.*, 182(10), P 2811–2822

20. Cao, J.G., and Meighen, E. A. (1989). Purification and structural identification of an autoinducer for the luminescence system of *Vibrio harveyi. J. Biol. Chem.,* 264(36), P 21670-21676

21. Carl Branden and John Tooze (1999). Introduction to protein structure. 2nd edition. Garland Publishing, Inc. New York.

22. Chatterjee J., Miyamoto C.M., Meighen E.A. (1996). Autoregulation of luxR: the *Vibrio harveyi* lux-operon activator functions as a repressor. *Mol. Microbiol.,* 20(2), P 415-425

23. Chen F., Chen C.C., Riadi L., and Ju L.K. (2004). Modeling rhl Quorum-Sensing Regulation on Rhamnolipid Production by Pseudomonas aeruginosa. *Biotechnol. Prog.* 20, P 1325-1331

24. Chen S., Lesnik E.A., Hall T.A., Sampath R., Griffey R.H., Ecker D.J., Blyn L.B. (2002). A bioinformatics based approach to discover small RNA genes in the *Escherichia coli* genome. *BioSystems,* 65(2-3), P 157-177

25. Chen, X., Schauder, S., Potier, N., Dorsselaer, A.V., Pelczer, I., Bassler, B.L., Hughson, F.M. (2002). Structural identification of a bacterial quorum-sensing signal containing boron. *Nature,* 415(6871), P 545– 549

26. Chenna R., Sugawara, H., Koike, T., Lopez R., Gibson T.J., Higgins D.G., Thompson, J.D. (2003). Multiple sequence alignment with the clustal series of programs. *Nucleic Acids Res.,* 31(13), P 3497-3500

27. Choi S.H. and Greenberg E.P. (1992). Genetic dissection of DNA binding and luminescence gene activation by the *Vibrio fischeri* LuxR protein. *J. Bacteriol.*, 174(12), P 4064-4069

28. Christie G.E., Farnham P.J., Platt T.(1981). Synthetic sites for transcription termination and a functional comparison with tryptophan operon termination sites in vitro. *PNAS,* 78(7), P4180-4184

29. Collins C.H., Arnold F.H., and Leadbetter J.R. (2005). Directed evolution of *Vibrio fischeri* LuxR for increased sensitivity to a broad spectrum of acyl-homoserine lactones. *Molecular Microbiology*, 55(3), P 712-723

30. Corana A., Marchesi M., Martini C., and Ridella S. (1987). Minimizing multimodal functions fo continuous variables with the "simulated annealing" algorithm. ACM Transactions on Mathematical Software, 13(3), P 262-280

31. Cox C.D., Peterson G.D., Allen M., Lancaster J.M., McCollum J.M., Austin D., Yan L., Sayler G.S. and Simpson M.L. (2003). Analysis of noise in quorum sensing. Omics: *A Journal of Integrative Biology,* 7(3), P 317-334

32. Dassow G.V., Meir E., Munro E.M. and Odell G.M. (2000). The segment polarity network is a robust development module. Nature, 406(13), P188-192

33. Devine J.H., Countryman C., and Baldwin T.O. (1988). Nucleotide sequence of the *lux*R and *luxI* genes and structure of the primary regulatory region of the *lux* regulon of *Vibrio fischeri* ATCC 7744. *Biochemistry*, 27, 837-842

34. Devine J.H., Shadel G.S., Baldwin T.O. (1989). Identification of the operator of the *lux* regulon from the *Vibrio fischeri* strain ATCC 7744. *Proc Natl Acad Sci U S A*, 86(15), P 5688-5692

35. Dockery J.D. and Keener J.P. (2000). A mathematical model for quorum sensing in *Pseudomonas aeruginosa. Bulletin of Mathematical Biology*. P 1-22

36. Dove J.E., Yasukawa K., Tinsley C.R., Nassif X. (2003). Production of the signalling molecule, autoinducer-2, by *Neisseria meningitidis*: lack of evidence for a concerted transcriptional response. *Microbiol.*, 149(7), P 1859-1869

37. Dunlap P.V. and Greenberg E.P. (1985). Control of *Vibrio fischeri* luminescence gene expression in *Escherichia coli* by cyclic AMP and cyclic AMP receptor protein. *J. Bacteriol.*, 164 (1), P 45–50

38. Dunlap P.V. and Greenberg E. P. (1988). Control of *Vibrio fischeri lux* gene transcription by a cyclic AMP receptor protein-LuxR protein regulatory circuit. *J. Bacteriol.*, 170(9), P 4040-4046

39. Dunlap P.V. and Kuo A. (1992). Cell density-dependent modulation of the *Vibrio fischeri* luminescence system in the absence of autoinducer and LuxR protein. *J. Bacteriol.*, 174(8), P 2440-2448

40. Dunlap P.V. (1999). Quorum regulation of luminescence in *Vibrio fischeri. J. Mol. Microbiol. Biotechnol.*, 1(1), P 5-12

41. Eberhard. A., Burlingame A.L., Eberhard, C., Kenyon G.L., Nealson K.H. and Oppenheimer N.J. (1981). Structural identification of autoinducer of *Photobacterium fischeri* luciferase. *Biochemistry,* 20(9), P 2444-2449

42. Egland K.A. and Greenberg E.P. (1999). Quorum sensing in *Vibrio fischeri*: elements of the LuxI promoter. *Mol. Microbiol.*, 31(4), P 1197-1204

43. Egland K. A. and Greenberg E. P. (2001). Quorum sensing in *Vibrio fischeri*: Analysis of the LuxR DNA Binding Region by Alanine-Scanning Mutagenesis. *J. Biotechnol.*, 183(1), P 382-386

44. Engebrecht J., Silverman M. (1987). Nucleotide sequence of the regulatory locus controlling expression of bacterial genes for bioluminescence. *Nucleic Acids Res.*, 15(24), P 10455-10467

45. Farnham P. J., Platt T. (1981). Rho-independent termination: dyad symmetry in DNA causes RNA polymerase to pause during transcription in vitro. *Nucleic Acids Res.*, 9(3), P 563-577

46. Federle M.J. and Bassler B.L. (2003). Interspecies communication in bacteria. *J. Clin Invest.*, 112 (9), P 1291–1299

47. Fidopiastis P.M., Miyamoto C. M., Jobling M.G., Meighen E. A. and Ruby E. G. (2002). LitR, a new transcriptional activator in Vibrio fischeri, regulates luminescence and symbiotic light organ colonization. *Mol. Microbiol.*, 45(1), P 131-143

48. Finney A.H., Blick R.J., Murakami K., Ishihama A., Stevens A.M. (2002). Role of the C-terminal domain of the alpha subunit of RNA polymerase in LuxR-dependent transcriptional activation of the *lux* operon during quorum sensing. *J. Bacteriol.,* 184(16), P 4520-4528

49. Freeman J. A. and Bassler B. L. (1999a). Sequence and function of LuxU: a two-component phosphorelay protein that regulates quorum sensing in *Vibrio harveyi. J. Bacteriol.*, 181(3), P 899-906

50. Freeman J. A. and Bassler B. L. (1999b). A genetic analysis of the function of LuxO, a two component response regulator involved in quorum sensing in *Vibrio harveyi. Mol. Micro.,* 31(2), P 665-677

51. Freeman J. A., Lilley, B. N. and Bassler B. L. (2000). A genetic analysis of the function of the LuxN: a two-component hybrid sensor kinase that regulates quorum sensing in *Vibrio harveyi. Mol. Micro.*, 35(1), P 139-149

52. Fuqua C. and Greenberg E.P. (1998). Self perception in bacteria: quorum sensing with acylated homoserine lactones. *Current Opinion in Microbiology*, 1(2), P 183-189

53. Fuqua, W.C., Winans, S.C.and Greenberg, E.P. (1994). Quorum sensing in bacteria: the LuxR-LuxI Family of cell density-responsive transcriptional regulators. *J. Bacteriol.*, 176(2), P 269-275

54. Fuqua C., Weans S.C. and Greenberg E.P. (1996). Census and consensus in bacterial ecosystems: the LuxR-LuxI family of quorum sensing transcription regulators. *Annu. Rev. Microbiol.,* 1996(50), P 727-751

55. Fuqua C., Parsek M.R., Greenberg E.P. (2001). Regulation of gene expression by cell-to-cell communication: acyl-homoserine lactone quorum sensing. *Annu Rev Genet.,* 35(35), P 439-468

56. Gasteiger E., Hoogland C., Gattiker A., Duvaud S., Wilkins M.R., Appel R.D., Bairoch A (2005). Protein Identification and Analysis Tools on the ExPASy Server. (In) John M. Walker (ed): The Proteomics Protocols Handbook, Humana Press, P 571-607

57. Gilson L., Kuo A, and Dunlap P.V. (1995). AinS and a new family of autoinducer synthesis proteins. *J. Bacteriol.*, 177 (23), P 6946–6951

58. Goffe W.L., Ferrier G.D., Rogers J.(1994). Global optimization of statistical functions with simulated annealing. *Journal of Econometrics*, 60(1/2), P 65-100

59. Goryachev AB, Toh DJ, Wee KB, Lee T, Zhang HB, Zhang LH (2005). Transition to Quorum Sensing in an *Agrobacterium* Population: A Stochastic Model. *PLoS Comput Biol*, 1(4), e37.

60. Gottesman S. (2004). The small RNA regulators of *Escherichia coli*: roles and mechanisms. *Annu Rev Microbiol.*, 58, P 303-328

61. Gray K.M., Greenberg E.P.(1992). Physical and functional maps of the luminescence gene cluster in an autoinducer-deficient *Vibrio fischeri* strain isolated from a squid light organ. *J. Bacteriol.*, 174(13), P 4384-4390

62. Gray K.M. and Greenberg E.P. (1992). Sequencing and analysis of *luxR* and *luxI*, the luminescence regulatory genes from the squid light organ symbiont *Vibrio fischeri* ES114. *Molecular Marine Biology and Biotechnology*. 1 (6), P 414-419

63. Gray K.M., Passador L., Iglewski B.H., and Greenberg E.P. (1994). Interchangeability and specificity of components from the quorum-sensing regulatory systems of Vibrio fischeri and Pseudomonas aeruginosa. *J. Bacteriol.*, 176(10), P 3076-3080

64. Gregory N. Stphano poulos, Aristos A. Aristidoll and Jens Nielsen (1998). Metabolic Engineering Principle and Methodologies. Academic Press.

65. Hanzelka B.L. and Greenberg E.P.(1996). Quorum sensing in *Vibrio fischeri*: evidence that S-adenosylmethionine is the amino acid substrate for autoinducer systhesis. *J. Bacteriol.*, 178(17), P 5291-5294

66. Hanzelka B.L., Parsek M.R., Val D.L., Dunlap P.V., Cronan J.E., JR., and Greenberg E. P. (1999). Acylhomoserine lactone synthase activity of the *Vibrio fischeri* AinS Protein. *J. Bacteriol.*, 181(18), P 5766–5770

67. Harlev, C.B., and Reynolds, R.P. (1987) Analysis of *E. coli* promoter sequences. *Necleic Acids Res.*, 15(5), P 2343-2361

68. Haygoodt M.G. and Nealson K. (1985). Mechanisms of iron regulation of luminescence in *Vibrio fischeri. J. Bacteriol.*, 162(1), P 209-216

69. Heath M.T.(2002) Scientific Computing, An Introductory Survey, 2nd edition, McGraw-Hill, New York.

70. Hershberg R., Altuvia S., Margalit H. (2003). A survey of small RNA-encoding genes in *Escherichia coli. Nucleic Acids Res.*, 31(7), P 1813-1820

71. Hertz G.Z. and Stormo G.D. (1999). Identifying DNA and protein patterns with statistically significant alignments of multiple sequences. *Bioinformatics*, 15, P 563-577

72. James S., Nilsson P., James G., Kjelleberg S. and Fagerstrom T. (1999). Luminescence control in the marine bacterium *Vibrio fischeri*: An analysis of the dynamics of *lux* regulation. *J. Mole. Biol.*, 296(4), P 1127-1137

73. Jennifer M.H. and Bonnie L.B. (2004). Three parallel quorum-sensing systems regulate gene expression in *Vibrio harveyi*. *J. Bacteriol.*, 186(20), P 6902–6914

74. Jennigs V. K., Rayner-Brandes M.H., and Bird D.J.(2001) Assessing chemical toxicity with the bioluminescent photobacterium(*Vibrio fischeri*): a comparion of three commercial systems. *Wat. Res.*, 35(14), P 448-3456

75. Juhas M., Eberl L. and Tümmler B. (2005). Quorum sensing: the power of cooperation in the world of *Pseudomonas*. *Environmental Microbiology,* 7(4), P 459–471

76. Kaiser K.L. (1998). Correlations of *Vibrio fischeri* bacteria test data with bioassay data for other organisms. *Environ Health Perspect,* 106(Suppl 2), P 583-591

77. Kaplan H.B. and Greenberg E.P. (1985). Diffusion of autoinducer is involved in regulation of the *Vibrio fischeri* luminescence system. *J. Bacteriol.,* 163 (3), P 1210–1214

78. Karlsson D, Karlsson S, Gustafsson E, Normark BH, Nilsson P (2006). Modeling the regulation of the competence-evoking quorum sensing network in *Streptococcus pneumoniae. Biosystems,* doi:10.1016/j.biosystems.2006.08.005

79. Kievit T.R. and Iglewski B.H. (2000). Bacterial quorum sensing in pathogenic relationships. *Infection and Immunity*, 68(9), P 4839–4849

80. Kirkpatrick S., Gelatt C.D. and Vecchi M.P. (1983). Optimization by simulated annealing. *Science*, 220(4598), P 671-680.

81. Kleerebezem M., Quadri L.E., Kuipers O.P. and de Vos WM(1997). Quorum sensing by peptide pheromones and two-componont signal-transduction systems in Gram-positive bacteria. *Mol. Microbiol.*, 24(5), P 895-904

82. Kolibachuk D., Greenberg E.P. (1993). The *Vibrio fischeri* luminescence gene activator LuxR is a membrane-associated protein. *J. Bacteriol.*,175(22), P 7307-7312

83. Kuo A., Blough N.N., and Dunlap P.V. (1994). Multiple N-Acyl-L-homoserine lactone autoinducers of luminescence in the marine symbiotic bacterium *Vibrio fischeri*. *J. Bacteriol.*, 176(24), P 7558-7565

84. Kuo A., Callahan S.M., and Unlap P.V. (1996). Modulation of luminescence operon expression by N-octanoyl-L-homoserine lactone in *ainS* mutants of *Vibrio fischeri. J. Bateriol.*, 178(4), P 971–976

85. Lam SH and Goussis DA (1994). The CSP method for simplifying kinetics. *International Journal of Chemical Kinetics,* 26, P 461-486

86. Lapertot M.E. and Pulgarin C. (2006). Biodegradability assessment of several priority hazardous substances: choice, application and relevance regarding toxicity and bacterial activity. *Chemosphere*, 65, P682-690

87. Leis JR and Kramer MA (1988). The simultaneous solution and sensitivity analysis of systems described by ordinary differential equations. *ACM Transactions on Mathematical Software*, 14(1), P 45-60

88. Leadbetter J.R., Greenberg E.P. (2000). Metabolism of acyl-Homoserine lactone quorum-sensing signals by *Variovorax paradoxus. J. Bacteriol.*, 182(24), P 6921-6926

89. Lenz D.H., Mok K.C., Lilley B.N., Kulkarni R.V., Wingreen N.S., Bassler B.L. (2004). The small RNA chaperone Hfq and multiple small RNAs control quorum sensing in *Vibrio harveyi* and *Vibrio cholerae. Cell*, 118(1), P 69-82

90. Lewin, B. (1994). Control by RNA structure: Termination and Antitermination. Oxford University Press, Oxford, P 461-462

91. Li H.L., Fu C.J. (2005). A linear programming approach for identifying a consensus sequence on DNA sequences, 21(9), P 1838-1845

92. Li J., Stewart V. (1992). Localization of upstream sequence elements required for nitrate and anaerobic induction of fdn(Formate Dehydrogenase-N) operon expression in *Escherichia coli* K-12. *J Bacteriol.*, 174(15), P 4935-4942

93. Lilley B.N. and Bassler B.L. (2000). Regulation of quorum sensing in *Vibrio harveyi* by LuxO and Sigma-54. *Molecular Microbiol.*, 36(4), P 940-954

94. Lin Y.H., Miyamoto C., and Meighen E.A. (2000). Functional studies of a *lux*O regulator *Lux*T from *Vibrio harveyi. Biochimica Biophysica Acta.,* 1494(3), P 226-235

95. Luo Z.Q., Farrand S.K. (1999). Signal-dependent DNA binding and functional domains of the quorum-sensing acitvator TraR as indentified by repressor activity. *Proc. Natl. Acad. Sci.*, 96(16), P 9009-9014

96. Lupp C., Urbanowski M, Greenberg E.P. and Ruby E.G. (2003). The *Vibrio fischeri* quorum-sensing systems *ain* and *lux* sequentially induce luminescence

gene expression and are important for persistence in the squid host. *Mol. Microbiol.* 50(1), P319-331

97. Lupp C. and Ruby E.G. (2004). *Vibrio fischeri* LuxS and AinS: comparative study of two signal synthases. *J. Bacteriol.*, 186(12), P 3873-3881

98. McLean R.J., Whiteley M., Stickler D.J. and Fuqua W.C.(1997). Evidence fo autoinducer activity in naturally occurring biofilms. *FEMS Microbio. Lett.*, 154(2), P 259-263

99. Meighan, E. A. (1988). Enzymes and genes from the *lux* operons of luminescent bacteria. *Ann. Rev. Microbiol.*, 42, P 154-176

100. Meighen E.A. (1994). Genetics of Bacterial Bioluminescence. *Annual Review of Genetics,* 28, P 117-139

101. Miller M.B. and Bassler B.L. (2001). Quorum Sensing in Bacteria. *Annu. Rev. Microbiol.,* 55, P 165–199

102. Miller M. B., Skorupski K., Lenz D.H., Taylor R. K., and Bassler B. L. (2002). Parallel quorum sensing systems converge to regulate virulence in *Vibrio cholerae. Cell,* 110(3), P 303-314

103. Milton D.L.(2006). Quorum sensing in *vibrios*: complexity for diversification. Int. *J. Med. Microbiol.*, 296(2-3), P 61-71

104. Miyamoto C.M., Dunlap P.V., Ruby E.G., Meighen E.A. (2003). LuxO controls LuxR expression in *Vibrio harveyi*: evidence for a common regulatory mechanism in *Vibrio. Mol. Microbiol.*, 48(2), P 537-548

105. Mount D.W. (2004). Bioinformatics sequence and Genome Analysis Cold Spring Harbor Laboratory Press, New York

106. Nealson, K.H. and Hastings, J.W. (1979). Bacterial bioluminescence: its control and ecological significance. *Microbiol. Rev.,* 43(4), P 469-518

107. Neiditch M.B., Federle M.J., Miller S.T., Bassler B.L., Hughson F.M. (2005). Regulation of LuxPQ receptor activity by the quorum-sensing signal autoinducer-2. *Mol Cell.,* 18(5), P 507-518

108. Nicolella C., van Loosdrecht M.C., Heijnen J.J. (2000). Wastewater treatment with particulate biofilm reactors. *J Biotechnol.* 80(1), P 1-33

109. Nishiguchi M.K., Ruby E.G. and J McFall-Ngai M. J. (1998). Competitive dominance among strains of luminous bacteria provides an unusual form of evidence for parallel evolution in Sepiolid Squid-*Vibrio* symbioses. *Applied and Environmental Microbiology*, 64(9), P 3209–3213

110. Nishiguchi M.K. and Nair V.S. (2003). Evolution of symbiosis in the *Vibrionaceae*: a combined approach using molecules and physiology. *International Journal of Systematic and Evolutionary Microbiology*, 53, P 2019-2026.

111. Nyholm S.V. and McFall-Ngai M.J. (2004). The winnowing: establishing the squid-Vibrio symbiosis. *Nature reviews,* 2(8), P 632-642

112. Odegaard H.(2006). Innovations in wastewater treatment: the moving bed biofilm process. *Water Sci. Technol.*, 53(9), P17-33

113. Pappas K.M., Weingart C.L. and Weans S.C. (2004). Chemical communication in proteobacteria: biochemical and structural Studies of signal synthases and receptors required for intercellular signaling. *Mol. Microbiol.,* 53(3), P 755-769

114. Parsek M.R., Val D.L., Hanzelka B.L., Cronan J.E., and Greenberg E.P. (1999). Acyl homoserine-lactone quorumsensing signal generation. *Proc. Natl. Acad. Sci. USA,* 96(8), P 4360-4365

115. Parsek M.R. and Greenberg E.P. (2000). Acyl-homoserine lactone quorum sensing in Gram-negative bacteria: a signaling mechanism involved in associations with higher organisms. *PNAS*, 97 (16), P 8789–8793

116. Parvez S., Venkataraman C., and Mukherji S.(2006). A revew on advantages of implementing luminescence inhibition test (Vibrio fischeri) for acute toxicity prediction of chemicals. *Environ. Int.*, 32(2), P 265-268

117. Perry L.L., Bright, N.G., Carroll Jr. R.J., Scott M.C., Allen M.S., and Applegate B.M. (2005). Molecular characterization of autoinduction of bioluminescence in the Microtox indicator strain *Vibrio fischeri* ATCC 49387. *Can. J. Microbiol.*, 51(7), P 549-557

118. Pesci E.C. and Iglewski B.H.(1997). The chain of command in *Pseudomonas* quorum sensing. *Trends Microbiology*. 5(4), P 134-135.

119. Ramos J.L., Martinez-Bueno M., Molina-Henares A.J., Teran W., Watanabe K., Zhang X., Gallegos M.T., Brennan R., Tobes R. (2005). The tetR family of transcriptional repressors. *Microbiology and Molecular Biology Reviews*, 69(2), P 326–356

120. Ravn L., Christensen A.B., Molin S., Givskov M., Gram L. (2001). Methods for detecting acylated homoserine lactones produced by Gram-negative bacteria and their application in studies of AHL-production kinetics. *J Microbiol Methods,* 44(3), P 239-51

121. Reitzer L., Schneider B.L. (2001). Metabolic context and possible physiological themes of sigma(54)-dependent genes in *Escherichia coli. Microbiol Mol Biol Rev.*, 65(3), P 422-444

122. Rodney M.D. (2002). Biofilms: microbial life on surfaces. *Emerg. Infect Dis,* 8(9), P 881-890

123. Rouault T.A., Klausner R.D. (1996). Iron-sulfur clusters as biosensors of oxidants and iron. *Trends Biochem Sci.,* 21(5), P 174-177

124. Ruby, E.G., and Nealson K.H. (1976). Symbiotic associations of Photobacterium fischeri with the marine luminous fish Monocentris japonica: a model of symbiosis based on bacterial studies. *Biol. Bull.*, 151(3), P 574–586

125. Ruby E.G. (1996). Lessons from a cooperative, bacterial-animal association: the Vibrio fischeri-Euprymna scolopes light organ symbiosis. *Annu. Rev. Microbiol.*, 50, P 591–624

126. Ruby E.G., Urbanowski M., Campbell j., Dunn A., Faini M., Gunsalus R., Lostroh P., Lupp C., McCann J., Millikan D., Schaefer A., Stabb E., Stevens A., Visick K., Whistler C., and Greenberg E.P. (2005). Complete Genome Sequence of Vibrio fischeri: A symbiotic bacterium with pathogenic congeners. *PNAS*, 102(8), P 3004-3009

127. Schaefer A.L., Val D.L., Hanzelka B. L., Cronan J.E., JR., and Greenberg E.P. (1996a). Generation of cell-to-cell signals in quorum sensing: Acylhomoserine lactone synthase activity of a purified *Vibrio fischeri* LuxI protein. *Proc. Natl. Acad. Sci.*, 93(18), P 9505–9509

128. Schaefer A.L., Hanzelka B.L., Eberhard A., Greenberg E.P. (1996b). Quorum sensing in *Vibrio fischeri*: probing autoinducer-LuxR interactions with autoinducer analogs. *J. Bacteriol.,* 178(10), P 2897-901

129. Shadel GS, Young RY, Baldwin TO (1990). Use of regualted cell lysis in a lethal genetic selection in *Escherichia*: identification of the autoinducer-binding region of the LuxR Protein from *Vibrio fischeri* ATCC7744. *J. Bacteriol.,* 172(7), P 3980-3987

130. Schauder S., Shokat K., Surette M.G., Bassler B.L. (2001). The LuxS family of bacterial autoinducers: biosynthesis of a novel quorum-sensing signal molecule. *Mol. Microbiol.*, 41(2), P 463-476

131. Schembri M.A., Givskov M., and Klemm P. (2002). An attractive surface: gram-negative bacterial biofilms. *Sci. STKE*, 14,132, P re6

132. Schupp P.J., Charlton T.S., Taylor M.W., Kjelleberg S. and Steinberg P.D. (2005). Use of solid-phase extraction to enable enhanced detection of acyl homoserine lactones (AHLs) in environmental samples. *Anal. Bioanal. Chem.* 383, P 132-137

133. Schuster M., Urbanowski M.L., and Greenberg E.P. (2004). Promoter specificity in *Pseudomonas aeruginosa* quorum sensing revealed by DNA binding of purified LasR. *Proc Natl Acad Sci U S A,* 101(45), P 15833–15839

134. Shadel G.S., Young R.Y., and Baldwin T.O. (1990). Use of regualted cell lysis in a lethal genetic selection in *Escherichia*: identification of the autoinducer-binding region of the LuxR Protein from *Vibrio fischeri* ATCC7744. *J. Bacteriol.,* 172(7), P 3980-3987

135. Shade G.S. and Baldwin T. O. (1992) Identification of a distantly located regulatory element in the luxD gene required for negative autoregulation of the Vibrio fischeri luxR gene. *Journal of Biological Chemistry*, 267(11), P 7690-7695

136. Shao C. P. and Hor L. I. (2001). Regulation of Metalloprotease Gene Expression in *Vibrio vulnificus* by a *Vibrio harveyi* LuxR Homologue. *J. Bacteriol.* 183(4), P 1369–1375

137. Shaw P.D., Ping G., Daly S.L., Cha C., Cronan Jr. J.E., Rinehart K.L., and Farrand S.K. (1997). Detecting and characterizing N-acyl-homoserine lactone signal molecules by thin-layer chromatography. *Proc. Natl. Acad. Sci. USA,* 94(12), P 6036-6041

138. Shin D.H., Shin W.S., Kim Y.H., Han M.H., and Choi S.J.(2006). Application of a combined process of moving-bed biofilm reactor (MBBR) and chemical coagulation for dyeing wastewater treatment. *Water Sci. Technol.*, 54(9), P181-189

139. Shiner E.K., Rumbaugh K.P., Williams S.C. (2005). Inter-kingdom signaling: deciphering the language of acyl homoserine lactones. *FEMS Microbiol Rev.,* 29(5), P 935-947

140. Sitnikov D.M., Schineller J.B., and Baldwin T.O. (1995). Transcriptional regulation of bioluminescence genes from *Vibrio fischeri. Mol. Microbiol.*, 17(5), P 801-812

141. Spiro S., Guest J.R. (1987). Regulation and over-expression of the fnr gene of *Escherichia coli. J Gen Microbiol.*, 133(12), P 3279-3288

142. Spiro S, Guest J.R.(1990). FNR and its role in oxygen-regulated gene expression in *Escherichia coli. FEMS Microbiol Rev.,* 6(4), P 399-428

143. Taga M.E., Semmelhack J.L., Bassler B.L. (2001). The LuxS-dependent autoinducer AI-2 controls the expression of an ABC transporter that functions in AI-2 uptake in *Salmonella Typhimurium. Mol. Microbiol.*, 42(3), P 777-793

144. Taga M.E. and Bassler B.L. (2003). Chemical communication among bacteria. *Proc. Natl. Acad. Sci.*, 100(suppl.2), P 14549–14554

145. Thattai M. and Oudenaarden A.V. (2001). Intrinsic noise in gene regulatory networks. *PNAS,* 98(15), P 8614-8619

146. Teresa R. de K. and Barbara H.I. (2000). Bacterial Quorum Sensing in Pathogenic Relationships. *Infect. Immun.*, 68(9), P 4839–4849

147. Trott A.E. and Stevens A.M. (2001). Amino acid residues in LuxR Critical for Its mechanism of transcriptional activation during quorum sensing in *Vibrio fischeri. J. Bacteriol.*, 183(1), P 387-392

148. Turanyi T (1990). Sensitivity analysis of complex kinetic systems tools and applications. *Journal of mathematical chemistry*, 5, P 203-248

149. Ulitzur S. (1998). LuxR controls the expression of Vibrio fischeri luxCDABE clone in *Echerichia coli* in the absence of *luxI* gene. *J. Biolumin Chemilumin.*, 13(6), P 365-369

150. Urbanowski M. L., Lostroh C. P., and Greenberg E. P. (2004). Reversible Acyl-Homoserine Lactone Binding to Purified *Vibrio fischeri* LuxR Protein *J. Bacteriol.*, 186(3), P 631–637

151. Vicente J.D., Lanchares J., and Hermida R. (2003). Placement by thermodynamic simulated annealing. *Physics* Letters, A 317, P 415-423

152. Viretta A. U. and Fussenegger M. (2004). Modeling the quorum sensing regulatory network of Human-pathogenic *Pseudomonas aeruginosa. Biotechnol. Prog.*, 20, P 670-678

153. Visick K.L., Foster J., Doino J., McFall-Ngai M., and Ruby E.G. (2000). *Vibrio fischeri lux* genes play an important role in colonization and development of the host light organ. *J. Bacteriol.*, 182(16), P 4578-4586

154. Visick K.L. (2005). Layers of Signaling in a Bacterium-Host Association. *J. Bacteriol.*, 187(11), P 3603-3606

155. Visick K.L., and Fuqua C. (2005). Decoding microbial chatter: cell-cell communication in bacteria. *J. Bacteriol.*,187(16), P 5507–5519

156. Visick K.L., and Ruby E.G. (2006). *Vibrio fischeri* and its host: it takes two to tango. *Current Opinion in Microbiology*, 9, P 632-638

157. Von Bodman S.B., Bauer W.D., Coplin D.L. (2003). Quorum sensing in plant-pathogenic bacteria. *Annu Rev Phytopathol.*, 41, P 455-482

158. Vosahlikova M., cajthaml T., Demnerova K. and Pazlarova J. (2006). Effect of methyl tert-butyl ether in standard tests for mutagenicity and environmental toxicity. *Environmental Toxicology,* 21(6), P 599-605

159. Wang L., Hashimoto Y., Tsao C.Y., Valdes J.J., Bentley W.E. (2005). Cyclic AMP (cAMP) and cAMP receptor protein influence both synthesis and uptake of extracellular autoinducer 2 in *Escherichia coli. J Bacteriol.*, 187(6), P 2066-2076

160. Watson W.T., Minogue T.D., Val D.L., von Bodman S.B., Churchill M.E. (2002). Structural basis and specificity of acyl-homoserine lactone signal production in bacterial quorum sensing. *Molecular Cell*, 9(3), P 685–694

161. Whitehead N.A., Barnard A.M., Slater H., Simpson N.J., Salmond G.P. (2001) Quorum-sensing in Gram-negative bacteria. *FEMS Microbiology Reviews,* 25(4), P 365-404

162. Wilusz CJ, Wilusz J.(2005). Eukaryotic Lsm proteins: lessons from bacteria. *Nat Struct Mol Biol.,* 12(12), P 1031-1036

163. Winans S.C. and Bassler B.L. (2002). Mob Psychology. *J. Bacteriol.* , 184(4), P 873–883

164. Winson M.K., Swift S., Fish L., Throup J.P., Jorgensen F., Chhabra S.R., Bycroft B.W., Williams P., Stewart G.S. (1998). Construction and analysis of *lux*CDABE-based plasmid sensors for investigating N-acyl homoserine lactone-mediated quorum sensing. *FEMS Microbiol Lett,* 163(2), P 185-192

165. Winzer K., Hardie K.R., Burgess N., Doherty N., Kirke D., Holden M.T., Linforth R., Cornell K.A., Taylor A.J., Hill P.J., Williams P. (2002). LuxS: Its role in central metabolism and the in Vitro synthesis of 4-hydroxy-5-methyl-3(2H)-furanone. *Microbiol.,* 148(Pt4), P 909-922

166. Wisniewski-Dye F. and Downie J.A. (2002). Quorum-sensing in Rhizobium. *Antonie Van Leeuwenhooek*, 81, P 397-407

167. Wright D.A., Dawson R., Cutler S.J., Culter H.G., Orano-Dawson C.E., and Graneli E (2007). Naphthoquinones as broad spectrum biocides for treatment of ship's ballast water: Toxicity to phytoplankton and bacteria. *Water Research*, 41, P1294-1302

168. Xavier K.B., Bassler B.L. (2003). LuxS quorum sensing: more than just a numbers game. *Current Opinion in Microbiology*, 6(2), P 191-197

169. Xavier K.B., Bassler B.L. (2005a). Interference with AI-2-mediated bacterial cell-cell communication. *Nature* 437(7059), P 750-753

170. Xavier K.B., Bassler B.L. (2005b). Regulation of uptake and processing of the quorum-sensing autoinducer AI-2 in *Escherichia coli. J Bacteriol.,* 187(1), P 238-248

171. Yan L, Allen MS, Simpson ML, Sayler GS, Cox CD (2007). Direct quantification of N-(3-oxo-hexanoyl)-l-homoserine lactone in culture supernatant using a whole-cell bioreporter. *J Microbiol Methods*. 68(1), P 40-45

172. Zuker M. and Stiegler P. (1981). Optimal computer folding of large RNA sequences using thermodynamics and auxiliary information. *Nucleic Acids Res.*, 9(1), P 133-148

173. Zhang A., Wassarman K.M., Ortega J., Steven A.C., Storz G.(2002). The Sm-like Hfq protein increases OxyS RNA interaction with target mRNAs. *Molecular Cell*, 9(1), P 11-22

Appendixes

Table A-1. The important sigma factors and their functions

Sigma factors	Gene	Function	[a]Locus in *V. fischeri*	[b]RNAp core recognition position in *E. coli.*	[b]RNAp core recognition position in *V. fischeri*
Sigma-70	*rpoD*	Housekeeping sigma factor	VF2254	-35: TTGACA -10: TATAAT (Harlev and Reynolds, 1987)	-35: ATG/CA/TCA/C -10: TGT/ATATA
Sigma-54	*rpoN*	Transcribing nitrogen-regulated genes, additional activators are required	VF0387	-24: CTGGNA -12: TTGCA	-24: TGGCACGA -12: GNNNTTGCA/T(Barrios et al., 1999)
Sigma-32	*rpoH* (*htpR*)	Heat shock sigma factor	VF2449, VF2450	-35: CTTGAAA -10: CCCCATNTA	NA
Sigma-S (sigma -38)	*rpoS*	Stationary phase sigma factor	VF2067	-35: TTGACA -10: CTATTT	NA
Sigma-28		Regulate expression of flagella operon (involved in cell motion)	VF2093, VFA0766	-35: TAAA -10: GCCGATAA	NA

[a]: Locus tag: VF means the gene is in Chromosome I; VFA means the gene is in Chromosome II

[b]: N means any nucleotide

Appendix B. The procedures for sequencing the putative sRNA DNA sequence.

DNA extraction

Genomic DNA of *V. fischeri* was extracted from cell cultures grown overnight using the Wizard® Genomic DNA Purification Kit (Promega, Madison, WI) according to the manufacturer's protocol. The quantity of the extracted DNA was measured using a DyNA Quant TM 200 fluorometer (Amersham Biosciences, Piscataway, NJ), and the integrity of extracted genomic DNA was analyzed by electrophoresis using 0.8% (w/v) agarose gel (Agarose Low EEO Electrophoresis Grade, Fisher Scientific). After that, the DNA extracts were stored at -20°C for the next procedures.

Sequencing

The primers designed for sequencing the whole small RNA were synthesized by Fisher Oligo. The target sequences were amplified by PCR (polymerase chain reaction) with the forward and reverse primer sequences of CACGCTCCCTGCAATAGGTA and CAACATGCGAAAGACTTGGA respectively. The total volume of each PCR reaction was 25 µL including one puReTaq™ Ready-To-Go™ PCR bead (Amersham Biosciences, Piscataway, NJ), 22.0µL of nucleic acid-free HPLC grade water, 1 µL of each primer (final concentration 400 nM), and 1.0 µL of 1:10 diluted extracted genomic DNA. The PCR program was as follows: 2 min at 94°C, followed by 36 cycles, each consisting of 1 min at 94°C, 1 min at 55°C, and 1 min at 72°C, and a final cycle at 72°C for 7 min. The PCR product was then checked by separation via 3% (w/v) agarose gel electrophoresis. After that, the PCR products were cloned into the plasmid vector (pCR®4-TOPO®) by one-shot chemical transformation following the manufacturer's protocol (TOPO TA Cloning® Kit for Sequencing, Invitrogen, Carlsbad, CA). The plasmid DNA of selected clones were isolated by Wizard® Plus SV Minipreps DNA Purification System (Promega, Madison, WI). The purified plasmid DNA was digested using the EcoRI restriction enzyme to confirm the insertion of the target sequence. Subsequently, the purified plasmid DNAs with the target sequences of interest were

sequenced at the Molecular Biology Resource Facility at the University of Tennessee using an Applied Biosystems 373™ DNA sequencer (Perkin-Elmer) equipped with an ABI PRISM dye terminator cycle sequencing kit, AmpliTaq® DNA polymerase, and M13f or M13r primers. The alignment of the amplified sequences is as follows:

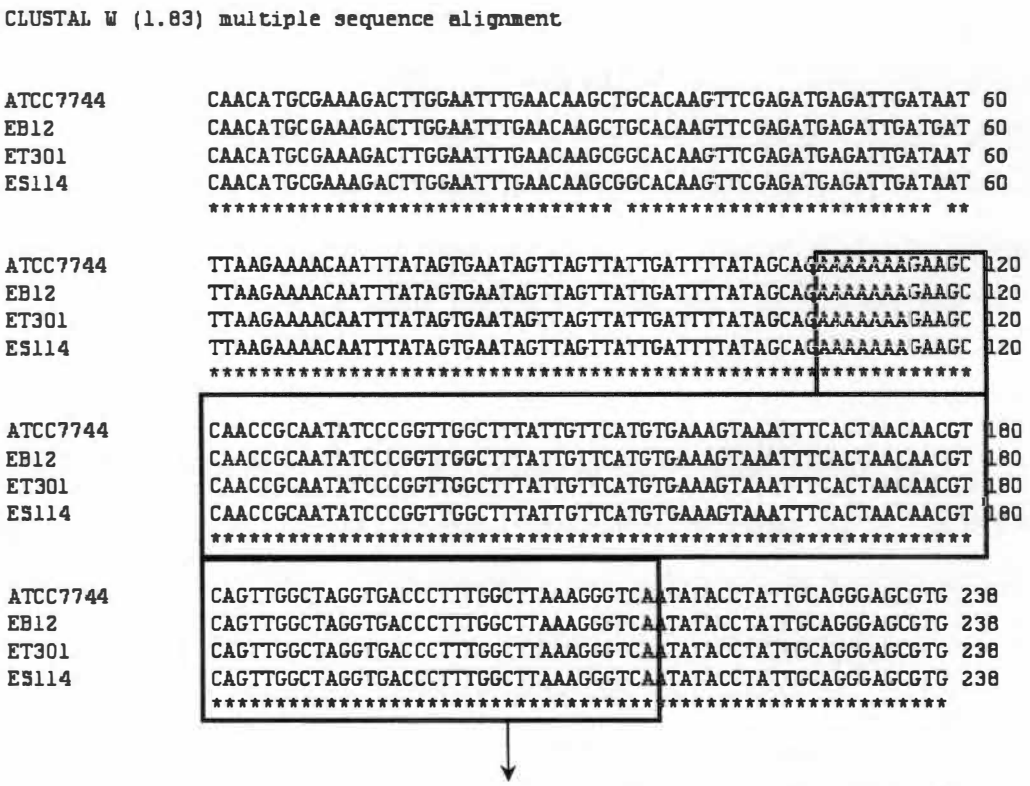

The full DNA sequences of the Putative small RNA

Appendix C. The important proteins in the QS regulatory network

Table C-1. The physical and chemical parameters of important quorum sensing related proteins

Protein	Formula	Molecular weight	-[b]	+[c]	Estimated half time *Escherichia coli, in vivo*	Estimate of the stability in a test tube	AN
LuxR	$C_{1275}H_{2005}N_{337}O_{382}S_{11}$	28519.6	27	31	>10 hours	stable	YP_206883
LuxI	$C_{965}H_{1528}N_{262}O_{293}S_7$	21712.7	27	24	>10 hours	unstable	YP_206882
AinS	$C_{1998}H_{3082}N_{508}O_{576}S_{13}$	43852.2	39	39	>10 hours	unstable	YP_204420
AinR	$C_{4349}H_{6764}N_{1058}O_{1206}S_{19}$	93777.0	74	75	>10 hours	stable	YP_204419
LitR	$C_{1023}H_{1605}N_{283}O_{318}S_9$	23245.2	29	20	>10 hours	stable	YP_205560
LuxO	$C_{2487}H_{3969}N_{685}O_{751}S_{18}$	56059.0	62	56	>10 hours	unstable	YP_206984

[a]: The amino acids information is from NCBI, and the parameters are estimated by ProtParam(Gasteiger et al., 2005)
[b] Total number of negatively charged residues (Asp + Glu)
[c]: Total number of positively charged residues (Arg + Lys)

LuxR(AAQ90196)

LuxI(AAQ90197)

AinR(YP_204419)

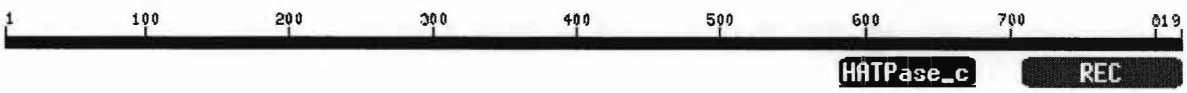

LitR(YP_205560)

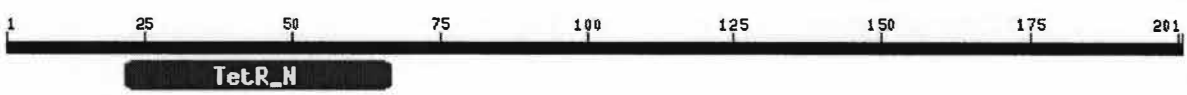

LuxO(AAF66011)

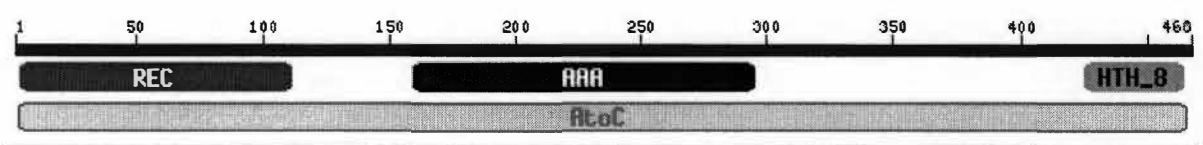

Figure C-1. The conserved domains of the important proteins in the quorum sensing regulation of *V. fischeri*

The meaning of each conserved domain is as follows (NCBI):

AAA: AAA-superfamily of ATPases associated with a wide variety of cellular activities, including membrane fusion, proteolysis, and DNA replication.
AtoC: Response regulator containing CheY-like receiver, AAA-type ATPase, and DNA-binding domains.

Autoind_bind: Autoinducer binding domain. This domain is found in a large family of bioluminescence operon transcriptional regulators. This domain specifically binds to autoinducer molecules.
Autoind_synth: Autoinducer synthase
HATPase_c: Histidine kinase-like ATPases
HTH_8: Bacterial regulatory protein, Fis family.
HTH_LUXR: helix_turn_helix, *Lux* Regulon; *lux* regulon (activates the bioluminescence operon)
REC: Signal receiver domain, and this domain receives the signal from the sensor partner in a two-component system; contains a phosphoacceptor site that is phosphorylated by histidine kinase homologs; usually found in a N-terminal to a DNA binding effector domain; forms homodimers
TetR_N: Bacterial regulatory proteins, tetR family.

Appendix D. The Fortran 77 codes

Print the results –program

```
      external  f1, jac1
      integer nspec, nrxn, nreact(100), nprod(100),
     1   irid(100, 100), ipid(100, 100),
     2   ircoef(100,100), ipcoef(100,100), nout, outid(100),
     3   ntime, nvari, idvari(100),
     4   neq, itol, itask, istate, iopt, lrw, iwork(120),liw, mf

      double precision spepop(100), ratek(100),extime(100),rtol,
     1    y(100), time, tout, atol,rwork(12000)


      character*15 spid(100)
      common / rate info / ratek, nreact, irid, ircoef,
     1    ipid, ipcoef, nrxn, nprod

      open (15, FILE='model.txt', STATUS='OLD')
      read (15, *) nspec
      print *, nspec
      read (15, *) (spid(i), i=1, nspec)
      print *, (spid(i), i=1, nspec)
      read (15, *) (spepop(i),i=1,nspec)
      print *, (spepop(i), i = 1, nspec)
      read (15, *) nrxn
      print *, nrxn
      do 100 i = 1, nrxn
         read (15, *) nreact(i), (ircoef(i,j), irid(i,j),j=1,nreact(i)),
     1   nprod(i), (ipcoef(i,jj), ipid(i,jj),jj=1,nprod(i)), ratek(i)

c      print *, irid(1,1)
       print *, nreact(i), (ircoef(i,j), irid(i,j),j=1,nreact(i)),
     1 nprod(i), (ipcoef(i,jj), ipid(i,jj),jj=1,nprod(i)), ratek(i)
100   continue
c      stop
      read (15, *) nout
      print *, nout
      read (15, *) (outid(i),i=1,nout)
      print*,(outid(i),i=1,nout)

c ******print all the reactions*******************
      open (25, FILE='reactions.txt', STATUS='new')
          Do 202 i=1,nrxn
            Do 225 j=1,nreact(i)-1
            write(25,107)ircoef(i,j),spid(irid(i,j)),'+'
225         continue
            write(25,1071)ircoef(i,nreact(i)),spid(irid(i,nreact(i)))
            write(25,1090)'==>'
            do 2251 k=1,nprod(i)-1
            write(25,108) ipcoef(i,k),spid(ipid(i,k)),'+'
2251        continue
            write(25,1071)ipcoef(i,nprod(i)),spid(ipid(i,nprod(i)))
            write(25,1082)'K',i,':',ratek(i)
```

```
202       continue

107   format(I2,a10,A1,$)
1071  format(I2,a10,$)
1090  format(A3,$)
108   format(I2,a10,A1,$)
1082  format(/,TR65,A1,I2,A1,g12.5,/,/)

c   ***********************************************

      open (20, FILE ='printtimeall.txt', STATUS='OLD')
      read (20, *) ntime, nvari
      print*,ntime,nvari
      read (20, *) (idvari(i), i=1, nvari)
      print*,(idvari(i), i=1, nvari)
      read (20,*)(extime(i),i=1,ntime)
      print*,(extime(i), i=1,ntime)
      close(20)


      open (30, FILE ='timeseries.txt', STATUS='new')
      write(30,303)'time  '
303   format(A5,$)
      write(30,304) (spid(outid(i)),i=1,nout)
304   format(100A10)

************************************************************
      neq = nspec
      itol = 1
      rtol = 1.0d-6
      atol = 1.0d-12
      itask = 1
      istate = 1
      iopt = 1
      lrw = 12000
      liw = 120
      mf = 21
      time = 0.0d0

      do 45 i = 5, 10
      iwork(i) = 0
      rwork(i) = 0
45    continue
      iwork(6) = 50000
      do 139 i = 1, nspec
      y(i) = spepop(i)
139   continue


      tout = extime(1)
      call dlsode(f1,neq,y,time,tout,itol,rtol,atol,itask,istate,
     1      iopt,rwork,lrw,iwork,liw,jac1,mf)

      do 200 i = 1, ntime
      iflag = 0
```

```
      do 220 k = 1, 500
      tout = tout + 100
      if (tout.ge.extime(i)) then
        tout = extime(i)
        iflag = 1
      else
      end if
        call dlsode(f1,neq,y,time,tout,itol,rtol,atol,itask,istate,
     1      iopt,rwork,lrw,iwork,liw,jac1,mf)

      if (iflag.eq.1) then
         go to 221
      else
      end if
c      print *, time, (y(outid(j)), j = 1, nout)
220   continue
221   continue

      write(30,305) time, (y(outid(j)), j = 1, nout)
305   format(g7.2,100g16.6)

200   continue
      end

*************************************************************************
      subroutine f1 (neq, t, y, ydot)
      integer neq, nrxn, nreact(100), irid(100,100), ircoef(100,100),
     1  ipid(100,100), ipcoef(100,100), nprod(100)
      double precision t, y(neq), ydot(neq), rate(100),
     1   ratek(100)
      common / rate info / ratek, nreact, irid, ircoef,
     1    ipid, ipcoef, nrxn, nprod
      do 10 i = 1, nrxn
      rate(i) = ratek(i)
      do 20 j = 1, nreact(i)
c      print *, "irid", i, j, irid(i,j), y(irid(i,j))
      rate(i) = rate(i)*y(irid(i,j))**ircoef(i,j)
c      print *, rate(i)
20    continue
10    continue
      do 30 i = 1, neq
      ydot(i) = 0
      do 40 j = 1, nrxn
      do 45 k = 1, nreact(j)
      if (irid(j,k).eq. i) then
        ydot(i) = ydot(i) - ircoef(j,k)*rate(j)
      else
      endif
45    continue
      do 46 k = 1, nprod(j)
      if (ipid(j,k) .eq. i) then
        ydot(i) = ydot (i) + ipcoef(j,k)*rate(j)
      else
      endif
46    continue
```

```
40    continue
c      print *, ydot (i)
30    continue
      return
      end


      subroutine  jac1 (neq, t, y, ml, mu, pd, nrowpd)
      integer  neq, ml, mu, nrwopd, nrxn, nreact(100), irid(100,100),
     1  ipid(100,100), ircoef(100,100), ipcoef(100,100), iflag,
     1  nprod(100)
      double precision  t, y(neq), pd(nrowpd,neq), term1, term2,
     1  flag1, ratek(100)
      common / rate info / ratek, nreact, irid, ircoef,
     1    ipid, ipcoef, nrxn, nprod
c      print *, neq
c      print *, (y(i), i=1, neq)
      do 10 i = 1, neq
      do 20 j = 1, neq
      pd(i,j) = 0
      do 30 k = 1, nrxn
      flag1 = 0.0d0
      do 31 kk = 1, nreact(k)
      if (irid(k,kk) .eq. i) then
        flag1 = (-1)*ircoef(k,kk)
      else
      endif
31    continue
      iflag = 0
      do 32 kk = 1, nreact(k)
      if (irid(k,kk) .ne. j) then
        flag1 = flag1*y(irid(k,kk))**ircoef(k,kk)
      else
       iflag = 1
       flag1 = flag1*ircoef(k,kk)*y(j)**(ircoef(k,kk)-1)
      endif
32    continue
      term1 = ratek(k) * iflag * flag1
      pd(i,j) = pd(i,j) + term1
      flag1 = 0.0d0
      do 33 kk = 1, nprod(k)
      if (ipid(k,kk) .eq. i) then
        flag1 = ipcoef(k,kk)
      else
      endif
33    continue
      iflag = 0
      do 34 kk = 1, nreact(k)
      if (irid(k,kk) .ne. j) then
        flag1 = flag1*y(irid(k,kk))**ircoef(k,kk)
      else
       iflag = 1
       flag1 = flag1*ircoef(k,kk)*y(j)**(ircoef(k,kk)-1)
      endif
34    continue
```

```
      term1 = ratek(k) * iflag * flag1
      pd(i,j) = pd(i,j) + term1
30    continue
c      print *, pd(i,j)
20    continue
10    continue
      return
      end
```

modelall.txt

37

gbLuxR	gbLuxI	gbAinS	gbAinR	gbLitR	gbsRNA	mLuxR	mLuxI	mAinS	mAinR	mLitR	sRNA	pLuxR
pLuxI	pAinS	pAinR	pLitR	giLuxR	giLuxIC6	giLuxIC8	gisRNA	C6AIout	C8AIout	Biomass	Substrate	GC
C6AI	C8AI	LuxRC6	LuxRC8	AinRC6	giAinSC6	pLuxOp	pLuxO	AinRC8	Nil	giAinSC8		
1	1	1	1	1	1	0	0	0	0	0	0	100
0	0	100	10	0	0	0	0	10000	1500	1	2500	0
0	0	0	0	0	0	1000	0	0	0	0		
61												
2	1	25	1	24	1	1	26	1.00E-04				
1	1	26	2	1	25	1	24	6.67E-01				
1	1	26	1	2	24	9.00E-04						
1	1	27	1	1	22	3.92E+08						
1	1	22	1	1	27	1.9132						
2	1	24	1	14	3	1	22	1	24	1	14	8.30E-02
2	1	16	2	22	1	1	31	2.48E-06				
1	1	31	2	1	16	2	22	4.1251				
1	1	8	2	1	14	1	8	7.80E-01				
1	1	14	1	1	36	5.76E-03						
1	1	28	1	1	23	3.92E+08						
1	1	23	1	1	28	1.91						
2	1	15	1	24	3	1	23	1	15	1	24	10
2	1	16	2	23	1	1	35	9.41E-06				
1	1	35	2	1	16	2	23	1.8824				
1	1	9	2	1	15	1	9	8.20E-02				
1	1	15	1	1	36	5.76E-03						
2	1	16	1	34	2	1	33	1	16	35.659		
2	1	31	1	34	2	1	33	1	31	1000		
2	1	35	1	33	2	1	34	1	35	100		
2	1	33	1	6	1	1	21	7.62E-02				
1	1	21	2	1	6	1	33	108.83				
1	1	21	2	1	12	1	21	1				
2	1	11	1	12	1	1	36	1				
1	1	12	1	1	36	0.00577						
1	1	5	2	1	11	1	5	0.6				
1	1	11	2	1	17	1	11	1.16E-01				
1	1	17	1	1	36	1.52E-04						
2	2	29	1	3	1	1	32	1.00E-06				
1	1	32	2	2	29	1	3	1				
1	1	32	2	1	9	1	32	1.20E-03				
1	1	3	2	1	9	1	3	5.00E-05				
1	1	9	1	1	36	5.77E-03						
2	2	17	1	1	1	1	18	9.21E-11				
1	1	18	2	2	17	1	1	0.64459				
1	1	18	2	1	7	1	18	0.0338				
1	1	7	1	1	36	5.77E-03						
2	1	13	1	27	1	1	29	1.20E+01				
1	1	29	2	1	27	1	13	1.00E+00				
1	1	29	1	1	36	2.46E-04						
2	1	28	1	13	1	1	30	3.00E+00				
1	1	30	2	1	13	1	28	1				
1	1	30	1	1	36	2.46E-04						
1	1	13	1	1	36	2.46E-04						
1	1	7	2	1	13	1	7	1.16E-01				
2	2	29	1	2	1	1	19	2.00E-06				
1	1	19	2	2	29	1	2	1.00E+00				
1	1	19	2	1	8	1	19	0.038				
2	2	30	1	2	1	1	20	2.00E-06				
1	1	20	2	2	30	1	2	1				
1	1	20	2	1	8	1	20	1.84E-02				
1	1	8	1	1	36	5.78E-03						
1	1	11	1	1	36	5.78E-03						
2	1	26	1	14	3	1	14	1	26	1	22	8.30E-02
2	1	26	1	15	3	1	15	1	26	1	23	10
2	2	30	1	3	1	1	37	2.00E-03				
1	1	37	2	2	30	1	3	1				
1	1	37	2	1	9	1	37	1.80E-04				

1	1	22	1	1	36	6.93E-05			
1	1	23	1	1	36	6.93E-05			
1	1	2	2	1	2	1	8	1.00E-04	
37									
1	2	3	4	5	6	7	8	9	10
11	12	13	14	15	16	17	18	19	20
21	22	23	24	25	26	27	28	29	30
31	32	33	34	35	36	37			

printtimeall.txt

53 37
1 2 3 4 5 6 7 8 9 10 11 12 13 14 15 16 17 18 19 20 21 22 23 24 25 26 27 28 29 30 31 32
33 34 35 36 37
0
1000 2000 3000 4000 5000 6000 7000 8000 9000 10000 11000 12000 13000 14000
15000 16000 17000 18000 19000 20000 21000 22000 23000 24000 25000 26000
27000 28000 29000 30000 31000 32000 33000 34000 35000 36000 37000 38000
39000 40000 41000 42000 43000 44000 45000 46000 47000 48000 49000 50000
51000 52000

Vita

Ling Yan received her B.S and M.S. degree in Environmental Engineering from Tianjin University, China in August 1998 and March 2001 respectively. She started to pursue her Ph.D. degree in the Civil & Environmental Engineering Dept., the University of Tennessee, Knoxville, in August 2002, and expects to graduate in May 2007.